Dissertation
submitted to the
Combined Faculties for the Natural Sciences and for Mathematics
of the Ruperto-Carola University of Heidelberg, Germany
for the degree of
Doctor of Natural Sciences

presented by

Dipl. Biochemist Sandra Christochowitz
born in Berlin

Oral Examination: 17th May 2018

Novel insights into the contribution of IL-13 to the pathogenesis of muco-obstructive lung disease

Referees: Prof. Dr. Stefan Wölfl

Prof. Dr. Marcus Mall

Table of contents

Table of contents ..... **V**

Abbreviations ..... **VIII**

List of figures ..... **X**

List of tables ..... **XI**

Abstract ..... **XII**

Zusammenfassung ..... **XIV**

1 Introduction **1**

1.1 Pathophysiological aspects of muco-obstructive lung diseases 1

1.2 Mucus clearance system of the lung 2

1.3 Abnormal mucus properties in CF, COPD, and asthma 3

1.4 IL-13-mediated inflammation and muco-obstructive lung diseases 5

1.5 Mouse models for muco-obstructive lung diseases 7

1.5.1 *Scnn1b*-Tg mouse model 7

1.5.2 *Il13*-Tg mouse model 8

1.6 Aim of the thesis 8

2 Material and Methods **9**

2.1 Experimental animals 9

2.2 Aspergillus fumigatus instillation 10

2.3 Hypertonic saline treatment 10

2.4 IL-33 instillation 10

2.5 Bronchoalveolar lavage and cytokine measurements 11

2.6 Flow cytometry 11

2.7 Histology and morphometry 12

2.7.1 Tissue embedding and sectioning 12

2.7.2 Histology 13

2.7.3 Immunohistochemisty 13

2.7.4 Morphometry....14
2.8 Laser micro-dissection....14
2.9 Mucociliary clearance....15
2.10 *Ex vivo* micro-computed tomography....15
2.11 Murine primary tracheal epithelial cell cultures....16
2.12 RNA extraction and real time RT-PCR....18
2.12.1 RNA extraction and RT-PCR....18
2.12.2 Real-time PCR....19
2.12.3 Generation of plasmid standards for real-time PCR....19
2.13 Statistics....20
3 Results....21
3.1 Airway epithelial cells express IL-13....21
3.1.1 Type 2 airway inflammation in juvenile naïve and Af-challenged *Scnn1b*-Tg mice....21
3.1.2 Airway epithelial cells are a cellular source of IL-13 in naïve and Af-challenged *Scnn1b*-Tg mice....23
3.1.3 IL-33 induces *Il13* expression via the St2/Myd88/p38 signaling pathway in epithelial cells *in vitro*....25
3.1.4 *In vivo* role of IL-33 on epithelial IL-13 production....27
3.2 Relative contributions of IL-13-induced mucin hypersecretion and airway surface dehydration to airway mucus obstruction....28
3.2.1 Airway mucus obstruction is more severe in *Scnn1b*-Tg mice with airway surface dehydration than in mice with IL-13-mediated mucin hypersecretion....29
3.2.2 IL-13 regulates *Muc5ac* and *Muc5b* expression....31
3.2.3 Airway surface dehydration but not IL-13-mediated mucin hypersecretion impairs mucociliary transport....33
3.2.4 Eosinophilic and neutrophilc inflammation in *Scnn1b*-Tg and *Il13*-Tg mice....34

3.2.5 IL-13-induced mucin hypersecretion in *Scnn1b*-Tg mice causes neonatal mortality due to severe airway mucus plugging 35

3.2.6 Increased *Muc5ac* and *Muc5b* expression in *Scnn1b*-Tg/*Il13*-Tg/*Il13*$^{-/-}$ mice ..38

3.2.7 Hypertonic saline treatment does not prevent early mortality of *Scnn1b*-Tg/*Il13*-Tg/*Il13*$^{-/-}$ mice 40

4 Discussion....**41**

4.1 Airway epithelial cells contribute to IL-13 production in mice with muco-obstructive lung disease 41

4.2 Epithelial IL-13 production is mediated by IL-33 via the St2/Myd88/p38 signaling pathway 43

4.3 Airway surface dehydration and IL-13-induced mucin hypersecretion act synergistically in the *in vivo* pathogenesis of airway mucus plugging 46

4.4 Muc5ac and Muc5b contribute to airway mucus plugging....49

4.5 Conclusions and future perspectives....51

5 References....**53**

Publications....**65**

Acknowledgements....**67**

Abbreviations

ABPA	Allergic bronchopulmonary aspergillosis
AB-PAS	Alcian blue periodic acid-Schiff
ACOS	Asthma-COPD-overlap syndrom
Actb	β-Actin
Af	*Aspergillus fumigatus* allergen
AHR	Airway hyperresponsiveness
ALI	Air-liquid interface
AMs	Airway macrophages
APC	Allophycocyanin
ASL	Airway surface liquid
BSA	Bovine serum albumin
BAL	Bronchoalveolar lavage
BV	Brilliant violet
Ca^{2+}	Calcium ion
CCSP	Club cell secretory protein
CF	Cystic fibrosis
CFTR	Cystic fibrosis transmembrane conductance regulator
Cl^-	Chloride ion
COPD	Chronic obstructive pulmonary disease
CT	Computed tomography
Cy	Cyanine
DAB	3, 3'-Diaminobenzidine
dd	Double distilled
DNase	Deoxyribonuclease
ENaC	Epithelial sodium channel
FACS	Fluorescence-activated cell sorting
FBS	Fetal bovine serum
FITC	Fluorescein isothiocyanate
Foxa	Forkhead box protein A
GCM	Goblet cell metaplasia
Gob5	Chloride channel accessory 1
HCO^{3-}	Bicarbonate

IL	Interleukin
ILC2s	Type 2 innate lymphoid cells
LPS	Lipopolysaccharides
MAPK	Mitogen-activated protein kinases
MCC	Mucociliary clearance
Myd88	Myeloid differentiation primary-response protein 88
Na^+	Sodium ion
PBS	Phosphate-buffered saline
PCL	Periciliary liquid layer
PCR	Polymerase chain reaction
PE	Phycoerythrin
PerCP	Peridinin-chlorophyll-protein complex
PMA	Phorbol 12-myristate 13-acetate
PND	Postnatal day
RT	Reverse transcription
Scnn1b	Gene of the β-subunit of the epithelial sodium channel
Spdef	SAM pointed domain containing ETS transcription factor
St2	Suppression of tumorigenicity 2
Stat6	Signal transducer and activator of transcription 6
Th	T helper
Tg	Transgenic
TGF-β	Transforming growth factor β
TMEM16A	Transmembrane member 16A
TNF-α	Tumor necrosis factor α
Tslp	Thymic stromal lymphopoietin
WT	Wild-type

List of figures

Figure 1. IL-13 effector functions in the lung.....5
Figure 2. Mechanisms of IL-13-induced goblet cell metaplasia.....6
Figure 3. *Il13* expression in the absence of doxycycline in CCSP-rtTA-*Il13*-Tg mice. 9
Figure 4. Murine primary tracheal epithelial cell cultures. 17
Figure 5. Spontaneous and exaggerated allergen-induced airway inflammation in juvenile *Scnn1b*-Tg mice.....22
Figure 6. Exaggerated type 2 cytokine concentrations after allergen exposure in juvenile *Scnn1b*-Tg mice.....23
Figure 7. Increased IL-13 expression in airway epithelial cells from *Scnn1b*-Tg mice.....24
Figure 8. IL-33 triggers epithelial *Il13* expression via St2/Myd88/p38 signaling *in vitro*.....26
Figure 9. Increased *Il33* expression in juvenile *Scnn1b*-Tg mice. 27
Figure 10. Epithelial IL-13 expression in response to exogenous IL-33 in WT mice.....28
Figure 11. IL-13-(in)dependent mucus accumulation in mouse models that mimic muco-obstructive airway disease. 29
Figure 12. Mucus obstruction is more severe in *Scnn1b*-Tg mice than in *Il13*-Tg mice.....30
Figure 13. IL-13 drives *Muc5ac* and *Muc5b* expression in juvenile *Scnn1b*-Tg and *Il13*-Tg mice. 31
Figure 14. Increased *Spdef* and *Foxa3* expression in *Il13*-Tg mice but not in *Scnn1b*-Tg mice.....32
Figure 15. Mucociliary transport is reduced in *Scnn1b*-Tg mice but not in *Il13*-Tg mice.....33
Figure 16. Eosinophilc and neutrophilc inflammation in *Scnn1b*-Tg and *Il13*-Tg mice.....34
Figure 17. Neonatal death of *Scnn1b*-Tg/*Il13*-Tg/*Il13*$^{-/-}$ mice.....35
Figure 18. Severe airway mucus obstruction in airways of neonatal *Scnn1b*-Tg/*Il13*-Tg/*Il13*$^{-/-}$ mice. 36
Figure 19. Severe mucus plugging and atelectasis in neonatal *Scnn1b*-Tg/*Il13*-Tg/*Il13*$^{-/-}$ mice visualized by µ-CT measurements.....37
Figure 20. Increased *Muc5ac* and *Muc5b* transcripts in neonatal *Il13*-Tg/*Il13*$^{-/-}$ and *Scnn1b*-Tg/*Il13*-Tg/*Il13*$^{-/-}$ mice. 39
Figure 21. Treatment with 7 % HS does not rescue *Scnn1b*-Tg/*Il13*-Tg/*Il13*$^{-/-}$ mice. 40
Figure 22. IL-33-mediated signaling pathway leading to IL-13 expression in airway epithelial cells.....45

List of tables

Table 1. Antibody master mix for the detection of leukocytes from BAL fluid by flow cytometry. 12
Table 2. Substances and conditions used for treatment of murine primary tracheal epithelial cell cultures. 18
Table 3. Sense and antisense primers used for preamplification....19
Table 4. Sense and antisense primers used for amplifiction of *Muc5ac* and *Muc5b*. 20
Table 5. Stimuli tested for induction of *Il13* expression in primary tracheal epithelial cell cultures from WT and *Scnn1b*-Tg mice. 25

Abstract

Airway mucus obstruction is a key feature of a spectrum of chronic lung diseases such as cystic fibrosis (CF), chronic obstructive pulmonary disease (COPD), and asthma. Mucus dehydration and mucin hypersecretion have been implicated in the pathogenesis of airway mucus plugging. However, understanding of relative contributions and combined effects of these abnormalities remain poorly understood. Mucus accumulation in the airways is associated with chronic airway inflammation. The type 2 cytokine interleukin (IL)-13 has been shown to play a crucial role during type 2 airway inflammation. Furthermore, IL-13 mediates mucin overproduction by acting on airway epithelial cells. If the airway epithelium itself contributes to IL-13 production under conditions of muco-obstructive lung disease is not well understood.

In this study, the airway epithelium was investigated as a cellular source for IL-13 production in transgenic (Tg) mice with airway-specific overexpression of the β-subunit of the epithelial sodium channel (*Scnn1b*) exhibiting airway mucus obstruction due to airway surface dehydration and a spontaneous type 2 airway inflammation at juvenile ages. IL-13 protein and gene expression was studied in the airway epithelium from naïve and allergen-treated wild-type (WT) and *Scnn1b*-Tg mice. *In vitro* studies were performed to elucidate signaling pathways that induce epithelial IL-13 expression. To better understand the *in vivo* pathogenesis of airway mucus obstruction, the relative roles of airway surface dehydration and IL-13-mediated mucin hypersecretion were investigated. Therefore, juvenile *Scnn1b*-Tg mice with genetic deletion of IL-13 (*Scnn1b*-Tg/*Il13*$^{-/-}$) were studied and the phenotypes of *Scnn1b*-Tg mice were compared to mice with airway-specific overexpression of IL-13 (*Il13*-Tg). By studying *Scnn1b*-Tg/*Il13*-Tg/*Il13*$^{-/-}$ mice, the combined effect of both defects were investigated.

The airway epithelium from *Scnn1b*-Tg mice was shown to produce increased levels of IL-13. Epithelial IL-13 production was induced by IL-33 via the St2/Myd88/p38 signaling pathway. Furthermore, IL-13 specifically overexpressed in airway epithelial cells (*Il13*-Tg/*Il13*$^{-/-}$) was sufficient to cause muco-obstructive lung disease associated with mucus plugging, severe goblet cell metaplasia (GCM), and airway inflammation. *Scnn1b*-Tg/*Il13*$^{-/-}$ mice displayed neither goblet cells nor mucin hypersecretion, but mucus plugging persisted in the airways. In *Scnn1b*-Tg mice, airway mucus plugging was more severe than in *Il13*-Tg mice, although *Il13*-Tg mice demonstrated a pronounced GCM and *Muc5ac* expression. These differences were associated with an impaired mucociliary transport in *Scnn1b*-Tg mice and a normal mucociliary transport in *Il13*-Tg mice. Combination of airway surface

dehydration and IL-13-induced mucin hypersecretion produced severe mucus plugging causing neonatal mortality of *Scnn1b*-Tg/*Il13*-Tg/*Il13*$^{-/-}$ mice.

In summary, these results demonstrate that the airway epithelium provides a source of IL-13 production in spontaneous and allergen-induced type 2 airway inflammation in juvenile *Scnn1b*-Tg mice and indicates that IL-33 contributes to this process *in vivo*. Further, these results suggest that both airway surface dehydration and IL-13-induced mucin hypersecretion have detrimental effects in the *in vivo* pathogenesis of airway mucus obstruction.

Zusammenfassung

Mukusobstruktion von Atemwegen ist ein Hauptmerkmal von chronischen Lungenkrankheiten wie zystischer Fibrose (CF), chronisch obstruktiver Lungenerkrankung (COPD) und Asthma. Es wird angenommen, dass eine Überproduktion von Mukus und die Dehydratation der Atemwegsoberfläche zur Ausbildung von hyperkonzentriertem und sehr viskosem Mukus führen. Die relative Bedeutung dieser pathologischen Mechanismen auf die Mukusobstruktion ist bisher nicht untersucht worden. Die Pathogenese der Mukusobstruktion geht mit einer chronischen Entzündung der Atemwege einher. Hierbei nimmt das Typ 2 Zytokin Interleukin (IL)-13 eine zentrale Rolle ein, da es die Typ 2 Atemwegsentzündung fördert und eine vermehrte Muzinproduktion in den Becherzellen des Atemwegepithels induziert. Inwiefern Epithelzellen in muko-obstruktiven Atemwegen selbst IL-13 produzieren können, ist jedoch nicht bekannt. Deshalb wurde in dieser Arbeit die epitheliale IL-13 Produktion in juvenilen transgenen (Tg) Mäusen mit einer atemwegsspezifischen Überexpression der β-Untereinheit des epithelialen Natriumkanals (*Scnn1b*) untersucht. Diese Mäuse weisen aufgrund einer Atemwegsdehydratation einen muko-obstruktiven Phänotyp sowie eine Typ 2 Atemwegsentzündung auf. Im Atemwegsepithel von naiven und allergenbehandelten Wildtyp (WT)- und *Scnn1b*-Tg Mäusen wurde die Protein- und Genexpression von IL-13 bestimmt sowie die zugrunde liegende Signalkaskade *in vitro* untersucht. Des Weiteren sollte geklärt werden, welchen Einfluss die Atemwegsdehydratation im Vergleich zur IL-13-vermittelten Muzinhypersekretion auf die Pathogenese der Mukusobstruktion *in vivo* haben. Zum einen wurden hierzu juvenile IL-13-defiziente *Scnn1b*-Tg (*Scnn1b*-Tg/*Il13*$^{-/-}$) Mäuse untersucht und zum anderen wurden *Scnn1b*-Tg Mäuse mit atemwegsspezifisch IL-13-überexprimierenden Mäusen verglichen (*Il13*-Tg). Mit Hilfe von *Scnn1b*-Tg/*Il13*-Tg/*Il13*$^{-/-}$ Mäusen wurde untersucht, welche Auswirkung das gleichzeitige Auftreten von Atemwegsdehydratation und IL-13-vermittelter Muzinhypersekretion auf die Mukusobstruktion hat.

Es konnte gezeigt werden, dass Atemwegsepithelzellen von *Scnn1b*-Tg Mäusen IL-13 produzieren und die epitheliale *Il13* Expression durch IL-33 via St2/Myd88/p38 induziert wird. Die Überexpression von IL-13 im Atemwegsepithel (*Il13*-Tg/*Il13*$^{-/-}$) war ausreichend, um Mukusobstruktion, Becherzellmetaplasie und Atemwegsentzündung in Mäusen hervorzurufen. Im Vergleich zu *Scnn1b*-Tg Mäusen wiesen *Scnn1b*-Tg/*Il13*$^{-/-}$ Mäuse weder Becherzellen noch eine vermehrte Muzinproduktion auf, jedoch keine verminderte Mukusobstruktion. In *Scnn1b*-Tg Mäusen war die Mukusobstruktion stärker ausgeprägt als

in *Il13*-Tg Mäusen, obwohl *Il13*-Tg Mäuse eine Becherzellmetaplasie und eine erhöhte Muc5ac Expression aufwiesen. Dieser Unterschied zwischen den Modellen korrelierte mit einer unterschiedlichen Effektivität des mukoziliären Transports, welcher in *Scnn1b*-Tg Mäuse deutlich vermindert und in *Il13*-Tg Mäusen nicht beeinträchtigt war. In *Scnn1b*-Tg/*Il13*-Tg/*Il13*$^{-/-}$ Mäusen hatte eine schwerwiegende Mukusobstruktion der Atemwege eine frühzeitige Mortalität innerhalb der ersten Lebenswoche zur Folge.

Zusammenfassend zeigt diese Arbeit, dass Atemwegsepithelzellen von juvenilen *Scnn1b*-Tg Mäusen mit einer Typ 2 Entzündung IL-13 produzieren und hierbei IL-33 als Stimulus eine wichtige Rolle spielt. Weiterhin deuten die Ergebnisse daraufhin, dass sowohl die Atemwegsdehydratation als auch die IL-13-vermittelte Muzinhypersekretion einen negativen Einfluss auf die Pathogenese der Mukusobstruktion von Atemwegen haben.

1 Introduction

1.1 Pathophysiological aspects of muco-obstructive lung diseases

Airway mucus obstruction is a critical pathogenic feature of several chronic lung diseases such as CF, COPD, and asthma. It contributes to airflow obstruction, pathogen colonization and chronic inflammation and affects disease severity.[1] CF is one of the most common autosomal recessive genetic diseases in Caucasian populations and results from mutations in the cystic fibrosis transmembrane conductance regulator (CFTR) gene leading to an imbalance of the ion transport on epithelial surfaces.[2-4] Although CF is a multi-organ disease, progressive lung disease associated with airway mucus obstruction is the major cause of morbidity and mortality in CF patients.[5] In CF lung disease, the build-up of thick and sticky mucus in the airways provides a nidus for bacterial infections with *Pseudomonas aeruginosa* being the most abundant pathogen.[6,7] This contributes to chronic airway inflammation dominated by neutrophilic infiltrates associated with elevated concentrations of IL-1, IL-6, IL-8, and tumor necrosis factor (TNF)-α.[8] COPD is primarily caused by cigarette smoking and characterized by chronic bronchitis and emphysema. Small airway mucus obstruction due to inflammation-induced mucus overproduction contributes to airflow limitations in COPD and correlates with disease severity.[9] Bacterial and viral infection are often associated with exacerbations and disease progression.[10] Airway inflammation in COPD is diverse; increased numbers of activated macrophages and neutrophils as well as $CD8^+$ and $CD4^+$ (predominantly T helper (Th)1 and Th17) lymphocytes are found in sputum and bronchoalveolar lavage (BAL) fluid of patients with COPD, and at least in subgroups of patients a type 2 immune response with increased levels of eosinophils and Th2 cells is observed.[11] An emerging concept is that mucus obstruction can trigger sterile inflammation. In recent years efforts were undertaken to investigate neutrophilic inflammation in the absence of infection, as observed in children with CF and patients with COPD.[12-14] Mucus plugging was shown to cause cellular hypoxia due to necrosis of epithelial cells[15], which is a potent stimulus for sterile neutrophilic inflammation in muco-obstructed airways.[16,17] Further, inhaled non-microbial irritants, such as cigarette smoke, accumulate in adhesive mucus and induce sterile inflammation by activating resident macrophages and airway epithelial cells to release inflammatory mediators attracting circulating leukocytes into the lung.[18] In patients with asthma, obstruction of the conducting airways is driven by mucus plug formation and

smooth muscle contraction in response to stimuli such as allergens or cold air leading to airway hyperresponsiveness (AHR).[19,20] Postmortem studies identified airway mucus plugging as the principle cause of death that is highlighted in fatal asthma cases.[21,22] Allergic asthma is primarily characterized by type 2 airway inflammation, which is initiated by the airway epithelium serving as a target and potent effector tissue for pulmonary immune responses against allergens. Through pattern-recognition receptors that recognize pathogen- and damage-associated molecular patterns, airway epithelial cells get activated and release chemokines, growth factors, endogenous danger signals, and cytokines including IL-25, IL-33, and thymic stromal lymphopoietin (Tslp).[23] The alarmin IL-33 was reported to most potently stimulate Th2 cells and type 2 innate lymphoid cells (ILC2s) to secrete IL-4, IL-5, and IL-13.[24-26] These type 2 signature cytokines in turn promote the recruitment of eosinophils and alternatively activated macrophage differentiation.[24]

1.2 Mucus clearance system of the lung

In health, airways are covered by a thin airway surface liquid (ASL) layer that mediates effective mucociliary clearance (MCC). The ASL consists of two gel layers, a mobile mucus layer that traps environmental irritants, inhaled pathogens, and cellular debris, and beneath a periciliary layer (PCL).[27] To keep airways free of potentially inflammatory stimuli, the mucus together with entrapped particles is propelled by ciliary beating within the PCL toward the pharynx where it can be swallowed or expectorated by coughing. Button *et al.* demonstrated that a dense mesh of large membrane-bound mucins, tethered to cilia and epithelial cells, prevent a penetration of secreted mucins and deposited particles from the mucus layer into the PCL.[27] The mucus layer is a viscoelastic gel that consists of secreted mucins, globular proteins, ions, lipids, and water. Mucins are complex glycoproteins characterized by large molecular weight and high carbohydrate content that are mostly O-linked glycans.[28] Their ability to form polymers is critical for gel formation and thus viscoelastic properties of mucus.[28] The mucins are stored in a condensed form in granules. Upon exocytosis, they are hydrated and unpacked by ion exchange of Na^+ for Ca^{2+}, which is chelated by HCO_3^- on the apical airway surface.[29] The major secreted mucins of the respiratory tract are MUC5B and MUC5AC. MUC5B is constitutively expressed and predominantly produced by secretory cells of the submucosal glands, whereas MUC5AC is secreted by goblet cells lining the airway surface and its expression is more regulated.[28,30] The pulmonary clearance system requires a coordinated regulation of mucin synthesis and secretion, coordinated ciliary beating and appropriate ion transport for a proper hydration

status. The hydration of airway surfaces is determined by transepithelial ion transport pathways that are mainly mediated by Na^+ absorption across the apical plasma membrane mediated by the epithelial Na^+ channel ENaC and Cl^- secretion driven by CFTR and alternative Cl^- channels, such as TMEM16A and SLC26A9.[5,31] The fluid passively follows along the electrochemical gradient, thereby regulating the ASL height.

1.3 Abnormal mucus properties in CF, COPD, and asthma

Several pathologies lead to a failure of the pulmonary mucus clearance system resulting in airway mucus obstruction. Current concepts predict that hyperconcentrated mucus is a critical factor causing impaired MCC.[27] The mucus concentration can be measured as percent solids and was shown to correlate with the mucus osmotic pressure. A high solid content of the mucus layer (hyperconcentrated mucus) increases its osmotic pressure by drawing water from the PCL. Above a certain threshold, the mucus layer-related osmotic pressure exceeds the osmotic pressure of the PCL, which results in the compression of subjacent cilia, impaired ciliary beating and mucus adhesion to airway cells.[27,32] Button *et al.* suggest two scenarios that lead to impaired MCC as a result of hyperconcentrated mucus.[27] First, mucus dehydration due to a dysregulation of the ion transport across the airway epithelium causes ASL volume depletion, thereby increasing the concentration of secreted mucins. This is most apparent in airways from CF patients, where Cl^- secretion is impaired and Na^+ absorption is increased. Consequently, water is removed osmotically from the PCL creating a dehydrated airway surface, which results in highly viscous mucus and mucus adhesion. Second, excessive secretion of mucins triggered by a broad spectrum of inflammatory stimuli increases the mucus concentration and removes water from the PCL, thus slowing mucus clearance, which can end up in mucus stasis. Increased mucin expression is an issue in CF airways, but upregulated mucin expression occurs rather secondary to mucus plugging as a result of inflammation and bacterial infection. Studies from Henderson *et al.* indicate that in CF airways mucus obstruction is primarily caused by airway dehydration.[33] This is supported by recent *in vitro* data from Abdullah *et al.* showing that the failure of proper fluid secretion rather than abnormal inflammation-induced mucin secretion affects the formation of hyperconcentrated mucus in CF.[34] Another factor that alters mucus structure and impairs MCC is mucin crosslinking via disulfide bonds in response to oxidative stress, such as reactive oxygen species arising from airway inflammation.[35] Further, HCO_3^- deficiency in CF airways, due to a reduced CFTR-mediated HCO_3^- secretion, impairs proper mucin hydration by reduced Ca^{2+} chelation and contributes

to viscous mucus formation.[29] *In vitro* studies by Abdullah *et al*. indicate that airway dehydration rather than low HCO_3^- concentrations is the major determinant for defective mucin unfolding in CF.[36]

In COPD, the muco-obstructed phenotype is most likely driven by both mucin hypersecretion and airway dehydration. A recent study by Anderson *et al.* demonstrates that in patients with chronic bronchitis, mucus hyperconcentration is associated with impaired MCC and disease severity.[32] Emerging evidence suggests that cigarette smoke causes CFTR dysfunction and thus a reduced capacity to secrete fluid due to an ion transport imbalance.[31] Further, cigarette smoke can directly upregulate mucin expression via cigarette smoke-containing toxins, or indirectly by activation (e.g. through reactive oxygen species) of epithelial cells and innate immune cells, such as neutrophils and macrophages, which in turn produce mucin-inducing factors.[18,37-40] In addition, viral and bacterial infections contribute to mucus overproduction in COPD.[41,42]

Asthma has also been associated with impaired MCC[43,44] and airway mucus hypersecretion constitutes a typical pathophysiological feature of asthma.[45,46] It is well established that inflammatory cells and their mediators, such as IL-13, induce an increase in mucus-producing cells as well as mucin synthesis and secretion in asthmatic airways.[47] However, the relationship between hyperconcentrated mucus, reduced MCC, and mucin hypersecretion in asthma is not well known. Recent studies on the role of mucus composition and the functional properties of MUC5AC and MUC5B yielded new insights to this issue. Mucus composition in COPD and CF differs from that in asthma patients. In COPD, both mucins are upregulated[48], whereas increased MUC5B levels are characteristic for CF lung disease.[30] In asthmatic patients, gene expression for MUC5AC is increased in epithelial cells[49,50], and MUC5AC is the predominating mucin in sputum samples.[45,51,52] Recently it was observed that MUC5AC-rich mucus is tethered to airway epithelial cells, thereby making the mucus more adhesive[53], and Muc5ac-meditated mucus plugging is required for airway hyperresponsiveness in allergic airway diseases.[54] Further, Muc5ac is highly fucosylated, increasing mucus viscoelasticity and promoting mucus aggregation.[55] MUC5B levels remained stable in some asthma patients, but in most patients they were reduced and associated with pronounced eosinophilc inflammation.[45,49,51,56] Data by Dunican *et al.* indicate that mucin crosslinking due to eosinophil-driven oxidation contributes to mucus plug formation in asthma.[19] Of note, Roy *et al.* revealed the essential role of Muc5b for effective MCC in a mouse model[57], but whether a reduction in MUC5B contributes to mucus dysfunction in asthma is not known.

1.4 IL-13-mediated inflammation and muco-obstructive lung diseases

The type 2 signature cytokine IL-13 plays a central role in the pathogenesis of allergic airway inflammation and is increased in asthmatic patients.[56,58-61] Several studies demonstrated a contribution of type 2 inflammation with elevated IL-13 levels to chronic airway inflammation in CF and COPD.[62-66] Moreover, an increased type 2 immune response develops in patients with allergic bronchopulmonary aspergillosis (ABPA) that is a hypersensitivity reaction to the fungus *Aspergillus* occurring in patients with CF[6,67], COPD[68,69], and asthma[70,71]. Under conditions with overlapping clinical symptoms of asthma and COPD (asthma-COPD-overlap syndrome, ACOS), IL-13 effector function becomes even more relevant.[72-74] In airway inflammation IL-13 is predominantly produced by ILC2s and Th2 cells.[24,75] Mediated by the IL-4Rα/IL-13Rα1 receptor complex, IL-13 promotes subepithelial fibrosis, bronchial eosinophilic inflammation, activation of alternatively activated macrophages, AHR, and mucus overproduction (Figure 1).[76,77]

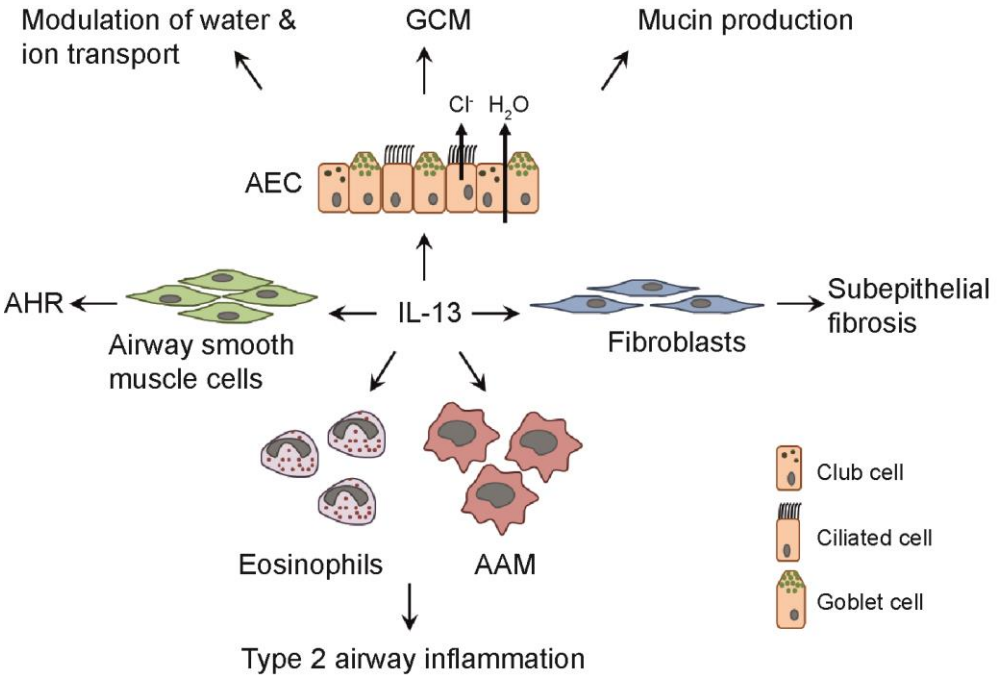

Figure 1. IL-13 effector functions in the lung. By acting on airway epithelial cells (AEC), IL-13 induces goblet cell metaplasia (GCM), mucin production, and Cl^- secretion. IL-13 activates fibroblasts and enhances extracellular collagen deposition causing subepithelial fibrosis. Recruitment of eosinophils and induction of alternatively activated macrophages (AAM) by IL-13 promotes type 2 airway inflammation. IL-13 induces proliferation and contraction of airway smooth muscle cells that triggers airway hyperresponsiveness (AHR). Modified from Gour *et al.*[78] and Oh *et al.*[79]

Despite sharing receptor components and regulatory pathways with IL-4, IL-13 possesses distinct effector functions in pulmonary inflammation independent of IL-4.[78] Kuperman *et al.* demonstrated that IL-13 is sufficient to induce AHR, goblet cell metaplasia, and mucin expression through direct interaction with airway epithelial cells.[77] Binding of IL-13 to the IL-4Rα/IL-13Rα1 receptor results in the activation of various transcription factors that are involved in mucus production (Figure 2). Induction of signal transducer and activator of transcription 6 (Stat6) activates expression of SAM pointed domain containing ETS transcription factor (Spdef).[80] Spdef inhibits forkhead box protein A 2 (Foxa2)[80], which is required for maintenance of normal differentiation of airway epithelial cells[81], allowing the induction of other genes important in goblet cell differentiation including Foxa3, chloride channel accessory 1 (Gob5), and transmembrane member 16A (TMEM16A).[82,83] The latter is a Ca^{2+}-activated Cl^- channel that was shown to be involved in Muc5ac expression[83] and mucin release from granules into the airway lumen.[84] Gob5 also induces *Muc5ac* expression via p38 mitogen-activated protein kinases (MAPK)-mediated signaling.[65]

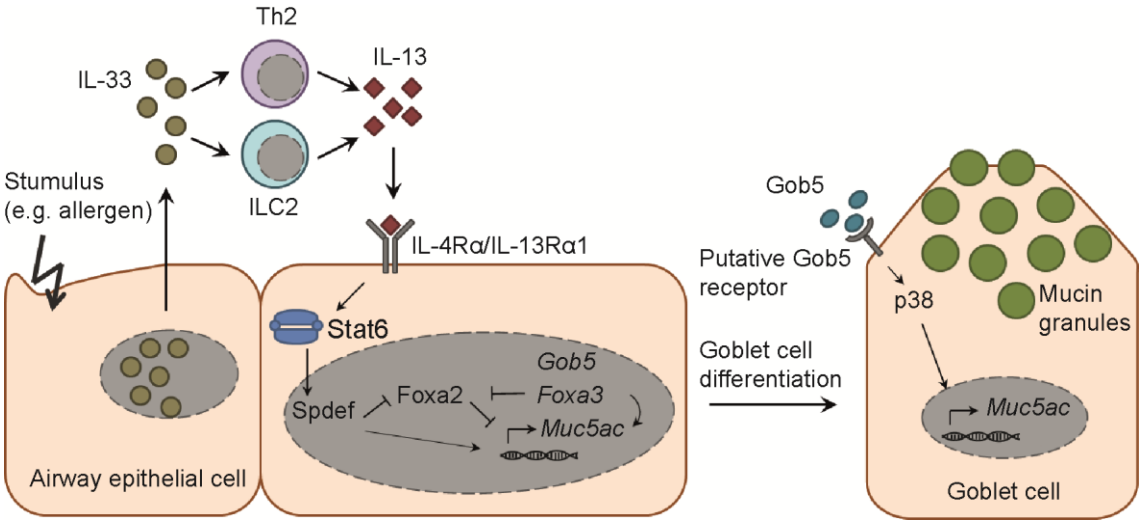

Figure 2. Mechanisms of IL-13-induced goblet cell metaplasia. Various stimuli (e.g. cell damage, inhaled allergens, respiratory viruses) induce the secretion of IL-33 by airway epithelial cells. As an alarmin, IL-33 is constitutively expressed and stored in the nucleus of airway epithelial cells. Upon release, IL-33 acts on Th2 cells and ILC2s, which then produce IL-13. IL-13 binds to the receptor complex IL-4Rα/IL-13Rα1 on airway epithelial cells leading to Stat6 activation. Stat6 hetero-dimers translocate to the nucleus and induce Spdef expression. Spdef inhibits Foxa2, which regulates normal airway epithelial differentiation, allowing the induction of genes associated with goblet cell differentiation including *Gob5*, *Foxa3*, and *Muc5ac*. Gob5 increases *Muc5ac* expression by activation of p38 MAPK via a putative Gob5 receptor. Mucin transcription is further induced by Foxa3. Mucin molecules are tightly packed in secretory granules within the goblet cell. Modified from Gour *et al.*[78] and Erle *et al.*[85]

The transcription factor FOXA3 was found to be elevated in goblet cells in tissue from COPD and asthma patients and can also be activated by IL-13, independent of SPDEF.[86] IL-13 is thought to decrease ciliary beat frequency, as shown in primary human nasal epithelial cells *in vitro*.[87] Further, IL-13 modulates the ion transport across the airway epithelium by mediating down-regulation of Na^+ absorption and up-regulation of Cl^- secretion, and by the induction of many genes encoding for ion channels and transporters, such as TMEM16A.[88-90] Recent data identified the alternative Cl^- channel Slc26a9 to be stimulated by IL-13 *in vivo* and a polymorphism in the SLC26A9 gene causing a reduced protein expression, was linked to asthma.[91]

1.5 Mouse models for muco-obstructive lung diseases

1.5.1 *Scnn1b*-Tg mouse model

The *Scnn1b*-Tg mouse mimics key pathologies of muco-obstructive lung diseases including CF, COPD, and asthma. In this mouse model, the β subunit of the epithelial Na^+ channel (βENaC, encoded by the *Scnn1b* gene) is constitutively overexpressed under control of the club cell secretory protein (CCSP) promoter. This leads to an airway-targeted exaggerated Na^+ and water absorption from the airway lumen causing ASL volume depletion, mucus hyperconcentration, and impaired MCC.[92] Consequently, *Scnn1b*-Tg mice exhibit airway mucus obstruction, GCM, reduced bacterial clearance, spontaneous chronic airway inflammation, and structural lung damage including alveolar wall destruction and airspace enlargement.[15,92-94] Longitudinal studies demonstrated that chronic airway inflammation in adult *Scnn1b*-Tg mice is predominantly neutrophilic, whereas at neonatal and juvenile ages inflammatory response is skewed towards type 2 immunity including increased levels of eosinophils, IL-13, and alternatively activated macrophages.[15,95] Moreover, Fritzsching *et al.* recently demonstrated that in juvenile *Scnn1b*-Tg mice eosinophilic inflammation, secretion of type 2 signature cytokines and AHR are aggravated due to impaired allergen clearance and type 2 biased immunity at the juvenile age.[95] These studies demonstrated that the phenotype of the *Scnn1b*-Tg mouse model shares key features of muco-obstructive lung disease in humans[96-98], and beyond this provides a model to investigate mediators of the type 2 immune response and to study muco-obstructive lung disease primarily triggered by airway surface dehydration.

1.5.2 *Il13*-Tg mouse model

Initially, Zhu *et al.* demonstrated that mice with airway epithelial-specific overexpression of IL-13 (under control of CCSP promoter) develop a phenotype that recapitulates many features of asthma.[76] The pathology of *Il13*-Tg mice is characterized by AHR and spontaneous type 2 airway inflammation including eosinophilia and increased levels of eotaxin, IL-4, and IL-5.[76,77] GCM and overproduction of mucus associated with upregulated expression of Muc5ac are also striking pathologic features of this mouse model, thereby mimicking muco-obstructive lung disease.[76,77] Further, *Il13*-Tg mice show transforming growth factor (TGF)-β-mediated subepithelial fibrosis and develop enhanced lung volume and pulmonary compliance mediated by IL-13-induced matrix metalloproteinases and cathepsin-dependent emphysema.[99,100]

1.6 Aim of the thesis

Based on preliminary data from our group in which IL-13 could be detected in the airway epithelium from juvenile *Scnn1b*-Tg mice, the first goal of the thesis was to elaborate these findings by analyzing IL-13 production in airway epithelial cells from juvenile WT and *Scnn1b*-Tg mice by immunohistochemistry and laser micro-dissection. Previous studies demonstrated that type 2 inflammation is exaggerated in response to allergen challenge in juvenile *Scnn1b*-Tg mice with impaired MCC.[95] To study if epithelial IL-13 production is also affected, WT and *Scnn1b*-Tg mice were treated with the natural aeroallergen *Aspergillus fumigatus* (Af) and epithelial IL-13 production was determined. To elucidate a signaling pathway of epithelial-mediated IL-13 production, studies in murine primary tracheal epithelial cells were performed.

The second goal was to investigate the relative contributions of airway surface dehydration and IL-13-induced mucin hypersecretion to the pathogenesis of airway mucus obstruction. To achieve this goal, the muco-obstructive phenotype of *Scnn1b*-Tg mice was compared to that of *Il13*-Tg mice. Further, *Scnn1b*-Tg mice lacking IL-13 expression (*Scnn1b*-Tg/*Il13*$^{-/-}$) were studied. The severity of mucus plugging, goblet cell numbers, mucin expression levels, mucociliary transport efficiency, and airway inflammatory cells were determined in these mouse models. *Il13*-Tg/*Il13*$^{-/-}$ mice were used to study the *in vivo* effect of airway epithelial cell-mediated IL-13. Finally, mice that exhibit both airway surface dehydration and mucin hypersecretion were analyzed (*Scnn1b*-Tg/*Il13*-Tg/*Il13*$^{-/-}$) to evaluate combined effects of these pathologic features.

2 Material and Methods

2.1 Experimental animals

All animal studies were approved by the local animal welfare authority "Regierungspräsidium Karlsruhe, Germany" (35-9185.81/G-26/14). *Scnn1b*-Tg mice were generated as previously described[92], maintained as heterozygous and studied on the C57BL/6N background. *Il13*$^{+/eGFP}$ mice were kindly provided by the laboratory of Dr A.N.J. McKenzie and backcrossed onto the C57BL/6N background, and referred to as *Il13*$^{+/-}$. *Il13*$^{eGFP/eGFP}$ mice were used as knockout mice[101] and referred to as *Il13*$^{-/-}$. CCSP-rtTA-*Il13*-Tg mice (originally generated by Dr J. Elias) were kindly provided by Dr H. Fehrenbach, maintained as heterozygous on the C57BL/6N background, and referred to as *Il13*-Tg. These mice were not exposed to doxycycline containing water, because gene expression analysis of *Il13* in lung homogenates demonstrated a leaky rtTA-mediated expression of the transgene even in the absence of doxycycline (Figure 3).[102]

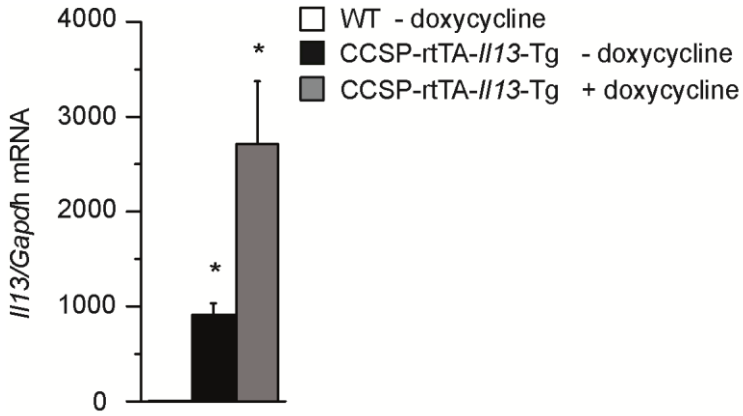

Figure 3. *Il13* expression in the absence of doxycycline in CCSP-rtTA-*Il13*-Tg mice. *Il13* levels in lung homogenates from WT mice and CCSP-rtTA-*Il13*-Tg mice exposed to normal water, and from CCSP-rtTA-*Il13*-Tg mice exposed to doxycycline containing water (1 mg/ml dissolved in 5 % sucrose) determined by real-time RT-PCR. n = 6–10 mice/group. *P < 0.05 compared with WT mice.

Scnn1b-Tg and *Il13*-Tg mice were intercrossed with *Il13*$^{-/-}$ mice to generate *Scnn1b*-Tg/*Il13*$^{+/-}$ and *Il13*-Tg/*Il13*$^{+/-}$ mice. Experimental animals were bred by intercrossing of *Scnn1b*-Tg/*Il13*$^{+/-}$ or *Il13*-Tg/*Il13*$^{+/-}$ mice with *Il13*$^{-/-}$ mice to obtain *Il13*$^{+/-}$, *Il13*$^{-/-}$, *Scnn1b*-Tg/*Il13*$^{+/-}$, *Scnn1b*-Tg/*Il13*$^{-/-}$, and *Il13*-Tg/*Il13*$^{+/-}$ and *Il13*-Tg/*Il13*$^{-/-}$ mice, respectively. This breeding strategy generated control groups heterozygous for the deletion of *Il13*, which are not expected to be different from wild-type mice.[103] To generate *Scnn1b*-Tg/*Il13*-Tg/*Il13*$^{-/-}$

mice, *Scnn1b*-Tg/*Il13*$^{-/-}$ mice were crossed with *Il13*-Tg/*Il13*$^{-/-}$ mice. *Stat6*$^{-/-}$ mice were backcrossed onto the C57BL/6N background (Jackson Laboratories, Bar Harbor, Me, USA). Mice were genotyped from tail biopsies by polymerase chain reaction (PCR) as previously described or as recommended by Jackson Laboratories.[76,92,103,104] Mice were either studied at neonatal (postnatal day (PND) 5.5) or juvenile (3–4 weeks old) ages. Littermates were used for all experiments. Mice were housed in a specific pathogen-free animal facility with a standard 12 hours day/night cycle at 22°C and had free access to food and water.

2.2 Aspergillus fumigatus instillation

To induce allergic airway inflammation, juvenile WT and *Scnn1b*-Tg mice were challenged by repeated sensitization with *Aspergillus fumigatus* (Af) extract (Hollister-Stier Laboratories, Spokane, WA, USA) according to a previously established protocol.[95] Mice were anesthetized with 3 % isoflurane (Baxter, Deerfield, Ill, USA) in oxygen, and 20 µl of Af (2 mg/ml) dissolved in 0.9 % NaCl (B. Braun, Melsungen, Germany), or equal volumes of vehicle (0.9 % NaCl) alone, were administered by means of intratracheal instillation every 48 hours for a period of 1 week. All endpoint studies were performed 24 hours after the last Af exposure.

2.3 Hypertonic saline treatment

For preventive hypertonic saline (HS) study, newborn *Il13*$^{-/-}$, *Scnn1b*-Tg/*Il13*$^{-/-}$, *Il13*-Tg/*Il13*$^{-/-}$, and *Scnn1b*-Tg/*Il13*-Tg/*Il13*$^{-/-}$ littermates were treated with 7 % HS directly after birth. 10 % NaCl (B. Braun, Melsungen, Germany) was dissolved in double distilled (dd) H_2O. Mice were anesthetized with 3 % isoflurane (Baxter, Deerfield, Ill, USA) in oxygen and treated with 7 % HS (1 µl/g body weight) by intranasal instillation 3 times per day for a period of 6 days.

2.4 IL-33 instillation

WT mice were anesthetized with 3 % isoflurane (Baxter, Deerfield, Ill, USA) in oxygen, and 20 µl of recombinant (r)IL-33 (5 µg; R&D Systems, Minneapolis, MN, USA) dissolved in 0.1 % bovine serum albumin (BSA) containing phosphate-buffered saline (PBS; Thermo Fisher Scientific, Darmstadt, Germany), or equal volumes of vehicle (0.1 % BSA in PBS) alone, were administered by means of intratracheal instillation every 48 hours for a period of 1 week. Endpoint studies were performed 24 hours after the last exposure.

2.5 Bronchoalveolar lavage and cytokine measurements

Juvenile mice were deeply anesthetized by intraperitoneal injection with ketamine (120 mg/kg) (Bremer Pharma, Warburg, Germany) and xylazine (16 mg/kg) (CP-Pharma, Burgdorf, Germany) and killed by exsanguination. The trachea was cannulated, the left main stem bronchus was ligated and right lobes were lavaged twice with sterile PBS (Thermo Fisher Scientific, Darmstadt, Germany) containing cOmplete Protease Inhibitor (Sigma-Aldrich, Taufkirchen, Germany) with a volume of 0.0175 ml/g body weight, as previously described.[95] For gene expression studies, right lobes were stored in RNAlater (Thermo Fisher Scientific, Darmstadt, Germany) at -80°C. For histological analysis, left lobes were left in 4 % buffered formalin overnight at 4°C, followed by a washing step with PBS and transferred to 70 % ethanol (Carl Roth, Karlsruhe, Germany) for longtime storing at 4°C. BAL fluid was centrifuged at 300 x *g* for 5 minutes at 4°C (Eppendorf, Wesseling-Berzdorf, Germany), the supernatant was stored at -80°C and subsequently used to determine the concentrations of IL-4, IL-5, and IL-13 by using the cytometric bead array enhanced sensitivity flex set (BD Biosciences, Heidelberg, Germany), according to the manufacturer's instructions. Flow cytometry was performed with cells from BAL fluid as described in section 2.6.

2.6 Flow cytometry

For isolation of leukocytes from BAL fluid, cells were transferred to 5-ml polystyrene round-bottom tubes (BD Biosciences, Heidelberg, Germany), 500 µl PBS and 2 ml 1.5 % sputolysin (Merck, Darmstatdt, Germany) diluted in nuclease-free H_2O was added and thoroughly vortexed to separate cells from mucus. After incubation of 15 minutes at room temperature, cells were washed 2 times by adding fluorescence-activated cell sorting (FACS) buffer, containing PBS supplemented with 1 % inactivated fetal bovine serum (FBS) (Thermo Fisher Scientific, Darmstadt, Germany) and 0.09 % sodium azide (Sigma-Aldrich, Taufkirchen, Germany) and centrifuged at 300 x g for 5 minutes at 4°C. Subsequently, cells were resuspended in FACS buffer and total cell numbers as well as viability were assessed in Neubauer counting chambers (Karl Hecht, Sondheim v. d. Rhön, Germany) by using the trypan blue exclusion test. Cell suspension was incubated with 1 µl FcBlock (BD Biosciences, Heidelberg, Germany) for 5 minutes at room temperature, followed by cell surface staining with 50 µl master mix of specific monoclonal fluorochrome-conjugated antibodies (Table 1) or respective isotype control antibodies for 30 minutes at 4°C in the

dark. Immediately after cellular staining flow cytometry was performed using a LSRFortessa flow cytometer (BD Biosciences, Heidelberg, Germany). After exclusion of debris, nonviable cells, and doublets, data were analyzed with FACSDiva software (v8.0.1; BD Biosciences, Heidelberg, Germany). BAL cells were characterized as follows: $CD4^+$ T cells ($CD3^+$, $CD4^+$, $F4/80^-$, and $CD11c^-$), neutrophils ($CD11b^+$, $Gr1^+$, $CD3^-$, and $F4/80^-$), eosinophils (Siglec-F^+, $CD11b^+$, $CD11c^-$, $Gr1^-$, and $CD3^-$), airway macrophages (AMs) (Siglec-F^+, $CD11c^+$, $MHCII^{mid}$, $F4/80^+$, $CD3^-$).

Table 1. Antibody master mix for the detection of leukocytes from BAL fluid by flow cytometry.

Antibody	Clone	Fluorophore	Supplier	Dilution
CD3e	500A2	V500	BD Biosciences	1:50
CD4	RM4-5	Fluorescein isothiocyanate (FITC)	Thermo Fisher	1:50
CD11b	M1/70	Brilliant violet (BV) 605	Biozol*	1:100
CD11c	HL3	Phycoerythrin (PE)- cyanine (Cy) Cy7	BD Biosciences	1:200
CD206	MR5D3	PE	Bio-Rad*	1:20
CD301	ER-MP23	Alexa Fluor 647	Bio-Rad	1:20
F4/80	BM8	Allophycocyanin (APC)-Cy7	Biozol	1:100
Gr1	RB-8C5	Peridinin-chlorophyll-protein complex (PerCP)- Cy 5.5	Thermo Fisher	1:50
MHCII	M5/114.15.2	eFluor 450	Thermo Fisher	1:400
Siglec-F	E50-2440	PE-CF594	BD Biosciences	1:50

*Biozol, Eching, Germany; Bio-Rad, Dreieich, Germany

2.7 Histology and morphometry

2.7.1 Tissue embedding and sectioning

Before paraffin embedding, left lobes were transversally cropped at the apical part. Tissue was dehydrated in embedding cassettes (Steinbrenner Laborsysteme, Wiesenbach, Germany) by ascending ethanol series (2 x 30 minutes 96 %, 2 x 45 minutes 100 %) (Carl Roth, Karlsruhe, Germany), cleared in xylene (Carl Roth, Karlsruhe, Germany) overnight, infiltrated with paraffin (Carl Roth, Karlsruhe, Germany) by applying vacuum for 2 hours, followed by 1 hour of atmospheric pressure, and finally embedded with the cropped surface facing downwards to ensure correct orientation of the tissue. Paraffin sections of 1.5 µm and 5 µm thickness were prepared with a microtome (Leica Microsystems, Nussloch, Germany).

Left lobes were sectioned transversally at the level of the proximal intra-pulmonary main axial airway near the hilus.

2.7.2 Histology

Before staining, sections were deparaffinized 2 x 10 minutes in xylene (Carl Roth, Karlsruhe, Germany), rehydrated by descending alcohol series (2 x 5 minutes 100 %, 2 x 3 minutes 96 %, 2 minutes 70 %) (Carl Roth, Karlsruhe, Germany), and finally rinsed in ddH_2O.
For mucus measurements and goblet cell counts, Alcian blue periodic acid-Schiff (AB-PAS) staining was performed on 5 µm and 1.5 µm sections of left lobe. Sections were immersed in Alcian blue solution containing 3 % acetic acid (Carl Roth, Karlsruhe, Germany), 1 % Alcian Blue 8GX (Sigma-Aldrich, Taufkirchen, Germany), and 1 crystal of Thymol (Sigma-Aldrich, Taufkirchen, Germany) for 30 minutes and subsequently rinsed in tab water for 2 minutes. After staining with 0.5 % periodic acid solution (Sigma-Aldrich, Taufkirchen, Germany) for 5 minutes, sections were rinsed 3 x in ddH_2O, followed by Schiff's reagent (Sigma-Aldrich, Taufkirchen, Germany) for 15 minutes and 1 minute in sulfur solution containing 1 % 5 M HCl (Merck, Darmstadt, Germany), 0.6 % sodium metabisulfit (Sigma-Aldrich, Taufkirchen, Germany), and subsequently rinsed in tab water. Finally, AB-PAS-stained sections were immersed in 96 % ethanol for 1 minute, 2 x 1 minute in 100 % ethanol, cleared in xylene for 3 minutes, and mounted with permanent mounting medium (Sigma-Aldrich, Taufkirchen, Germany).

2.7.3 Immunohistochemisty

To localize IL-13, immunohistochemical staining was performed on formalin-fixed, paraffin-embedded 1.5 µm lung sections of the left lobe by using a polyclonal goat anti-mouse IL-13 antibody (R&D Systems, Minneapolis, MN, USA) at a dilution of 1:1000. Unstained and hydrated paraffin sections were pretreated for 10 minutes with 3 % hydrogen peroxide, rinsed 3 x 2 minutes in PBS, followed by antigen retrieval with Citra plus buffer (BioGenex, San Ramon, CA, USA) and incubation with a nonspecific protein-blocking solution containing animal serum (Vector Laboratories, Burlingame, CA, USA) for 30 minutes. Tissue sections were incubated overnight at 4°C with the primary antibody. After washing with PBS, slides were incubated with a biotinylated rabbit anti-goat IgG antibody as secondary antibody for 30 minutes at room temperature. Immunoreactivity of IL-13 was visualized with Vectastain Elite Kit ABC Reagent (Vector Laboratories, Burlingame, CA, USA) according to the manufacturer's instructions, followed by 3, 3'-diaminobenzidine (DAB) substrate kit

(Vector Laboratories, Burlingame, CA, USA) for 3 minutes. As a negative control, each experiment included lung sections stained with secondary antibody only. Sections were counterstained with hematoxylin (Sigma-Aldrich, Taufkirchen, Germany) for 5 seconds, dehydrated, cleared and mounted.

2.7.4 Morphometry

For morphometric measurements, images were captured with an Olympus IX-71 microscope (Olympus, Hamburg, Germany) and analyzed by using Cell F analysis software (OSIS, Münster, Germany).

Goblet cells and IL-13$^+$ cells were determined in 1.5 µm lung sections from the left lobe stained with AB-PAS or anti-IL-13 antibody/DAB substrate, respectively, and identified by the presence of intracellular AB-PAS-positive and DAB-positive material. Numeric densities were quantified by counting the number of goblet cells and IL-13$^+$ cells per millimeter of the basement membrane.

Airway mucus content was determined on 5 µm AB-PAS-stained sections by using a defined threshold for the AB-PAS-positive material in the airway related to the area of the airway, which was derived from the length of the luminal membrane of the airway epithelium. This ratio was then normalized to the surface area per unit volume, as previously described.[15,105,106] Semi-quantitative assessment of airway mucus obstruction was determined by scoring for the absence or presence of intraluminal mucus accumulation, as defined by AB-PAS-positive material taking up ≥ 10 % of the cross-sectional area of the airway lumen.[91]

2.8 Laser micro-dissection

Juvenile mice were deeply anesthetized by intraperitoneal injection with ketamine (120 mg/kg) (Bremer Pharma, Warburg, Germany) and xylazine (16 mg/kg) (CP-Pharma, Burgdorf, Germany) and killed by exsanguination. The trachea was cannulated, the left main stem bronchus was ligated and right lobes were inflated with tissue-tek O.C.T. compound (Sakura Finetek, Torrance, CA, USA) diluted in PBS (1:1). The right superior lobes were embedded in Peel-A-Way Embedding Molds (Polysciences Europe, Eppelheim, Germany) containing tissue-tek O.C.T. compound, and subsequently frozen in liquid nitrogen. Lobes were sectioned transversally at 10 µm thickness with a cryostat CM1950 (Leica, Wetzlar, Germany) and mounted on MembraneSlides 1.0 PEN (Zeiss, Jena, Germany). Airway epithelium was identified by light microscopy, micro-dissected and catapulted in an adhesive

cap of a microfuge tube (Zeiss, Göttingen, Germany) using the MicroBeam system (PALM Microlaser Technologies, Bernried, Germany) consisting of a 337 nm nitrogen laser integrated in an inverted microscope (Axiovert 200, Zeiss, Göttingen, Germany).

2.9 Mucociliary clearance

Mucociliary clearance was determined by measuring the elimination of fluorochrome-labeled Af after intratracheal instillation, as previously described.[95] In brief, Af extract (Hollister-Stier Laboratories, Spokane, WA, USA) was labeled with Alexa Fluor 647 Microscale Protein Labeling Kit (Thermo Fisher Scientific, Darmstadt, Germany), according to the manufacturer's instructions. By intratracheal instillation, 2.5 µg of Alexa Fluor 647-labeled Af dissolved in 20 µl PBS was administered in WT, *Scnn1b*-Tg, and *Il13*-Tg mice after anesthesia with 3 % isoflurane (Baxter, Deerfield, Ill, USA) in oxygen. Either immediately (t = 0) or 1 hour after instillation mice were deeply anesthetized with intraperitoneal injections of ketamine (120 mg/kg) (Bremer Pharma, Warburg, Germany) and xylazine (16 mg/kg) (CP-Pharma, Burgdorf, Germany) and sacrificed by exsanguination. Lungs and tracheae were excised *en bloc* and homogenized in 500 µl PBS with a tissue homogenizer (IKA, Staufen, Germany). Fluorescence intensity was measured in a plate reader (Perkin Elmer, Waltham, MA, USA) and the percentage of clearance after 1 hour was calculated as follows: (1 - Fluorescence intensity at t = 1 hour / Fluorescence intensity at t = 0) x 100. Baseline (t = 0) fluorescence intensity did not differ between WT, *Scnn1b*-Tg, and *Il13*-Tg mice.

2.10 *Ex vivo* micro-computed tomography

To visualize pulmonary alterations of the whole lung, *ex vivo* micro-computed tomography (µ-CT) imaging was performed. Lungs were fixed by vasculature perfusion as previously described.[107] Mice were deeply anesthetized with intraperitoneal injections of ketamine (120 mg/kg) (Bremer Pharma, Warburg, Germany) and xylazine (16 mg/kg) (CP-Pharma, Burgdorf, Germany). To preserve airway mucus in its original location, tracheae of euthanized neonatal mice were tied to reserve the residual volume of air in the lungs, and no positive airway pressure was applied to inflate the lungs. The chest was opened and thymus and ribs were removed making the heart accessible for perfusion. The right ventricle was cannulated with a 22 G angiocatheter (Hospira, München, Germany) and the left atrium was cut for drainage. Lungs were perfused with Ringer solution (B. Braun, Melsungen, Germany) containing 5 % dextran 70 (Carl Roth, Karlsruhe, Germany), 0.02 % procaine

(Jenapharm, Jena, Germany) and 5 IU/ml heparin (Ratiopharm, Ulm, Germany) for 15 minutes to prevent blood clotting and to ensure vasodilation for homogeneous perfusion. For fixation, lungs were perfused with fixative solution containing ddH_2O supplemented with 25 % polyethylene glycol (Carl Roth, Karlsruhe, Germany), 10 % ethanol (Carl Roth, Karlsruhe, Germany) and 3.7 % formaldehyde (AppliChem, Darmstadt, Germany) for 30 minutes under a constant pressure of 20 cm. Lungs were removed and further processed using an osmium impregnation technique, as previously described.[108]

Imaging of explanted lungs was performed with a Bruker SkyScan 1176 µ-CT using the following acquisition settings, resulting in an acquisition time of 1.75 hours: 50 kV_p tube potential, 0.5 mm aluminum filtration, 500 µA tube current, 0.2° rotation step size over a full rotation of 360°, and detector pixel size of 8.65 µm (spatial resolution) applying a frame averaging of 5. Volume image data (897 slices of 1812×1812 pixels² each) were reconstructed with NRecon (v1.7.0.4; Bruker BioSpin, Rheinstetten, Germany) and analyzed with CTVox (v3.2.0; Bruker BioSpin) software.

Based on µ-CT image data, atelectasis and mucus plugging were graded semi-quantitatively on a 0 to 2 scale (0 = no, 1 = mild, 2 = severe) for each airway segment using an adapted mouse airway nomenclature suggested by Thiesse *et al*.[109] Airways in atelectatic areas were scaled with a score of 2 because mucus cannot be differentiated from atelectatic regions by µ-CT imaging.

2.11 Murine primary tracheal epithelial cell cultures

Mice were deeply anesthetized via intraperitoneal injection of ketamine (120 mg/kg) (Bremer Pharma, Warburg, Germany) and xylazine (16 mg/kg) (CP-Pharma, Burgdorf, Germany), killed via exsanguination and tracheae were removed. Isolation and culture of primary murine tracheal epithelial cells was performed according to Mayer *et al*.[110] Tracheae of 6–10-week-old mice were excised, cut open and transferred to collection medium containing DMEM/F-12 (1:1) (Thermo Fisher Scientific, Darmstadt, Germany) and 1 % Penicillin-Streptamycin (Thermo Fisher Scientific, Darmstadt, Germany). Tracheae were washed in PBS, transferred to 20 ml dissociation medium containing PBS (Thermo Fisher Scientific, Darmstadt, Germany) supplemented with 1.4 mg/ml Protease E (Sigma-Aldrich, Taufkirchen, Germany), 0.1 mg/ml DNase I (Sigma-Aldrich, Taufkirchen, Germany), 72 mg $NaHCO_3$, 0.1 µl FeN_3O_9, 0.2 µl Sodium Pyruvate (100 mM), and 0.6 % Penicillin-Streptamycin and incubated overnight at 4°C. After incubation for 1 hour at 37°C, 5 ml heat-inactivated FBS (Thermo Fisher Scientific, Darmstadt, Germany) was added to stop

enzymatic digestion. The cell suspension was filtered through a 100 µm cell strainer (Sigma-Aldrich, Taufkirchen, Germany), centrifuged 10 minutes at 1300 rpm, resuspended in DMEM/F-12 (1:1) medium supplemented with heat-inactivated FBS, insulin (human recombinant zinc) (Thermo Fisher Scientific, Darmstadt, Germany) and primocin (InvivoGen, Toulouse, France) and incubated at 37°C for 2 hours to separate adherent non-epithelial cells (fibroblasts). Epithelial cells were seeded on collagen IV-coated (0.5 mg/ml type IV placenta collagen diluted in 0.2 % acetic acid (Sigma-Aldrich, Taufkirchen, Germany)) transwell filters (Corning, Glendale, NY, USA). On day two of culture, medium of the apical surface was removed to establish air-liquid interface (ALI) conditions (Figure 4) for the purpose of resembling very closely *in vivo* conditions of the lung.

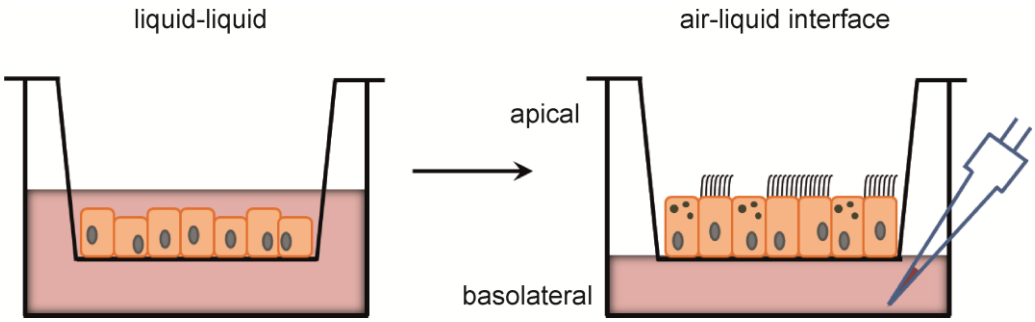

Figure 4. Murine primary tracheal epithelial cell cultures. Isolated cells were seeded and cultured under submerged conditions (left). After two days, air-liquid interface (ALI) conditions (right) were established, and substances were added to the basolateral site when cells reached confluence.

After reaching confluence, cells were treated with the substances as listed in Table 2 by adding to the basolateral side. For pharmacological inhibition study, ALI cultures were pre-incubated with anti-suppression of tumorigenicity 2 (St2) antibody, the myeloid differentiation primary-response protein 88 (MyD88) inhibitory peptide Pepinh-MYD, or the p38 MAPK inhibitor SB203580 as listed in Table 2, and subsequently stimulated with rIL-33 (10 ng/ml) for 3 hours. For the wound assay, circular wounds were made in confluent cell layer using 20 µl pipette tips (4 wounds per well).

Table 2. Substances and conditions used for treatment of murine primary tracheal epithelial cell cultures.

Treatment	Concentration	Incubation	Supplier
rIL-1α	100 ng/ml	24 h	R&D systems
rIL-4	10 ng/ml	24 h	R&D systems
rIL-9	10 ng/ml	24 h	R&D systems
rIL-13	10 ng/ml	24 h	R&D systems
rIL-33	0.025–100 ng/ml	24 h	R&D systems
rThymic stromal lymphopoietin (Tslp)	10 ng/ml	24 h	R&D systems
Aspergillus fumigatus	0.1–1 mg/ml	24 h	Hollister-Stier
Ionomycin	1 µg/ml	4 h	Sigma-Aldrich
Lipopolysaccharide (LPS)	0.001–1 µg/ml	24 h	Sigma-Aldrich
Wound assay		24 h	
Anti-St2 antibody	30 µg/ml	1 h	R&D systems
Pepinh-MYD	50 µM	6 h	InvivoGen
SB203580	20 µM	1 h	InvivoGen

2.12 RNA extraction and real time RT-PCR

2.12.1 RNA extraction and RT-PCR

Total RNA was isolated from lung tissue or from cell cultures. First, lung tissue was homogenized with a tissue homogenizer (IKA, Staufen, Germany) and murine primary tracheal epithelial cultures were washed with PBS. Total RNA was extracted by using the RNeasy Plus Mini Kit (Qiagen, Hilden, Germany) according to the manufacturer's protocol. Total RNA from micro-dissected tissue was isolated using the RNeasy Micro Kit (Qiagen, Hilden, Germany). Before extraction, micro-dissected samples were incubated in the provided lysis buffer for 30 minutes at room temperature, centrifuged at 12000 rpm for 5 minutes and proceeded according to the manufacturer's protocol. The cDNA was synthesized by reverse transcription (RT) of 1 µg of total RNA from lung homogenate and 10 µl total RNA from micro-dissected tissue and primary tracheal epithelial cells (Superscript III RT; Thermo Fisher Scientific, Darmstadt, Germany).

2.12.2 Real-time PCR

Real-time PCR was performed on an Applied Biosystems 7500 Real Time PCR System using TaqMan universal PCR master mix and inventoried TaqMan gene expression assays for β-Actin (*Actb)* (Mm00607939_s1), *Gapdh* (NM_008084.2), *Gob5* (Mm01320697_m1), *Il13* (Mm00434204_m1), *Il33* (Mm00505403_m1), *Muc5ac* (Mm01276718_m1), *Muc5b* (Mm00466391_m1), *Foxa3* (Mm00484714_m1) and *Spdef* (Mm00600221_m1) according to the manufacturer's instructions (Thermo Fisher Scientific, Darmstadt, Germany). For relative quantification, the relative fold changes of target gene expression were determined from the efficiency of the PCR reactions and the crossing point deviation between samples from the different genotypes in relation to WT vehicle-treated, *Il13*$^{+/-}$, or *Il13*$^{-/-}$ mice, as appropriate, and normalized to the expression of the reference gene *Actb* (or *Gapdh* as for Figure 3) as previously described.[111]

For micro-dissected airway epithelium, target sequences were preamplified before quantitative PCR using Platinum Taq DNA Polymerase (Thermo Fisher Scientific, Darmstadt, Germany) and the intron-spanning primers as listed in Table 3.

Table 3. Sense and antisense primers used for preamplification.

Gene		Sequence 5' → 3'
Il13	sense	5'-CTG TGT CTC TCC CTC TGA CCC-3'
	antisense	5'-CCA GGG CTA CAC AGA ACC CG-3'
Il33	sense	5'-ACA CAT TGA GCA TCC AAG GAAC-3'
	antisense	5'-AAG AAG GCC TGT TCC GGA GG-3'
Actb	sense	5'-AGA TCA AGA TCA TTG CTC CTC CT-3'
	antisense	5'-TGC TCC AAC CAA CTG CTG TC-3'

2.12.3 Generation of plasmid standards for real-time PCR

For absolute quantification of *Muc5ac* and *Muc5b* transcripts, copy numbers were calculated using a plasmid DNA standard curve. Intron-spanning primer pairs as listed in Table 4 were designed for *Muc5ac* and *Muc5b*, and target sequences were amplified with Platinum *Pfx* DNA Polymerase (Thermo Fisher Scientific, Darmstadt, Germany). PCR products were verified by gel electrophoresis and cloned into pCR-Blunt-II-TOPO vector using the Zero Blunt TOPO PCR Cloning Kit (Thermo Fisher Scientific, Darmstadt, Germany) according to the manufacturer's instructions. Recombinant vectors were transformed into chemically

competent *Escherichia coli* (One Shot TOP10, Thermo Fisher Scientific, Darmstadt, Germany) and transformations were spread on selective Luria-Bertani (LB) plates containing 50 µg/ml kanamycin (Carl Roth, Karlsruhe, Germany) and incubated overnight at 37°C. Picked colonies were cultured in culture tubes (Sarstedt, Nümbrecht, Germany) in kanamycin supplemented LB medium overnight at 200 rpm and 37°C. DNA plasmids were isolated with QIAprep Spin Miniprep Kit (Qiagen, Hilden, Germany) according to the manufacturer's instructions, followed by restriction digest (TatI, Thermo Fisher Scientific, Darmstadt, Germany) to confirm presence of inserts. After amplification with Platinum *Pfx* DNA Polymerase, a standard curve was prepared for *Muc5ac* and *Muc5b* and real-time PCR was performed as described above. Total copy numbers were calculated from the standard curve and then normalized to levels of *Actb*.

Table 4. Sense and antisense primers used for amplifiction of *Muc5ac* and *Muc5b*.

Gene		Sequence 5' → 3'
Muc5ac	sense	5'-CTG GAA GGA TGC TAT CCC AAG-3'
	antisense	5'-GCA GCC TCC TAT GCC ATC TG-3'
Muc5b	sense	5'-TGG AGA ATG AGA ACT TCG CCC-3'
	antisense	5'-AAG TAG CCC TTG GTT TGG GG-3'

2.13 Statistics

Data were derived from at least 3 independent experiments and were analyzed with SigmaPlot version 12.5 (Systat Software, Erkrath, Germany) and presented as mean ± SEM Statistical analysis were performed with one-way ANOVA, Tukey's post hoc test, Kruskal-Wallis ANOVA, Dunn's post hoc test, unpaired Student's *t*-test, Fisher's exact test, and Kaplan-Meier, as appropriate. $P < 0.05$ was accepted to indicate statistical significance.

3 Results

3.1 Airway epithelial cells express IL-13

Previous studies from our group demonstrated that juvenile *Scnn1b*-Tg mice with impaired MCC produce spontaneous transient type 2 airway inflammation including airway eosinophilia and elevated IL-13 levels that is exaggerated after allergen exposure.[15,95] Among leukocytes, ILC2 and Th2 cells were identified to provide sources of IL-13 in juvenile *Scnn1b*-Tg mice.[95] During airway disease the airway epithelium serves as an effector tissue for IL-13[23], but it also acts as a source of inflammatory mediators. If the airway epithelium itself produces IL-13 is not well studied. A few studies reported an IL-13 production by airway epithelial cells and preliminary data from our group indicated that the airway epithelium might contribute to the IL-13 production in *Scnn1b*-Tg mice.[112-116] However, recent data are not completely solid and stimuli inducing IL-13 in airway epithelial cells are not well known. To study an epithelial IL-13 production, protein and mRNA expression was analyzed in the airway epithelium from juvenile WT and *Scnn1b*-Tg mice, and *in vitro* studies were performed to elucidate the underlying signaling pathway. To analyze if allergen exposure fosters IL-13 production in airway epithelial cells, a previously established *Aspergillus fumigatus* challenge model was used.[95]

3.1.1 Type 2 airway inflammation in juvenile naïve and Af-challenged *Scnn1b*-Tg mice

Previous studies demonstrated that impaired mucus clearance exacerbates allergen-induced type 2 airway inflammation in juvenile *Scnn1b*-Tg mice.[95] To study whether airway epithelial cells produce IL-13 and contribute to elevated IL-13 levels in allergen-induced type 2 airway inflammation, 3–4-week-old WT and *Scnn1b*-Tg mice were challenged with intratracheal applications of the natural aeroallergen Af or vehicle alone. To characterize allergen-induced airway inflammation, the inflammatory cell counts and levels of the type 2 cytokines IL-4, IL-5, and IL-13 were measured in BAL fluid by flow cytometry. In WT mice short-term Af treatment induced a moderate increase in macrophage and neutrophil counts (Figure 5A), elevated concentrations of IL-5 and IL-13 (Figure 6B, C), and no change in eosinophil counts or in the alternatively activated phenotype of airway macrophages (Figure 5B, C). In unchallenged *Scnn1b*-Tg mice, eosinophil and CD4 T cell counts (Figure 5A), and IL-4, IL-5, and IL-13 levels (Figure 6) were spontaneously elevated. After Af exposure

airway eosinophilia and cytokine concentrations were significantly increased compared to vehicle-treated *Scnn1b*-Tg mice (Figure 5 and Figure 6).

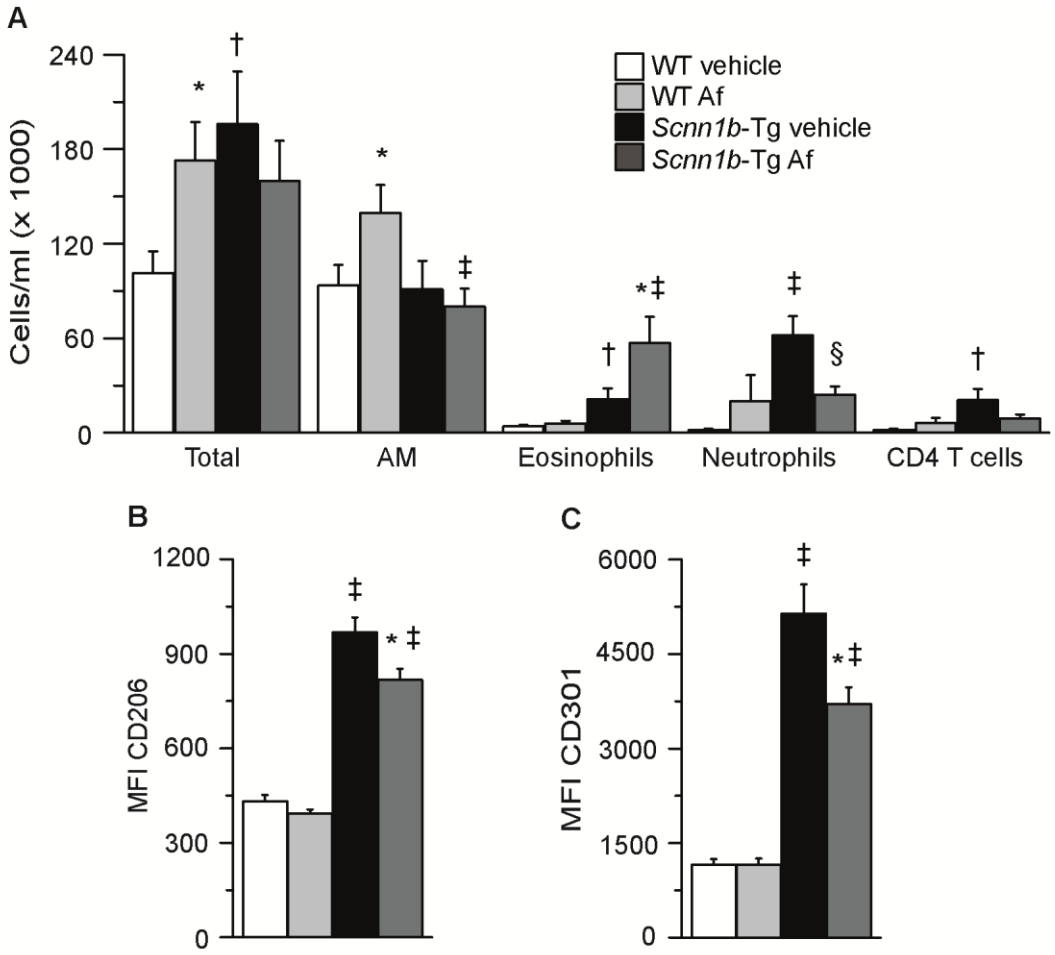

Figure 5. Spontaneous and exaggerated allergen-induced airway inflammation in juvenile *Scnn1b*-Tg mice. (**A–C**) Juvenile WT and *Scnn1b*-Tg mice were challenged with Af or vehicle alone. (**A**) Inflammatory cell counts in BAL fluid (Airway macrophages [AM]) determined by flow cytometry. n = 18–23 mice for each group. (**B, C**) Mean fluorescence intensity (MFI) of $CD206^+$ (**B**) and $CD301^+$ (**C**) AM in BAL fluid. n = 15–20 mice for each group. *P < 0.05, §P < 0.01 compared to vehicle-treated mice of the same genotype, †P < 0.05, ‡P < 0.01 compared with mice with the same treatment but different genotype.

Further, Af- and vehicle-treated *Scnn1b*-Tg mice exhibited alternatively activated airway macrophages, as shown by an up-regulated expression of CD206 and CD301 (Figure 5B, C) that is in line with increased IL-4 and IL-13 levels in *Scnn1b*-Tg mice (Figure 6). Taken together, these data confirm spontaneous and exaggerated allergen-induced type 2 airway inflammation associated with increased type 2 cytokine production in juvenile *Scnn1b*-Tg mice.

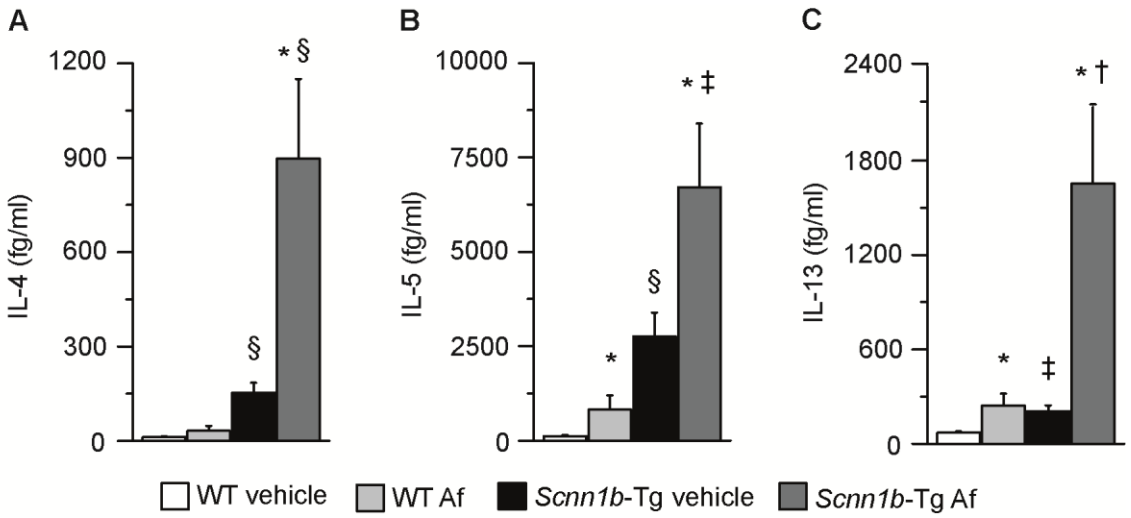

Figure 6. Exaggerated type 2 cytokine concentrations after allergen exposure in juvenile *Scnn1b*-Tg mice. (**A–C**) Juvenile WT and *Scnn1b*-Tg mice were challenged with Af or vehicle alone. IL-4 (**A**), IL-5 (**B**) and IL-13 (**C**) concentrations in BAL fluid measured by cytometric bead array. n = 9–11 mice for each group. *P < 0.05 compared with vehicle-treated mice of the same genotype, †P < 0.05, ‡P < 0.01, and §P < 0.001 compared to mice with the same treatment but different genotype.

3.1.2 Airway epithelial cells are a cellular source of IL-13 in naïve and Af-challenged *Scnn1b*-Tg mice

To determine if epithelial cells express IL-13, immunohistochemistry was performed for the detection of IL-13 protein in lung sections from juvenile WT and *Scnn1b*-Tg mice challenged with Af or vehicle alone. Results were confirmed by determining *Il13* transcript levels in micro-dissected airway epithelium. In naïve and Af-challenged WT mice, a few IL-13$^+$ cells were counted (Figure 7A, B); however, *Il13* transcripts were not detectable in WT mice (Figure 7C). In contrast, a distinct IL-13-positive staining was observed in epithelial cells from the conducting airways in Af- and vehicle-treated *Scnn1b*-Tg mice (Figure 7A, B) that was confirmed by *Il13* levels in micro-dissected tissue (Figure 7C). After Af challenge, the number of IL-13$^+$ cells and levels of *Il13* transcripts tended to be increased in *Scnn1b*-Tg mice, however, this trend did not reach statistical significance. Taken together, these results demonstrate that airway epithelial cells are a source of IL-13, and that IL-13 production is increased in spontaneous and allergen-induced type 2 airway inflammation in juvenile *Scnn1b*-Tg mice.

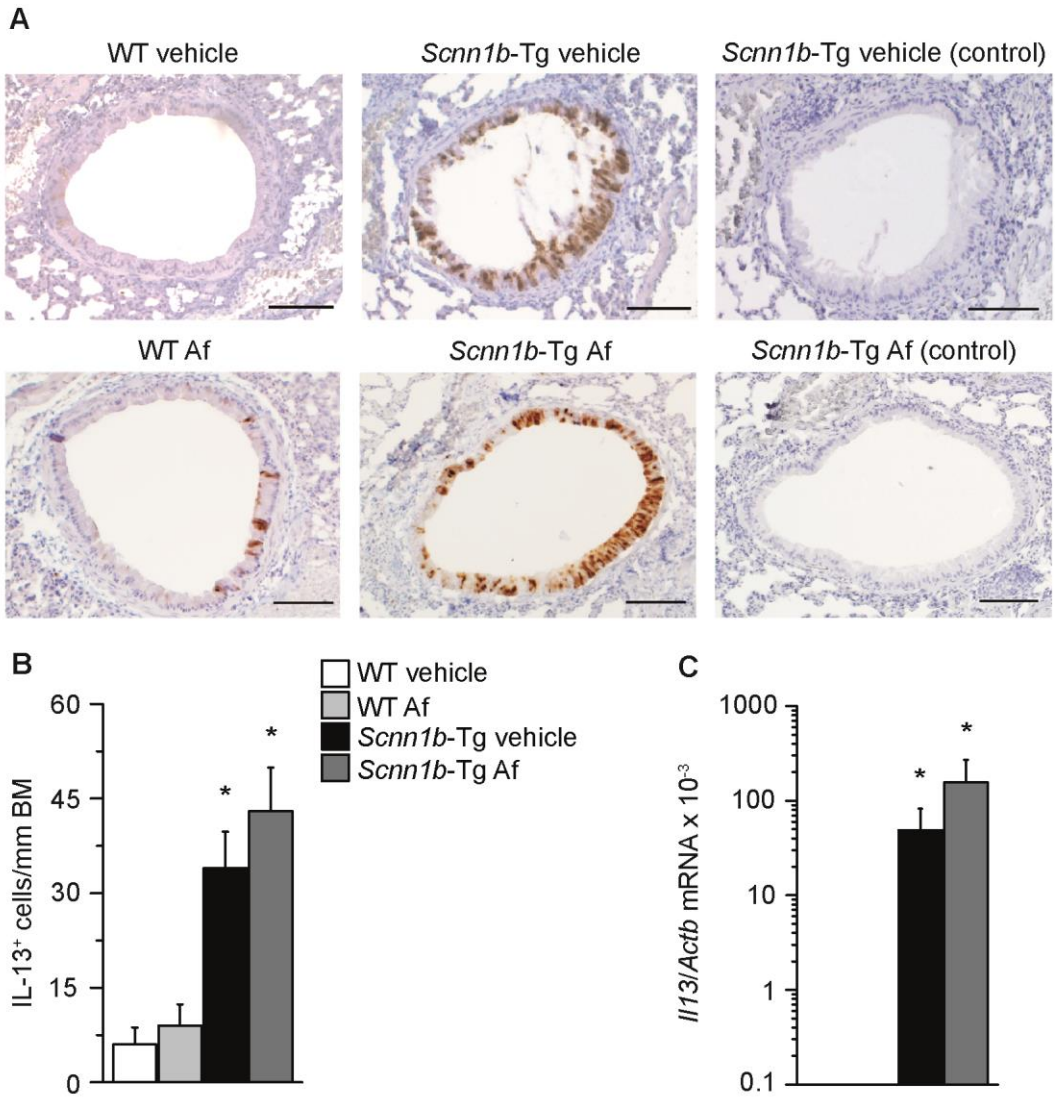

Figure 7. Increased IL-13 expression in airway epithelial cells from *Scnn1b*-Tg mice. (**A–C**) Juvenile WT and *Scnn1b*-Tg mice were challenged with Af or vehicle alone. (**A**) Representative images of immunohistochemical detection of IL-13 in lung sections from juvenile WT and *Scnn1b*-Tg mice. IL-13 staining was not detected in sections incubated with secondary antibody only (control). Scale bars = 100 µm. (**B**) IL-13$^+$ cells in the airway epithelium per mm of basal membrane (BM). n = 9–22 mice for each group. (**C**) Expression of *Il13* transcripts in laser micro-dissected airway epithelium from juvenile WT and *Scnn1b*-Tg mice determined by real-time RT-PCR. n = 7–11 mice for each group. *P < 0.05 compared with vehicle-treated mice of the same genotype.

3.1.3 IL-33 induces *Il13* expression via the St2/Myd88/p38 signaling pathway in epithelial cells *in vitro*

To identify the underlying signaling pathway of epithelial *Il13* expression, well polarized murine primary tracheal epithelial cell cultures from WT and *Scnn1b*-Tg mice were used. Cultures were treated with different stimuli followed by *Il13* transcript analysis. First, cultures were stimulated with recombinant (r) IL-9, rTslp, LPS and by inducing wounds in confluent cell layers, because these stimuli were reported to induce epithelial IL-13 expression.[112-114,116] Since airway epithelial cells bear the IL-4Rα/IL-13Rα1 receptor complex[85,117], cultures were treated with rIL-4 and rIL-13. To test whether Af directly induces epithelial *Il13* expression, cultures were further stimulated with Af. Under basal conditions and after treatment with rIL-4, rIL-9, rIL-13, rTslp, Af, LPS, or in response to the wound assay, *Il13* was not detected in primary tracheal epithelial cells neither derived from WT nor from *Scnn1b*-Tg mice (Table 5). In immune cells, the Ca^{2+} ionophore ionomycin is used as a non-specific stimulus for experimental cytokine production.[75,103,118] *In vivo*, IL-33 potently stimulates IL-13 production (e.g. by ILC2s and Th2 cells).[119,120] Stimulation with ionomycin and rIL-33 resulted in *Il13* expression in cultures from WT and *Scnn1b*-Tg mice (Table 5 and Figure 8A).

Table 5. Stimuli tested for induction of *Il13* expression in primary tracheal epithelial cell cultures from WT and *Scnn1b*-Tg mice.

None *Il13*-inducing stimuli	*Il13*-inducing stimuli
rIL-4	rIL-33
rIL-9	Ionomycin
rIL-13	
rTslp	
Af	
LPS	
Wound assay	

Due to the important role of IL-33 as an epithelial-derived alarmin orchestrating type 2 airway inflammation, the IL-33-induced epithelial IL-13 production was investigated. Dose-dependent induction of *Il13* revealed an effective concentration of 10 ng/ml for further experiments (Figure 8B). The transcription factor Stat6 is known to promote transcriptional activation of *Il13* in Th2 cells.[121,122] In primary tracheal epithelial cell cultures, *Il13* expression in response to rIL-33 was not impeded by genetic deletion of Stat6 (Figure 8C)

demonstrating a Stat6 independent mechanism. Another pathway in immune cells signals via the IL-33 receptor St2, Myd88, and MAPK.[119] It was shown that tracheal epithelial cells from both genotypes express *St2* (Figure 8D). IL-33-mediated *Il13* expression was blocked by using an anti-St2 antibody, the MyD88 inhibitory peptide Pepinh-MYD, or the p38 MAPK inhibitor SB203580 (Figure 8E). Collectively, these data show that epithelial IL-13 production is induced in response to IL-33 via the St2/Myd88/p38 signaling pathway.

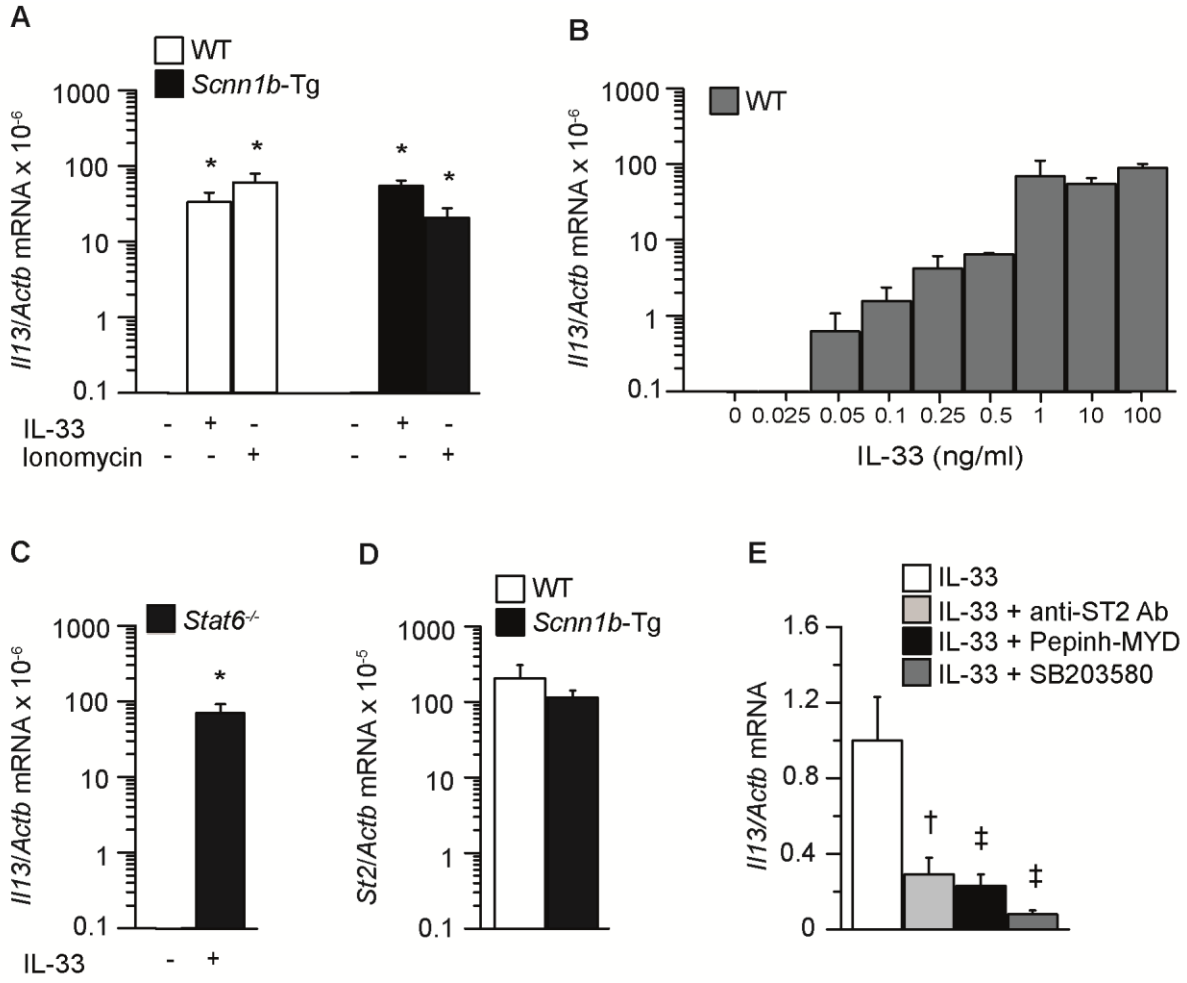

Figure 8. IL-33 triggers epithelial *Il13* expression via St2/Myd88/p38 signaling *in vitro*. (**A–E**) Primary tracheal epithelial cells were cultured under ALI conditions. mRNA expression was analyzed under basal conditions and after stimulation by the basolateral side. (**A**) Induction of *Il13* expression in murine primary tracheal epithelial cells derived from WT and *Scnn1b*-Tg mice by rIL-33 and ionomycin. (**B**) Dose-dependent induction of *Il13* expression in WT cultures in response to rIL-33. (**C**) Induction of *Il13* expression in response to rIL-33 in murine primary tracheal epithelial cells derived from *Stat6*$^{-/-}$ mice. (**D**) mRNA expression levels of the IL-33 recpetor St2 in WT and *Scnn1b*-Tg cell cultures. (**E**) Effects of the IL-33/St2 signaling pathway on *Il13* expression in primary tracheal epithelial cells of WT mice. n = 3–10 for each group. *P < 0.05 compared with vehicle-treated cultures of the same genotype; †P < 0.05 and ‡P < 0.01 compared with rIL-33-treated WT cultures.

3.1.4 *In vivo* role of IL-33 on epithelial IL-13 production

Based on these *in vitro* results, it was hypothesized that IL-33 might also be a stimulating factor *in vivo*. First, the transcript levels of *Il33* in lung homogenates and micro-dissected airway epithelium from naïve and Af-challenged WT and *Scnn1b*-Tg mice were determined. *Il33* transcripts were detectable in lung tissue and micro-dissected airway epithelia from WT mice independent of Af treatment (Figure 9). In *Scnn1b*-Tg mice, *Il33* expression in both tissues was significantly increased compared to WT mice (Figure 9). After Af challenge, *Il33* transcripts tended to be increased in lung homogenates from *Scnn1b*-Tg mice (Figure 9A). In airway epithelial tissue *Il33* levels did not differ between naïve and challenged *Scnn1b*-Tg mice (Figure 9B).

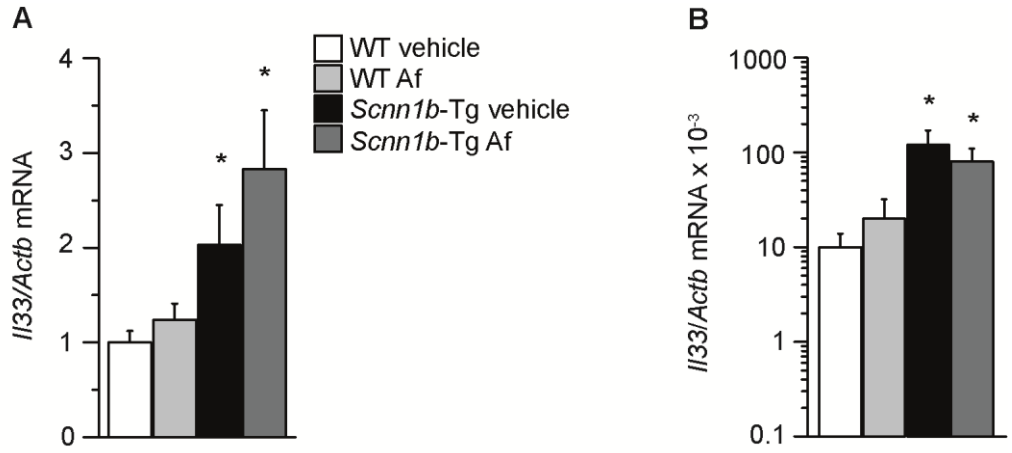

Figure 9. Increased *Il33* expression in juvenile *Scnn1b*-Tg mice. (**A, B**) Juvenile WT and *Scnn1b*-Tg mice were challenged with Af or vehicle alone. Expression of *Il33* transcripts in lung homogenates (**A**) and laser micro-dissected airway epithelium (**B**) from juvenile WT and *Scnn1b*-Tg mice measured by real-time RT-PCR. n = 7–11 mice for each group. *P < 0.05 compared with vehicle-treated mice of the same genotype.

As a proof of concept, it was tested if exogenous IL-33 induces epithelial IL-13 *in vivo*. Whilst vehicle-treated WT mice did not show positive anti-IL-13 staining, WT mice treated with rIL-33 revealed a distinct epithelial anti-IL-13-positive staining (Figure 10).

Taken together, under conditions of type 2 inflammation *Scnn1b*-Tg mice express increased levels of IL-33 by airway epithelial cells, and IL-33 is sufficient to induce epithelial IL-13 production *in vivo*.

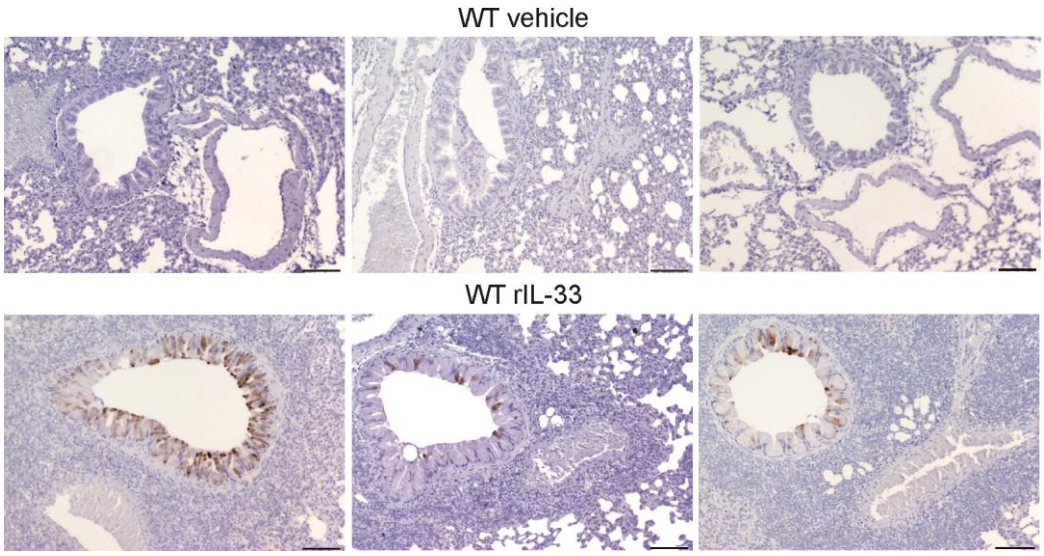

Figure 10. Epithelial IL-13 expression in response to exogenous IL-33 in WT mice. Immunohistochemical detection of IL-13 in lung sections from juvenile WT mice treated with rIL-33 or vehicle alone. Scale bars = 100 µm. n = 3 mice for each group

3.2 Relative contributions of IL-13-induced mucin hypersecretion and airway surface dehydration to airway mucus obstruction

Under conditions of type 2 airway inflammation where IL-13 induces GCM and mucin expression, it is not known to what extent airway surface dehydration and mucin hypersecretion affects airway mucus plugging. Therefore, the *in vivo* pathogenesis of airway mucus obstruction primarily triggered by airway surface dehydration or mainly induced by IL-13-induced mucin hypersecretion was studied. First, it was investigated if airway dehydration is sufficient to cause mucus plugging in the absence of the mucin-inducing cytokine IL-13 by using *Scnn1b*-Tg mice with genetic deletion of IL-13 (*Scnn1b*-Tg/*Il13*$^{-/-}$). Second, phenotypes of *Scnn1b*-Tg mice were compared to mice with overexpression of IL-13 (*Il13*-Tg) enabling an evaluation of the relative contributions of airway surface dehydration and IL-13-induced mucin hypersecretion to airway mucus obstruction. Third, the expression of IL-13 exclusively in the airway epithelium (*Il13*-Tg/*Il13*$^{-/-}$) allows conclusions on the impact of epithelium-mediated IL-13 on mucus plugging. Mice were studied at juvenile ages, because a spontaneous type 2 airway inflammation with increased IL-13 production and a most severe mucus plugging was demonstrated in *Scnn1b*-Tg mice at this age.[15,95] Finally, *Scnn1b*-Tg/*Il13*$^{-/-}$ and *Il13*-Tg/*Il13*$^{-/-}$ mice were crossed to evaluate the combined effects of airway surface dehydration and IL-13-mediated mucin hypersecretion.

3.2.1 Airway mucus obstruction is more severe in *Scnn1b*-Tg mice with airway surface dehydration than in mice with IL-13-mediated mucin hypersecretion

To compare the muco-obstructive phenotype caused by airway surface dehydration and by IL-13-induced mucin hypersecretion, goblet cell numbers and airway mucus plugging of main axial airways were analyzed in juvenile *Il13*$^{+/-}$, *Il13*$^{-/-}$, *Scnn1b*-Tg/*Il13*$^{+/-}$, *Scnn1b*-Tg/*Il13*$^{-/-}$, *Il13*-Tg/*Il13*$^{+/-}$, and *Il13*-Tg/*Il13*$^{-/-}$ mice. Neither goblet cells nor mucus were observed in the airways from *Il13*$^{+/-}$ and *Il13*$^{-/-}$ mice (Figure 11 and Figure 12). Airways of *Scnn1b*-Tg/*Il13*$^{+/-}$ mice showed elevated goblet cell numbers and mucus plugging compared to *Il13*$^{+/-}$ mice. The lack of IL-13 in juvenile *Scnn1b*-Tg mice significantly reduced goblet cell numbers that were similar to that in *Il13*$^{-/-}$ mice (Figure 12A). However, mucus plugging was still present and as severe as in *Scnn1b*-Tg/*Il13*$^{+/-}$ mice (Figure 12B, C). Overexpression of IL-13 induced strong GCM, consistent with published data[76], and mucus accumulation in *Il13*-Tg/*Il13*$^{+/-}$ and *Il13*-Tg/*Il13*$^{-/-}$ mice (Figure 11 and Figure 12). Goblet cell numbers and levels of airway mucus obstruction did not differ between *Il13*-Tg/*Il13*$^{+/-}$ and *Il13*-Tg/*Il13*$^{-/-}$ mice.

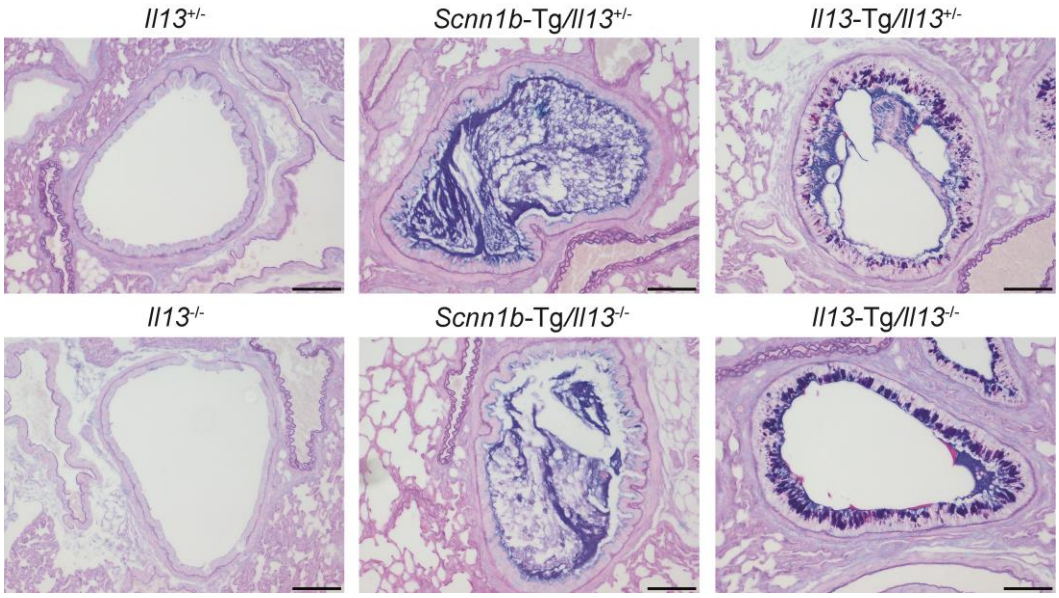

Figure 11. IL-13-(in)dependent mucus accumulation in mouse models that mimic muco-obstructive airway disease. Representative images of main axial airways stained with AB-PAS from juvenile *Il13*$^{+/-}$, *Il13*$^{-/-}$, *Scnn1b*-Tg/*Il13*$^{+/-}$, *Scnn1b*-Tg/*Il13*$^{-/-}$, *Il13*-Tg/*Il13*$^{+/-}$, and *Il13*-Tg/*Il13*$^{-/-}$ mice. Scale bars = 100 µm.

When compared to *Scnn1b*-Tg/*Il13*$^{+/-}$ mice, the amount of airway mucus was 3-fold lower in *Il13*-Tg/*Il13*$^{+/-}$ mice (Figure 12A, B), although the number of goblet cells was 3-fold increased in IL-13-overexpressing mice. Further, airway mucus obstruction was only observed in 45 % of *Il13*-Tg/*Il13*$^{+/-}$ and *Il13*-Tg/*Il13*$^{-/-}$ mice, whereas in > 90 % of *Scnn1b*-Tg/*Il13*$^{+/-}$ and *Scnn1b*-Tg/*Il13*$^{-/-}$ mice airways were obstructed (Figure 12C). Collectively, it was shown that lack of IL-13 abrogates GCM, but has no effect on mucus plugging in juvenile *Scnn1b*-Tg mice. Further, the data demonstrate that epithelial overexpression of IL-13 causes less severe airway mucus obstruction than under conditions of airway dehydration.

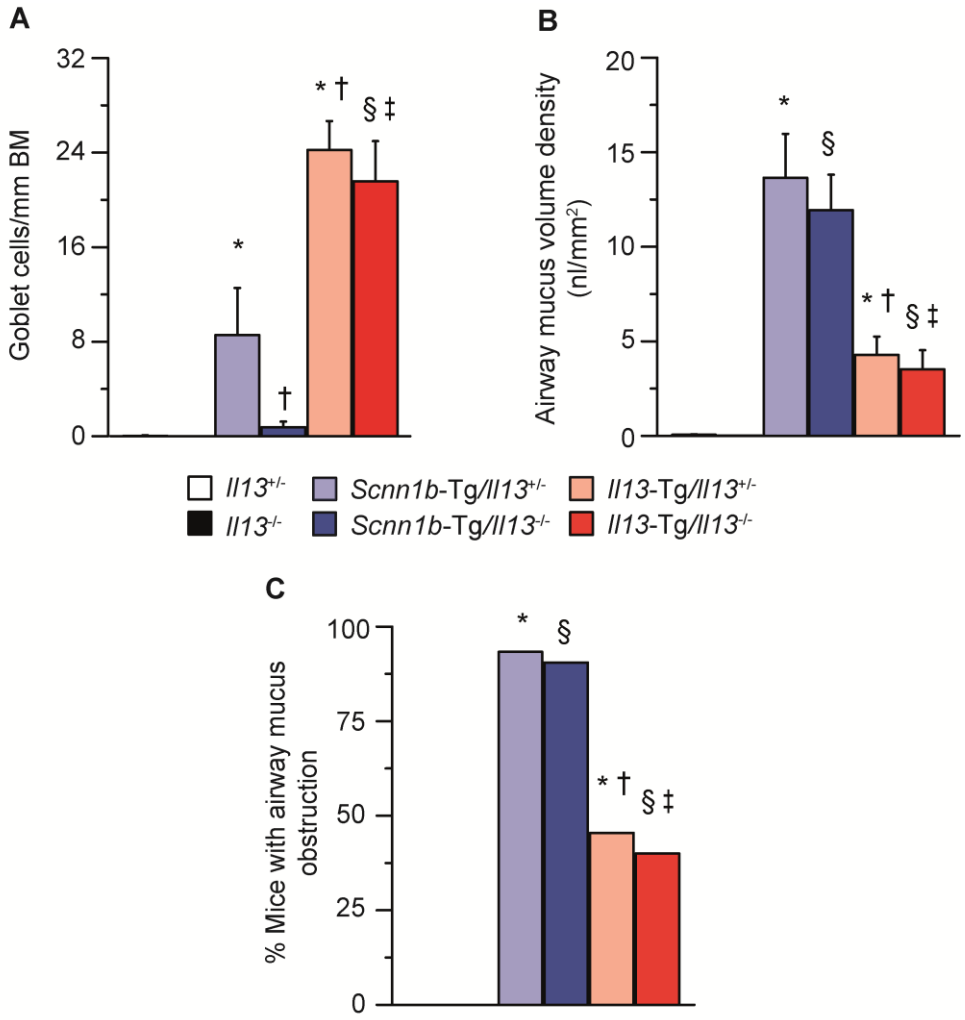

Figure 12. Mucus obstruction is more severe in *Scnn1b*-Tg mice than in *Il13*-Tg mice. Number of goblet cells per mm basal membrane (BM) (**A**), airway mucus content quantified from the AB-PAS-positive material in the airway lumen (**B**), and semi-quantitative analysis of % mice showing airway mucus obstruction (**C**) in juvenile *Il13*$^{+/-}$, *Il13*$^{-/-}$, *Scnn1b*-Tg/*Il13*$^{+/-}$, *Scnn1b*-Tg/*Il13*$^{-/-}$, *Il13*-Tg/*Il13*$^{+/-}$, and *Il13*-Tg/*Il13*$^{-/-}$ mice. n = 10–21 mice per genotype. *P < 0.05 vs. *Il13*$^{+/-}$, §P < 0.05 vs. *Il13*$^{-/-}$, †P < 0.05 vs. *Scnn1b*-Tg/*Il13*$^{+/-}$, ‡P < 0.05 vs. *Scnn1b*-Tg/*Il13*$^{-/-}$.

3.2.2 IL-13 regulates *Muc5ac* and *Muc5b* expression

Recent studies demonstrated that IL-13 mediates mucin gene expression, in particular that of *Muc5ac*[76,77], amongst others via Gob5, which serves as a goblet cell marker (Figure 2).[65] To determine how IL-13 affects mucin expression in the studied mouse models and to investigate whether the severity in mucus obstruction was due to different mucin expression levels, relative transcript levels of *Gob5*, *Muc5ac* and *Muc5b* were measured in lung homogenates from juvenile *Il13*$^{+/-}$, *Il13*$^{-/-}$, *Scnn1b*-Tg/*Il13*$^{+/-}$, *Scnn1b*-Tg/*Il13*$^{-/-}$, *Il13*-Tg/*Il13*$^{+/-}$, and *Il13*-Tg/*Il13*$^{-/-}$ mice. In *Il13*$^{-/-}$ mice, a trend towards a reduced expression of all 3 genes compared to *Il13*$^{+/-}$ mice was observed (Figure 13).

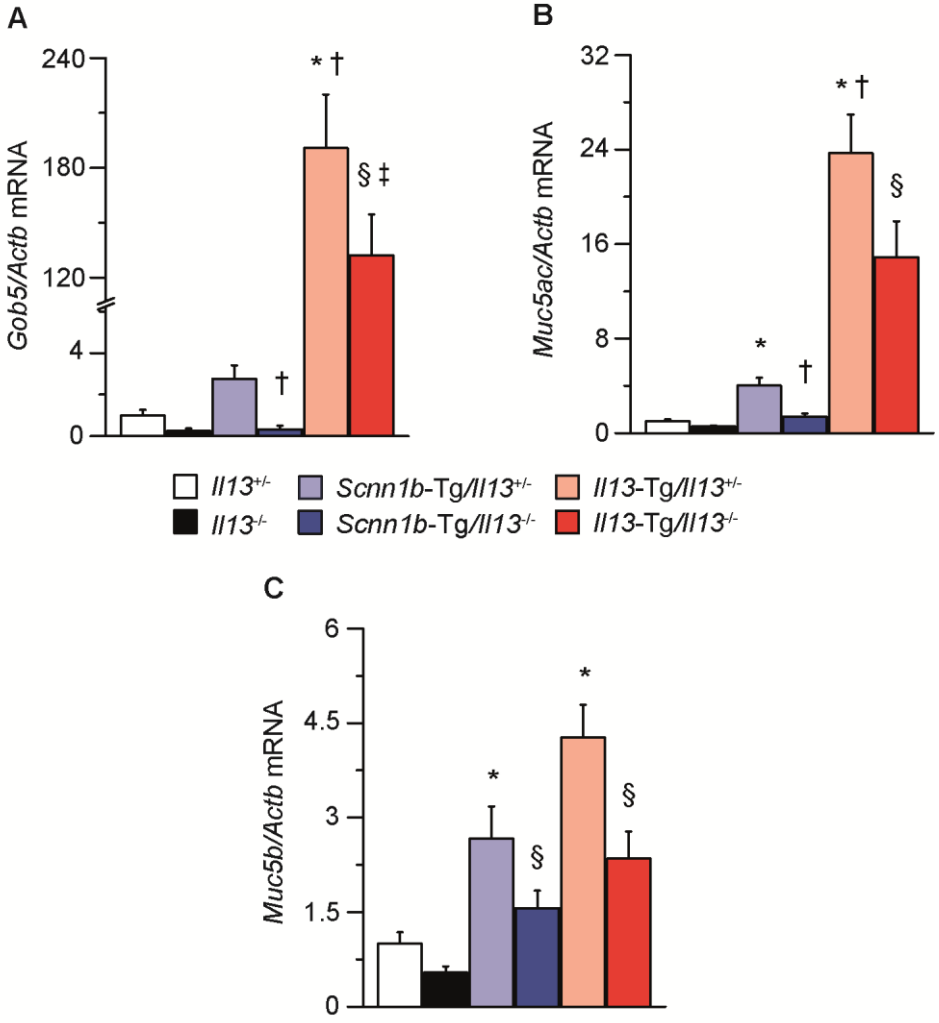

Figure 13. IL-13 drives *Muc5ac* and *Muc5b* expression in juvenile *Scnn1b*-Tg and *Il13*-Tg mice. Expression levels of *Gob5* (**A**), *Muc5ac* (**B**), and *Muc5b* (**C**) in lung homogenates from juvenile *Il13*$^{+/-}$, *Il13*$^{-/-}$, *Scnn1b*-Tg/*Il13*$^{+/-}$, *Scnn1b*-Tg/*Il13*$^{-/-}$, *Il13*-Tg/*Il13*$^{+/-}$, and *Il13*-Tg/*Il13*$^{-/-}$ mice determined by real-time RT-PCR. n = 10–16 mice per genotype. *P < 0.05 vs. *Il13*$^{+/-}$, §P < 0.05 vs. *Il13*$^{-/-}$, †P < 0.05 vs. *Scnn1b*-Tg/*Il13*$^{+/-}$, ‡P < 0.05 vs. *Scnn1b*-Tg/*Il13*$^{-/-}$.

Increased levels of *Gob5* and *Muc5ac* in *Scnn1b*-Tg/*Il13*$^{+/-}$ mice were significantly abrogated by deletion of IL-13 (Figure 13A, B). Consistent with the high number of goblet cells and previous reports[77], expression of *Gob5* and *Muc5ac* was strongly increased in IL-13-overexpressing mice compared to *Il13*$^{+/-}$ and *Il13*$^{-/-}$ mice (Figure 13A, B). When compared to *Scnn1b*-Tg/*Il13*$^{+/-}$ mice, *Il13*-Tg/*Il13*$^{+/-}$ mice displayed a 6-fold elevated *Muc5ac* expression. Further, an IL-13-dependent *Muc5b* expression was observed. *Muc5b* levels tended to be reduced in *Scnn1b*-Tg/*Il13*$^{-/-}$ and *Il13*$^{-/-}$ mice in comparison to mice sufficient for IL-13, and were significantly increased in *Il13*-Tg/*Il13*$^{+/-}$ and *Il13*-Tg/*Il13*$^{-/-}$ mice compared to *Il13*$^{+/-}$ and *Il13*$^{-/-}$ mice (Figure 13C). In mice expressing IL-13 exclusively in epithelial cells, all 3 genes tended to be reduced compared to *Il13*-Tg/*Il13*$^{+/-}$ mice (Figure 13).

Next, relative expressions of *Spdef* and *Foxa3* were quantified in lung homogenates. These transcription factors are involved in the down-stream signaling pathway of IL-13-mediated mucin expression and goblet cell differentiation (Figure 2).[80,86] Levels of *Spdef* and *Foxa3* did not change between *Scnn1b*-Tg/*Il13*$^{+/-}$, *Scnn1b*-Tg/*Il13*$^{-/-}$, *Il13*$^{+/-}$, and *Il13*$^{-/-}$ mice (Figure 14). In *Il13*-Tg/*Il13*$^{+/-}$ and *Il13*-Tg/*Il13*$^{-/-}$ mice, expression of both transcription factors was highly elevated to a similar level and increased compared to all other genotypes, as appropriate (Figure 14).

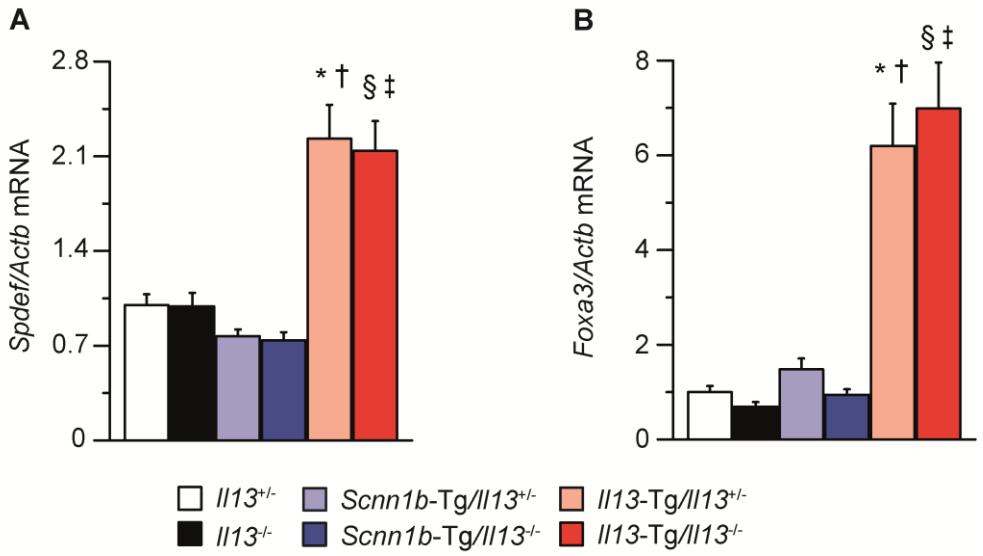

Figure 14. Increased *Spdef* and *Foxa3* expression in *Il13*-Tg mice but not in *Scnn1b*-Tg mice. Expression levels of *Spdef* (**A**) and *Foxa3* (**B**) in lung homogenates from juvenile *Il13*$^{+/-}$, *Il13*$^{-/-}$, *Scnn1b*-Tg/Il13$^{+/-}$, *Scnn1b*-Tg/*Il13*$^{-/-}$, *Il13*-Tg/*Il13*$^{+/-}$, and *Il13*-Tg/*Il13*$^{-/-}$ mice measured by real-time RT-PCR. n = 10–16 mice per genotype. *P < 0.05 vs. *Il13*$^{+/-}$, §P < 0.05 vs. *Il13*$^{-/-}$, †P < 0.05 vs. *Scnn1b*-Tg/*Il13*$^{+/-}$, ‡P < 0.05 vs. *Scnn1b*-Tg/*Il13*$^{-/-}$.

In summary, these results show that severe mucus plugging persists in *Scnn1b*-Tg/*Il13*$^{-/-}$ mice although deletion of IL-13 diminishes *Muc5ac* and *Muc5b* expression, and that *Muc5ac* levels are highly upregulated in IL-13 overexpressing mice compared to *Scnn1b*-Tg mice. Further, these data indicate that IL-13 not only regulates *Muc5ac* but also *Muc5b* expression.

3.2.3 Airway surface dehydration but not IL-13-mediated mucin hypersecretion impairs mucociliary transport

So far, the obtained data demonstrated that IL-13-induced mucin hypersecretion causes less severe mucus obstruction than airway surface dehydration in *Scnn1b*-Tg mice with mucus plugging persisting even in the absence of mucin hypersecretion. To test if these observations are due to differences in the ability to clear mucus, the mucociliary transport efficiency was determined. Fluorochrome-labeled allergen was instilled intratracheally in juvenile WT, *Scnn1b*-Tg, and *Il13*-Tg mice and allergen clearance of the whole lung was measured. Consistent with previously published data by Fritzsching *et al.*[95], *Scnn1b*-Tg mice displayed a mean mucociliary transport efficiency of 57 % after 1 hour, which was significantly reduced compared to WT mice with a mean efficiency of 74 % (Figure 15). In contrast, in *Il13*-Tg mice mucociliary transport was not impaired and similar as in WT mice, but significantly increased compared to *Scnn1b*-Tg mice (Figure 15). These data demonstrate that mucociliary transport is impaired in *Scnn1b*-Tg mice, whereas IL-13-induced mucin hypersecretion does not affect mucociliary transport.

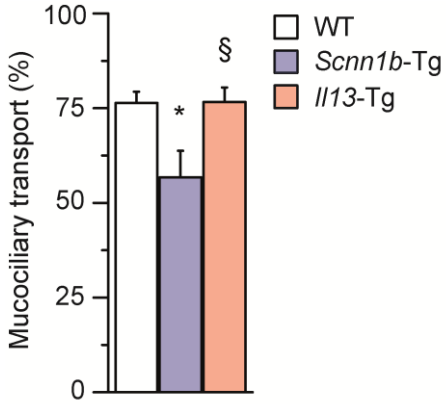

Figure 15. Mucociliary transport is reduced in *Scnn1b*-Tg mice but not in *Il13*-Tg mice. Mucociliary transport determined by the clearance efficiency of fluorochrome-labeled allergen 1 hour after intratracheal instillation in juvenile WT, *Scnn1b*-Tg, and *Il13*-Tg mice. n = 11–18 mice per genotype. *P < 0.05 vs. WT, §P < 0.05 vs. *Scnn1b*-Tg.

3.2.4 Eosinophilic and neutrophilc inflammation in *Scnn1b*-Tg and *Il13*-Tg mice

To compare the inflammatory phenotypes of the studied mouse models and thereby assessing the role of IL-13, eosinophil and neutrophil numbers were measured in BAL fluid by flow cytometry in juvenile *Il13*$^{+/-}$, *Il13*$^{-/-}$, *Scnn1b*-Tg/*Il13*$^{+/-}$, *Scnn1b*-Tg/*Il13*$^{-/-}$, *Il13*-Tg/*Il13*$^{+/-}$, and *Il13*-Tg/*Il13*$^{-/-}$ mice. Eosinophils and neutrophils were rarely detected in juvenile *Il13*$^{+/-}$ and *Il13*$^{-/-}$ mice, whereas both inflammatory cell types were significantly increased in juvenile *Scnn1b*-Tg/*Il13*$^{+/-}$ (Figure 16). Lack of IL-13 in *Scnn1b*-Tg mice caused a trend towards reduced eosinophil and increased neutrophil numbers compared to *Scnn1b*-Tg/*Il13*$^{+/-}$ mice (Figure 16A). Eosinophil and neutrophil counts remained significantly elevated in *Scnn1b*-Tg/*Il13*$^{-/-}$ mice compared to *Il13*$^{-/-}$ mice. As reported recently[77,123], significantly increased eosinophil and neutrophil counts were observed in *Il13*-Tg/*Il13*$^{+/-}$ and *Il13*-Tg/*Il13*$^{-/-}$ mice compared to *Il13*$^{+/-}$ and *Il13*$^{-/-}$ mice, respectively. Exclusive expression of IL-13 in the airway epithelium seemed to reduce eosinophilic inflammation in *Il13*-Tg/*Il13*$^{-/-}$, but this did not reach statistical significance (Figure 16A). With regard to the comparison of *Scnn1b*-Tg and *Il13*-Tg mice, eosinophils were increased to a similar level in both mouse models and neutrophils tended to be elevated in *Scnn1b*-Tg mice (Figure 16).

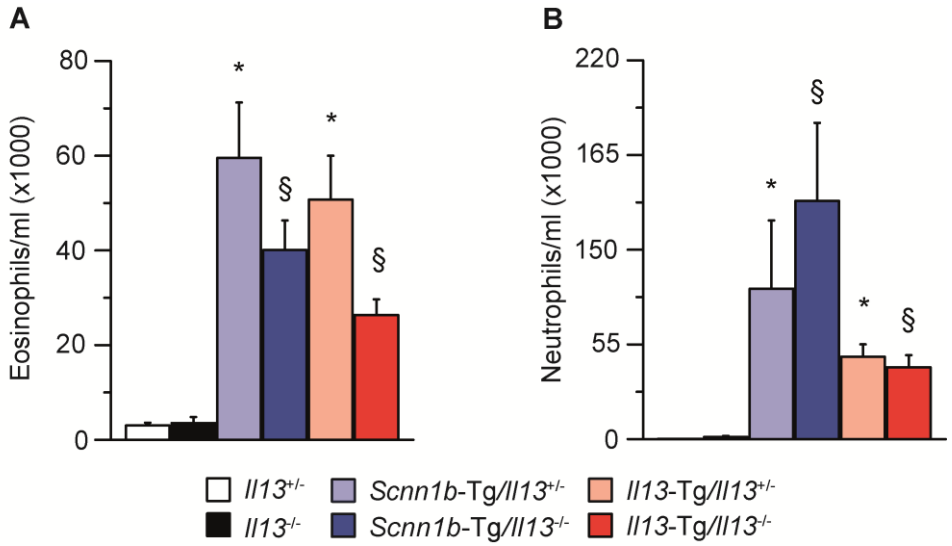

Figure 16. Eosinophilc and neutrophilc inflammation in *Scnn1b*-Tg and *Il13*-Tg mice. Eosinophils (**A**) and neutrophils (**B**) in BAL fluid from juvenile *Il13*$^{+/-}$, *Il13*$^{-/-}$, *Scnn1b*-Tg/*Il13*$^{+/-}$, *Scnn1b*-Tg/*Il13*$^{-/-}$, *Il13*-Tg/*Il13*$^{+/-}$, and *Il13*-Tg/*Il13*$^{-/-}$ mice determined by flow cytometry. n = 21–38 mice per genotype. *P < 0.05 vs. *Il13*$^{+/-}$, §P < 0.05 vs. *Il13*$^{-/-}$.

In summary, these data show that in the absence of IL-13 eosinophilic inflammation persists in juvenile *Scnn1b*-Tg mice. It was demonstrated that *Scnn1b*-Tg and *Il13*-Tg mice reveal eosinophilic and neutrophilc infiltration.

3.2.5 IL-13-induced mucin hypersecretion in *Scnn1b*-Tg mice causes neonatal mortality due to severe airway mucus plugging

To test combined effects of airway surface dehydration and IL-13-mediated mucin hypersecretion, both mouse models were crossed to generate *Scnn1b*-Tg/*Il13*-Tg/*Il13*$^{-/-}$ mice. First, the survival and growth of *Scnn1b*-Tg/*Il13*-Tg/*Il13*$^{-/-}$ mice and *Il13*$^{-/-}$, *Scnn1b*-Tg/*Il13*$^{-/-}$, *Il13*-Tg/*Il13*$^{-/-}$ littermates was monitored. All *Scnn1b*-Tg/*Il13*-Tg/*Il13*$^{-/-}$ mice died before PND6 (Figure 17A). Accordingly, a significant reduction in body weight on PND4 and PND5 was observed in *Scnn1b*-Tg/*Il13*-Tg/*Il13*$^{-/-}$ mice compared with *Il13*$^{-/-}$ littermates, whereas growth curves of *Scnn1b*-Tg/*Il13*$^{-/-}$ and *Il13*-Tg/*Il13*$^{-/-}$ mice did not differ from *Il13*$^{-/-}$ mice (Figure 17B).

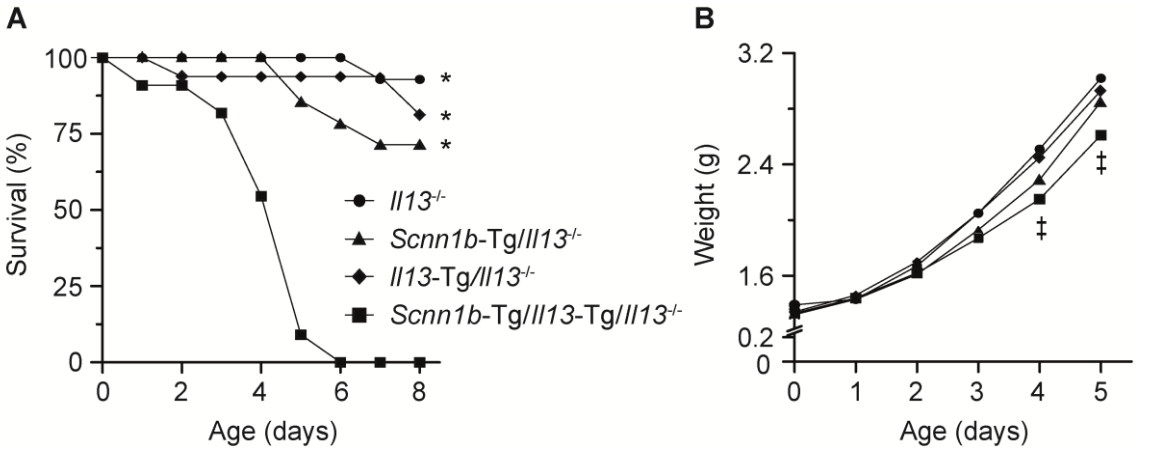

Figure 17. Neonatal death of *Scnn1b*-Tg/*Il13*-Tg/*Il13*$^{-/-}$ mice. Survival curves (**A**) and growth curves (**B**) of *Il13*$^{-/-}$, *Scnn1b*-Tg/*Il13*$^{-/-}$, *Il13*-Tg/*Il13*$^{-/-}$, and *Scnn1b*-Tg/*Il13*-Tg/*Il13*$^{-/-}$ littermates. n = 8–34 mice/genotype. *P < 0.0001 vs. *Scnn1b*-Tg/*Il13*-Tg/*Il13*$^{-/-}$, ‡P < 0.05 vs. Il13$^{-/-}$.

To determine the cause of neonatal mortality, goblet cell counts and airway mucus content were analyzed in airway sections from *Il13*$^{-/-}$, *Scnn1b*-Tg/*Il13*$^{-/-}$, *Il13*-Tg/*Il13*$^{-/-}$, and *Scnn1b*-Tg/*Il13*-Tg/*Il13*$^{-/-}$ mice on PND5.5. The number of goblet cells was elevated to a similar level in *Il13*-Tg/*Il13*$^{-/-}$ and *Scnn1b*-Tg/*Il13*-Tg/*Il13*$^{-/-}$ mice, whereas goblet cells were absent in airways from *Il13*$^{-/-}$ and *Scnn1b*-Tg/*Il13*$^{-/-}$ mice (Figure 18A, B). In contrast to juvenile mice (Figure 12), mucus obstruction was not different in neonatal *Scnn1b*-Tg/*Il13*$^{-/-}$ mice compared to *Il13*-Tg/*Il13*$^{-/-}$ mice (Figure 18C, D). In *Scnn1b*-Tg/*Il13*-Tg/*Il13*$^{-/-}$ mice, the airway mucus content was 3- to 4-fold increased

compared to *Il13*-Tg/*Il13*$^{-/-}$ and *Scnn1b*-Tg/*Il13*$^{-/-}$ mice. Airway mucus accumulation was observed in 40 % of *Scnn1b*-Tg/*Il13*-Tg/*Il13*$^{-/-}$ mice, but only in 9 % and 18 % of neonatal *Scnn1b*-Tg/*Il13*$^{-/-}$ and *Il13*-Tg/*Il13*$^{-/-}$ mice, respectively (Figure 18D).

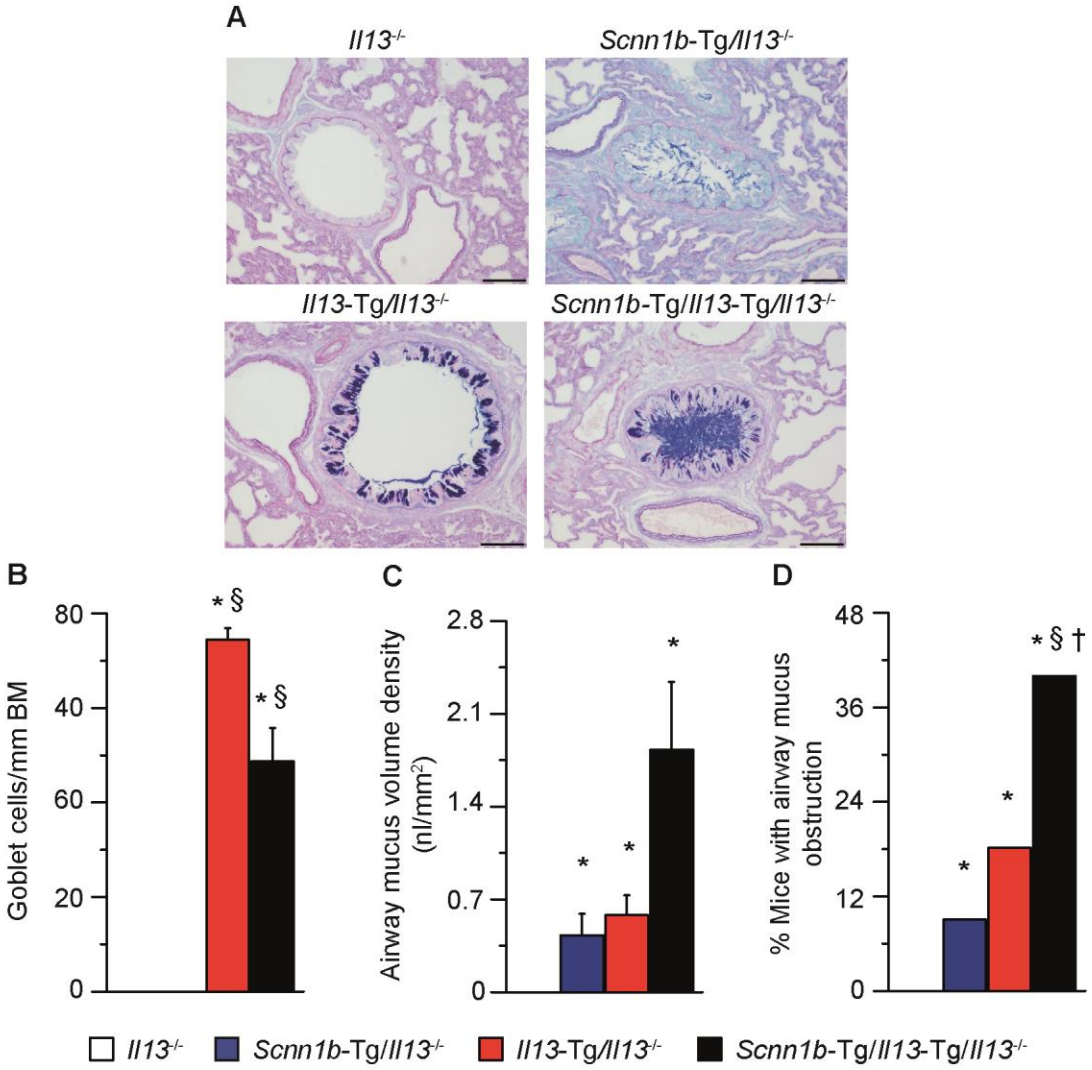

Figure 18. Severe airway mucus obstruction in airways of neonatal *Scnn1b*-Tg/*Il13*-Tg/*Il13*$^{-/-}$ mice. (**A**) Representative images of main axial airways stained with AB-PAS from neonatal *Il13*$^{-/-}$, *Scnn1b*-Tg/*Il13*$^{-/-}$, *Il13*-Tg/*Il13*$^{-/-}$, and *Scnn1b*-Tg/*Il13*-Tg/*Il13*$^{-/-}$ littermates. Scale bars = 100 µm. Number of goblet cells per mm basal membrane (BM) (**B**), airway mucus content quantified from the AB-PAS-positive material in the airway lumen (**C**), and semi-quantitative analysis of % mice showing airway mucus obstruction (**D**) in neonatal *Il13*$^{-/-}$, *Scnn1b*-Tg/*Il13*$^{-/-}$, *Il13*-Tg/*Il13*$^{-/-}$, and *Scnn1b*-Tg/*Il13*-Tg/*Il13*$^{-/-}$ mice. n = 10–12 mice per genotype. *P < 0.05 vs. *Il13*$^{-/-}$, §P < 0.05 vs. *Scnn1b*-Tg/*Il13*$^{-/-}$, †P < 0.05 vs. *Il13*-Tg/*Il13*$^{-/-}$.

Next, *ex vivo* µ-CT measurements we performed to visualize morphological alterations of the whole lung. Semi-quantitative analysis of all airways revealed mucus accumulation in neonatal *Scnn1b*-Tg/*Il13*$^{-/-}$, *Il13*-Tg/*Il13*$^{-/-}$, and *Scnn1b*-Tg/*Il13*-Tg/*Il13*$^{-/-}$ mice (Figure 19A, B).

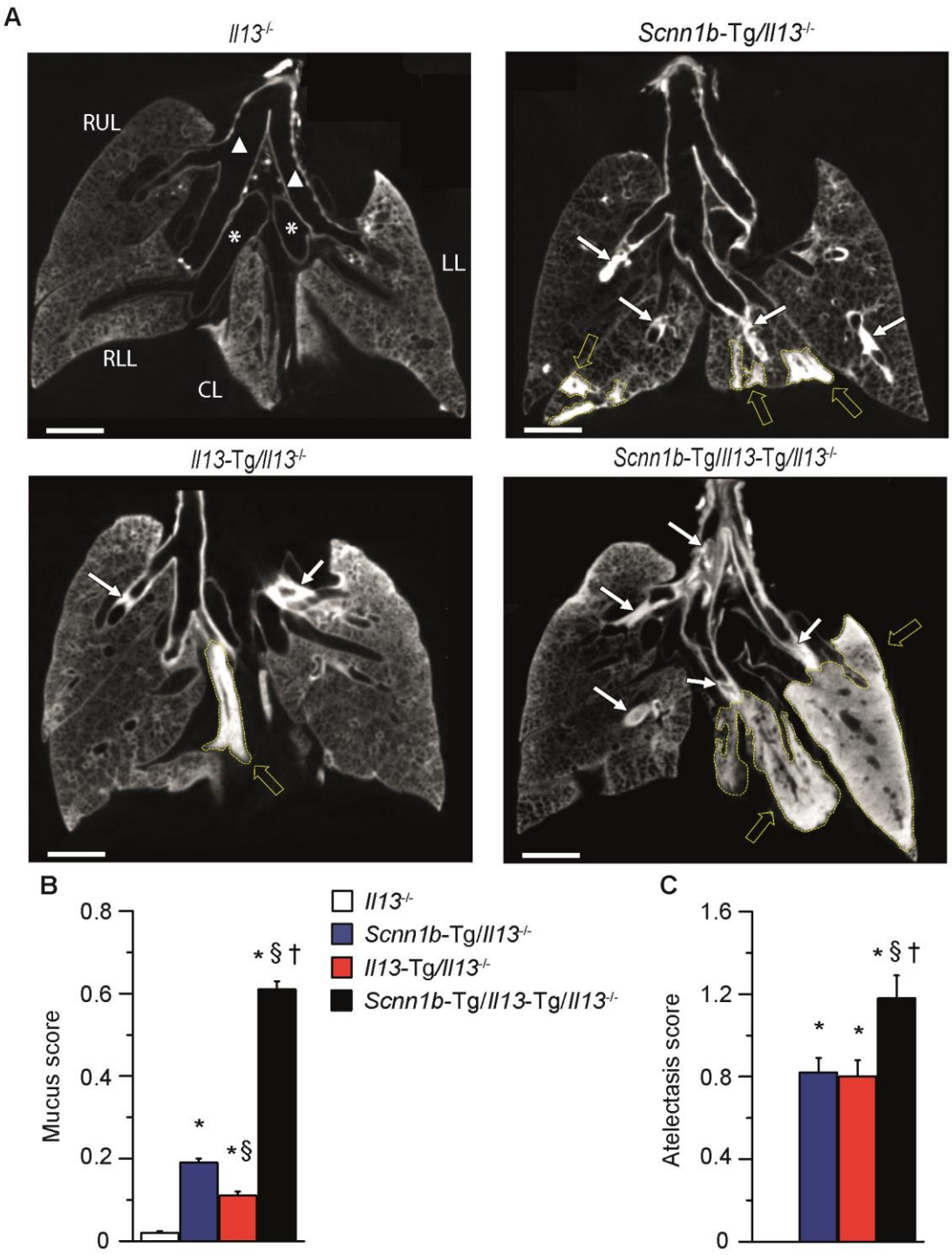

Figure 19. Severe mucus plugging and atelectasis in neonatal *Scnn1b*-Tg/*Il13*-Tg/*Il13*$^{-/-}$ mice visualized by µ-CT measurements. (**A**) Representative µ-CT scans of explanted lungs from neonatal *Il13*$^{-/-}$, *Scnn1b*-Tg/*Il13*$^{-/-}$, *Il13*-Tg/*Il13*$^{-/-}$, and *Scnn1b*-Tg/*Il13*-Tg/*Il13*$^{-/-}$ mice. Scale bars = 1 mm. CL, cardiac lobe; LL, left lobe; RLL, right lower lobe; RUL, right upper lobe. Mucus plugging (white arrows) (**B**) and atelectasis (yellow arrows, yellow framed areas) (**C**) were determined by semi-quantitative scoring of each airway and each lobe from µ-CT scans of neonatal *Il13*$^{-/-}$, *Scnn1b*-Tg/*Il13*$^{-/-}$, *Il13*-Tg/*Il13*$^{-/-}$, and *Scnn1b*-Tg/*Il13*-Tg/*Il13*$^{-/-}$ mice. Asterisks indicate blood vessels, triangles indicate airways. n = 8–11 mice per genotype. *P < 0.001 vs. *Il13*$^{-/-}$, §P < 0.001 vs. *Scnn1b*-Tg/*Il13*$^{-/-}$, †P < 0.001 vs. *Il13*-Tg/*Il13*$^{-/-}$.

In *Il13*-Tg/*Il13*$^{-/-}$ mice, the µ-CT-based mucus score was at its lowest level when compared to *Il13*$^{-/-}$ mice, and significantly reduced compared to *Scnn1b*-Tg/*Il13*$^{-/-}$ mice (Figure 19B). In *Scnn1b*-Tg/*Il13*-Tg/*Il13*$^{-/-}$ mice, the score was 3–5-fold increased in comparison to *Scnn1b*-Tg/*Il13*$^{-/-}$ and *Il13*-Tg/*Il13*$^{-/-}$ mice, respectively (Figure 19B). Complete occlusion of airways by mucus plugs can cause atelectasis that is the collapse of the lung parenchyma. Atelectatic areas were absent in *Il13*$^{-/-}$ mice (Figure 19C), but were detected in *Scnn1b*-Tg/*Il13*$^{-/-}$ and *Il13*-Tg/*Il13*$^{-/-}$ mice to a similar level. In line with severe mucus obstruction, the atelectasis score was significantly increased in *Scnn1b*-Tg/*Il13*-Tg/*Il13*$^{-/-}$ mice (Figure 19C). Taken together, these data demonstrate that combined effects of airway surface dehydration and IL-13-mediated mucin hypersecretion lead to lethal pulmonary alterations including severe airway mucus obstruction and serious atelectasis.

3.2.6 Increased *Muc5ac* and *Muc5b* expression in *Scnn1b*-Tg/*Il13*-Tg/*Il13*$^{-/-}$ mice

To clarify if the lethal mucus obstruction in *Scnn1b*-Tg/*Il13*-Tg/*Il13*$^{-/-}$ mice is driven by an exaggerated mucin expression, and to investigate if differences in Muc5ac and Muc5b content might contribute, expression levels of *Gob5*, *Muc5ac*, and *Muc5b* were determined in lung homogenates from neonatal *Il13*$^{-/-}$, *Scnn1b*-Tg/*Il13*$^{-/-}$, *Il13*-Tg/*Il13*$^{-/-}$, and *Scnn1b*-Tg/*Il13*-Tg/*Il13*$^{-/-}$ mice. When compared to *Il13*$^{-/-}$ mice, relative *Gob5*, *Muc5ac*, and *Muc5b* levels were not different in neonatal *Scnn1b*-Tg/*Il13*$^{-/-}$ mice (Figure 20A–C). In contrast, in *Il13*-Tg/*Il13*$^{-/-}$ and *Scnn1b*-Tg/*Il13*-Tg/*Il13*$^{-/-}$ mice highly increased expression levels for *Gob5* and both mucins were observed, with a >25-fold increase of *Mu5cac* expression compared to *Scnn1b*-Tg/*Il13*$^{-/-}$ mice (Figure 20 A–C). Transcript levels did not differ between *Il13*-Tg/*Il13*$^{-/-}$ and *Scnn1b*-Tg/*Il13*-Tg/*Il13*$^{-/-}$ mice.

Absolute quantification of *Muc5ac* and *Muc5b* copy numbers revealed a similar pattern as observed for relative expression levels. *Muc5ac* and *Muc5b* copy numbers were significantly increased to a similar level in *Il13*-Tg/*Il13*$^{-/-}$ and *Scnn1b*-Tg/*Il13*-Tg/*Il13*$^{-/-}$ mice when compared to *Il13*$^{-/-}$ and *Scnn1b*-Tg/*Il13*$^{-/-}$ mice (Figure 20D, E). The predominant mucin in all genotypes was *Muc5b* (Figure 20E), but in *Il13*-Tg/*Il13*$^{-/-}$ and *Scnn1b*-Tg/*Il13*-Tg/*Il13*$^{-/-}$ mice *Muc5ac* copy numbers were highly increased (Figure 20D). The *Muc5ac/Muc5b* ratio reflects that *Muc5ac* expression relative to *Muc5b* is low in *Scnn1b*-Tg/*Il13*$^{-/-}$ mice, whereas a high *Muc5ac* expression relative to *Muc5b* was observed in *Il13*$^{-/-}$, *Il13*-Tg/*Il13*$^{-/-}$ and *Scnn1b*-Tg/*Il13*-Tg/*Il13*$^{-/-}$ mice (Figure 20F). Collectively, these data demonstrate that total

mucin expression is not further exaggerated and that both *Muc5ac* and *Muc5b* are highly upregulated in neonatal *Scnn1b*-Tg/*Il13*-Tg/*Il13*$^{-/-}$ mice.

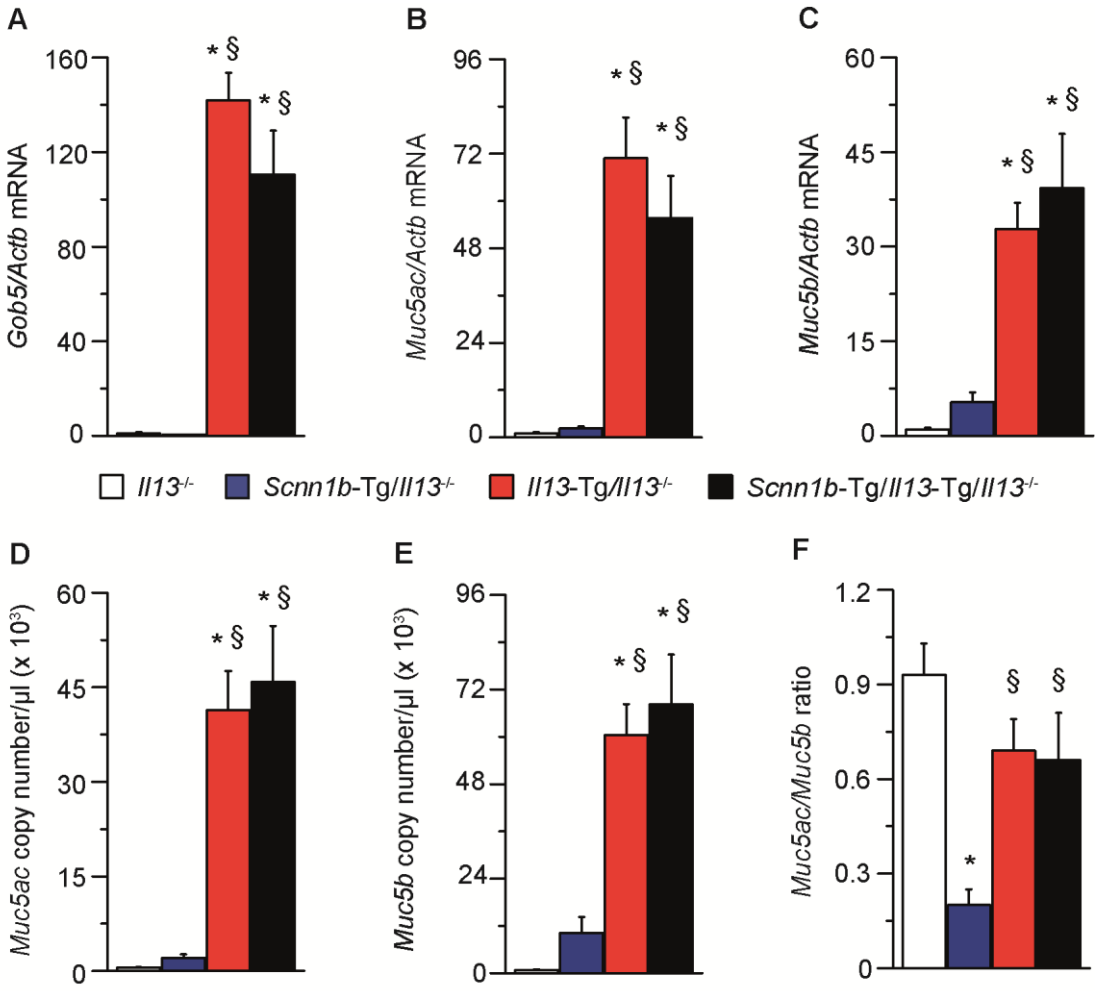

Figure 20. Increased *Muc5ac* and *Muc5b* transcripts in neonatal *Il13*-Tg/*Il13*$^{-/-}$ and *Scnn1b*-Tg/*Il13*-Tg/*Il13*$^{-/-}$ mice. (**A–C**) Relative expression levels of *Gob5* (**A**), *Muc5ac* (**B**), and *Muc5b* (**C**); (**D, E**) copy numbers of *Muc5ac* (**D**) and *Muc5b* (**E**), and ratio of *Mu5ac/Muc5b* copy numbers (**F**) in lung homogenates from neonatal *Il13*$^{-/-}$, *Scnn1b*-Tg/*Il13*$^{-/-}$, *Il13*-Tg/*Il13*$^{-/-}$, and *Scnn1b*-Tg/*Il13*-Tg/*Il13*$^{-/-}$ mice determined by real-time RT-PCR. n = 10–12 mice per genotype. *P < 0.05 vs. *Il13*$^{-/-}$, §P < 0.05 vs. *Scnn1b*-Tg/*Il13*$^{-/-}$.

3.2.7 Hypertonic saline treatment does not prevent early mortality of *Scnn1b*-Tg/*Il13*-Tg/*Il13*$^{-/-}$ mice

Previous studies demonstrated that preventive treatment with 7 % hypertonic saline (HS) improves airway surface dehydration and reduces the mortality of *Scnn1b*-Tg mice.[124] To test if improvement of airway surface hydration has benefits on the survival of *Scnn1b*-Tg/*Il13*-Tg/*Il13*$^{-/-}$ mice, *Il13*$^{-/-}$, *Scnn1b*-Tg/*Il13*$^{-/-}$, *Il13*-Tg/*Il13*$^{-/-}$, and *Scnn1b*-Tg/*Il13*-Tg/*Il13*$^{-/-}$ mice were treated from the first day of life with intranasal instillation of 7 % HS. This treatment did not rescue *Scnn1b*-Tg/*Il13*-Tg/*Il13*$^{-/-}$ mice from neonatal mortality (Figure 21). This indicates that improvement of airway surface hydration alone is not sufficient to circumvent early severe mucus obstruction and associated mortality in mice with airway dehydration and IL-13-induced mucin hypersecretion.

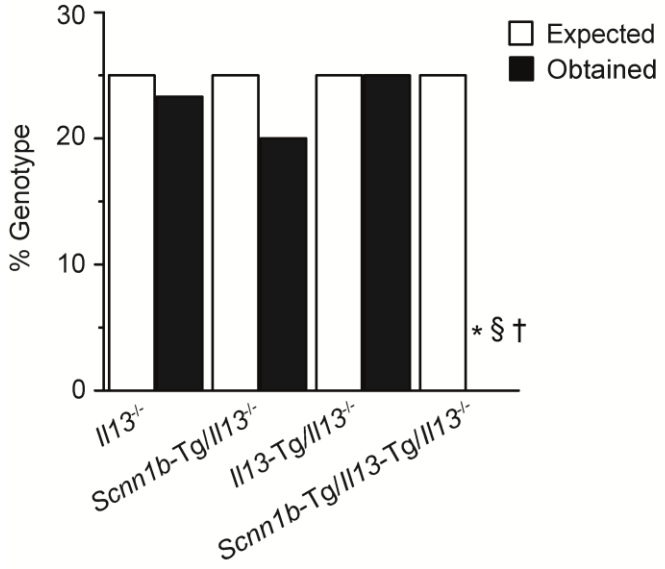

Figure 21. Treatment with 7 % HS does not rescue *Scnn1b*-Tg/*Il13*-Tg/*Il13*$^{-/-}$ mice. Newborn *Il13*$^{-/-}$, *Scnn1b*-Tg/*Il13*$^{-/-}$, *Il13*-Tg/*Il13*$^{-/-}$, and *Scnn1b*-Tg/*Il13*-Tg/*Il13*$^{-/-}$ littermates were treated with 7 % HS by intranasal instillation. Frequencies of expected versus obtained genotypes of mice that survived until PND6. n = 60 mice from 8 litters. *P < 0.01 vs. *Il13*$^{-/-}$, §P < 0.01 vs. *Scnn1b*-Tg/*Il13*$^{-/-}$, †P < 0.01 vs. *Il13*-Tg/*Il13*$^{-/-}$.

4 Discussion

The airway epithelium and the mucus layer provide the first line of defense against environmental pathogens, irritants, toxicants, and allergens through effective MCC and initiation of inflammatory responses at the airway surface. In chronic airway diseases associated with mucus accumulation, such as CF, COPD and asthma, epithelial dysfunction directly affects mucus properties either through an overproduction of mucins, or an epithelial ion transport dysfunction resulting in airway dehydration.[125] Reasons can be intrinsic due to a genetic disorder as in CF, environmental and/or inflammatory stimuli as in COPD and asthma. Reduced MCC associated with airway mucus accumulation and chronic airway inflammation are key features that promote airway mucus obstruction in these diseases. IL-13 is an important mediator in type-2 inflammation and causes mucin hypersecretion, but its cellular sources and the role of IL-13-mediated mucin hypersecretion in muco-obstructed airways are poorly understood. In this study, the airway epithelium's potential to produce IL-13 was analyzed. Further, the relative and combined effects of airway surface dehydration and IL-13-mediated mucin hypersecretion in the pathogenesis of airway mucus obstruction were investigated.

4.1 Airway epithelial cells contribute to IL-13 production in mice with muco-obstructive lung disease

IL-13 plays a crucial role in muco-obstructive airway diseases due to its effects on airway epithelial cells.[76,77,88,90] So far it is mainly believed that IL-13 is released by immune cells, such as ILC2 and Th2 cells. A few studies reported an IL-13 production by airway epithelial cells and preliminary studies from our group also suggested an epithelial IL-13 synthesis in juvenile *Scnn1b*-Tg mice with muco-obstructive lung disease. Therefore, an IL-13 production by airway epithelial cells was studied by analyzing protein and transcript levels, by investigating stimuli and signaling pathways, and by determining the impact on the *in vivo* pathogenesis of airway mucus obstruction.

Previous studies demonstrated that *Scnn1b*-Tg mice develop a spontaneous type 2-biased inflammatory response including elevated levels of IL-13 at juvenile ages.[15] To study an epithelial IL-13 production in juvenile WT and *Scnn1b*-Tg mice, spontaneous type 2 airway inflammation in juvenile *Scnn1b*-Tg mice was first confirmed. This was demonstrated by alternatively activated airway macrophages and increased numbers of eosinophils as well

as elevated concentrations of IL-4, IL-5, and IL-13 in *Scnn1b*-Tg mice (Figure 5 and Figure 6). To elucidate the impact of allergen exposure on IL-13 expression, juvenile WT and *Scnn1b*-Tg mice were exposed to the natural aeroallergen Af to induce allergic airway inflammation. An exaggerated type 2 immune response including increased IL-13 levels was observed after Af challenge in juvenile *Scnn1b*-Tg mice (Figure 5 and Figure 6). This observation is consistent with previously published data from our group using a house dust mite challenge model and can be ascribed to mucociliary dysfunction causing an impaired clearance of inhaled allergens.[95]

Immunohistochemical studies on human lung tissue sections by Hocke *et al.* and Park *et al.* indicated that bronchial epithelium and epithelial cells in bronchial glands from patients suffering from idiopathic pulmonary fibrosis or lung cancer, respectively, provide a source of IL-13.[115,116] By using immunohistochemistry, IL-13 was detected in a few airway epithelial cells from WT mice. In contrast, increased IL-13 protein expression was readily detected in airway epithelial cells from naïve juvenile *Scnn1b*-Tg mice. This finding was confirmed in laser micro-dissected airway epithelium on mRNA level revealing *Il13* expression in naïve juvenile *Scnn1b*-Tg mice (Figure 7). These data, for the first time, demonstrate an IL-13 production by airway epithelial cells in muco-obstructive lung disease.

Through recognition by Toll-like receptors (TLRs) Af activates airway epithelial cells[126], and Af-derived proteases were shown to contribute to type 2 inflammation[127] and to disrupt epithelial integrity leading to cytokine secretion.[128] In immune cells, allergens derived from Af are presented by antigen presenting cells to T cells.[70], and Af-specific Th2 cells were measured in patients with ABPA, allergic asthma, and CF.[70] In this study, total IL-13 concentration was highly upregulated in response to Af challenge (Figure 6), but in the airway epithelium the number of IL-13$^+$ cells and *Il13* levels were only slightly increased in *Scnn1b*-Tg mice after allergen exposure (Figure 7). Considering that Fritzsching *et al.* recently demonstrated an exaggerated number of IL-13$^+$ T cells in lungs of Af-challenged *Scnn1b*-Tg mice[95], these data indicate that exaggerated IL-13 levels in response to Af may be mainly produced by immune cells rather than airway epithelial cells in *Scnn1b*-Tg mice.

To assess the impact of epithelial-derived IL-13 on the *in vivo* pathogenesis of airway mucus obstruction, mice with (over)expression of IL-13 exclusively in the airway epithelium (*Il13*-Tg/*Il13*$^{-/-}$) were studied. *Il13*-Tg/*Il13*$^{-/-}$ mice revealed strong GCM, increased mucin expression, airway mucus plugging, and increased eosinophil and neutrophil numbers

compared to *Il13*$^{-/-}$ mice (Figure 12, Figure 13, and Figure 16). When compared to *Il13*-Tg/*Il13*$^{+/-}$ mice, mucin expression levels and eosinophil counts tended to be reduced in *Il13*-Tg/*Il13*$^{-/-}$ mice. This might be due to a higher IL-13 concentration in *Il13*-Tg/*Il13*$^{+/-}$ mice with immune cells contributing to IL-13 secretion. These data indicate that epithelial IL-13 contributes to the muco-obstructive phenotype including mucus plugging and airway inflammation. However, transgenic overexpression may cause a rather non-physiological situation with constitutively high concentrations of IL-13.

4.2 Epithelial IL-13 production is mediated by IL-33 via the St2/Myd88/p38 signaling pathway

To investigate factors responsible for epithelial IL-13 expression, *in vitro* studies using murine primary tracheal epithelial cell cultures from WT and *Scnn1b*-Tg mice were performed in the presence of various stimuli being reported to induce IL-13. In a rat model, it was shown that LPS induces epithelial IL-13 expression.[116] Temann *et al.* detected *Il13* in epithelial cells by *in situ* hybridization in IL-9-overexpressing mice in the absence of functional T cells.[113] TSLP and mechanical injury induced IL-13 production in human epithelial cell cultures.[112,114] However, in this study neither LPS, rIL-9, rTslp stimulation or mechanical injury induced *Il13* expression by primary epithelial cell cultures (Table 5). Stimulation with rIL-4 and rIL-13 did also not induce *Il13* expression suggesting no positive feedback loop via the IL-4Rα/IL-13Rα1 receptor. Moreover, Af treatment did not stimulate *Il13* expression further supporting the hypothesis that Af does not directly affect epithelial IL-13 expression.

Upon activation (e.g. by allergens), airway epithelial cells release pre-stored alarmins, such as IL-33, which recruits and/or activates amongst other immune cells dendritic cells, ILC2, and Th2 cells.[129] Interestingly, rIL-33 treatment induced expression of *Il13* in primary tracheal epithelial cell cultures from WT and *Scnn1b*-Tg mice (Figure 8). This suggests similar mechanisms in immune cells and epithelial cells. To identify the underlying signaling pathway, first, the role of Stat6 was studied, which is involved in *Il13* expression in Th2 cells.[121,122] The lack of *Stat6* in primary tracheal epithelial cultures did not abrogate *Il13* expression after rIL-33 treatment (Figure 8), which is consistent with a recent study in intestinal epithelium reporting Stat6-independent *Il13* expression in response to IL-33.[130] Second, the St2 receptor complex mediated pathway was elaborated, which was shown to drive IL-33-induced type 2 cytokine production in ILC2 and Th2 cells.[129,131] Consistent with

previous studies by Yagami *et al.* and Traister *et al.*, it was confirmed that primary tracheal epithelial cells express the IL-33 receptor St2.[132,133] Levels of *St2* did not differ between genotypes (Figure 8) suggesting that airway epithelial cells from WT and *Scnn1b*-Tg mice have the same potential to respond to IL-33. This might explain why *Il13* expression was similar in cultures from WT and *Scnn1b*-Tg mice. An anti-St2 antibody and inhibitors against Myd88 and p38 MAPK in the presence of IL-33 were used to interfere the reported signaling pathway. Blocking only the St2 receptor or inhibiting either Myd88 or p38 MAPK impeded IL-33-induced *Il13* expression in primary tracheal epithelial cultures (Figure 8). These data, for the first time, show that *Il13* expression in airway epithelial cells is induced by IL-33 and mediated by St2/Myd88/p38 signaling. However, these data do not exclude an involvement of other MAPK, such as signal-regulated kinase (ERK) and JUN N-terminal kinase (JNK), which become also activated by this pathway.[119] p38 MAPK was identified as the central target of IL-33-mediated cytokine production in human memory Th2 cells and murine peripheral blood mononuclear cells[131,134], whereas ERK was required in a human bronchial epithelial cell line. Inhibition of ERK or JNK might also block IL-33/St2-mediated *Il13* expression. A schematic overview of the IL-33-induced signaling pathway leading to IL-13 production is shown in Figure 22.

IL-33 is constitutively expressed and stored as a nuclear protein in various cell types especially of barrier tissues.[120] Hence, it is conclusive that *Il33* transcripts were readily detected in tissues from WT mice. Expression levels of *Il33* were significantly increased in *Scnn1b*-Tg mice compared to WT mice (Figure 9). This is in line with previous reports linking increased epithelial IL-33 levels to CF[135,136], COPD[137], and asthma.[138,139] Inflammation, infections, mechanical stress, and necrosis were shown to induce IL-33 production[140] and may contribute to elevated *Il33* expression in *Scnn1b*-Tg mice.[15,16] One may speculate that IL-13 synthesis in the airway epithelium from naïve *Scnn1b*-Tg is induced by elevated levels of IL-33. This assumption is supported by the observation of an IL-13 production in airway epithelial cells from WT mice after administration of rIL-33 (Figure 10).

In addition to IL-33, ionomycin stimulated *Il13* expression by murine primary tracheal epithelial cell cultures from WT and *Scnn1b*-Tg mice (Figure 8). Ionomycin is an ionophore that raises the intracellular Ca^{2+} concentration and is used to study the intracellular production of cytokines in immune cells.[75,103,118] *In vitro* experiments by Kouzaki *et al.* revealed an ionomycin-mediated translocation and release of nuclear-stored IL-33 from normal human bronchial airway epithelial cells due to increased Ca^{2+} concentrations.[140] This

might suggest that ionomycin promotes IL-33 release, which subsequently induces *Il13*. However the mechanism of ionomycin-mediated *Il13* expression in murine primary tracheal epithelial cells remains unknown.

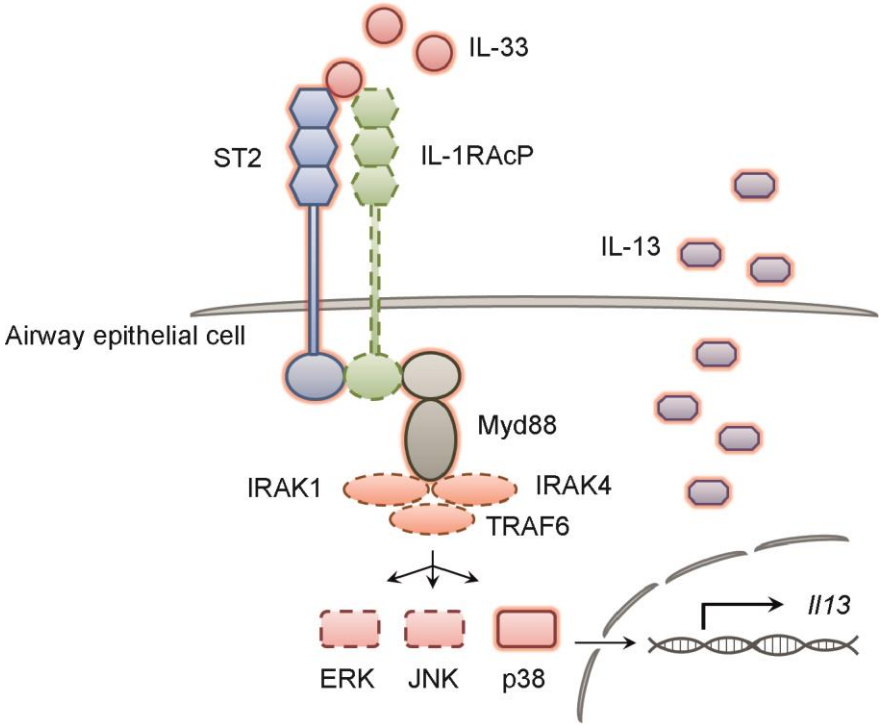

Figure 22. IL-33-mediated signaling pathway leading to IL-13 expression in airway epithelial cells. Red highlighted symbols indicate proteins that were studied in the presented study. Dotted lines indicate proteins that have been shown to be involved in the signaling pathway according to the literature. IL-33 signals through suppression of tumorigenicity 2 (ST2) and IL-1 receptor accessory protein (IL-1RAcP) receptor dimers. Upon binding myeloid differentiation primary-response protein 88 (Myd88), the kinases IL1R-associated kinase 1 (IRAK1) and IRAK4, and the adapter protein TNF receptor-associated factor 6 (TRAF6) are recruited. This leads to activation of the mitogen-activated protein kinases (MAPK), including extracellular signal-regulated kinases (ERK), Jun N-terminal kinases (JNK), and p38 to drive the synthesis of IL-13.

4.3 Airway surface dehydration and IL-13-induced mucin hypersecretion act synergistically in the *in vivo* pathogenesis of airway mucus plugging

In muco-obstructive airway diseases such as CF, COPD, and asthma, abnormal mucus production and/or hydration leads to highly viscous and adhesive mucus associated with impaired MCC. Although the initial reasons for airway mucus obstruction differ between muco-obstructive lung diseases, airway mucus plugging is often driven by both pathologies the overproduction of mucins and airway dehydration. In CF lung disease, mucus obstruction is primarily caused by airway dehydration and associated with mucin hypersecretion.[141] In COPD and asthma, inflammation in response to different triggers including tobacco smoke and inhaled allergens, respectively, initially induces mucin hypersecretion leading to airway obstruction.[142] Several studies also indicated that mucus hyperconcentration is a critical point in chronic bronchitis, which is a common clinical feature of asthma and COPD.[31,32,143] Further, cigarette smoke was shown to induce ASL volume depletion by the loss of the CFTR function[144,145], ascribing airway dehydration also to the pathogenesis of COPD. IL-13 plays a pivotal role in the overproduction of mucins, thereby contributing to airway mucus plugging. Besides asthma, COPD and CF are also associated with type 2 inflammation including increased IL-13 levels that might contribute to mucin hypersecretion.[62,64,65] Lately, efforts have been undertaken to understand the biophysical mechanism of mucus plugging[27], but the relative contribution of airway surface dehydration and IL-13-mediated mucin hypersecretion to the *in vivo* pathogenesis of airway mucus obstruction is not known. Therefore, the phenotype of *Scnn1b*-Tg mice lacking IL-13 (*Scnn1b*-Tg/*Il13*$^{-/-}$) was studied and *Scnn1b*-Tg mice (*Scnn1b*-Tg/*Il13*$^{+/-}$) were compared to IL-13-over-expressing mice (*Il13*-Tg/*Il13*$^{+/-}$). It will be referred to *Scnn1b*-Tg and *Il13*-Tg mice to discuss the comparison of *Scnn1b*-Tg/*Il13*$^{+/-}$ and *Il13*-Tg/*Il13*$^{+/-}$ mice. To gain new insights in the combined effects of both defects, *Scnn1b*-Tg/*Il13*-Tg/*Il13*$^{-/-}$ mice were generated.

Previous studies demonstrated that GCM and spontaneous as well as allergen-induced type 2 airway inflammation in neonatal/juvenile *Scnn1b*-Tg mice can be abrogated by the deletion of IL-4Rα[146] or Stat6[95]. The direct impact of IL-13 in *Scnn1b*-Tg mice with spontaneous type 2 airway inflammation, including increased IL-13 and IL-4 levels, is unclear with both cytokines signaling through IL-4Rα/Stat6.[147] In juvenile *Scnn1b*-Tg mice lacking IL-13, decreased mucin expression levels accompanied by absence of goblet cells

were observed (Figure 12 and Figure 13). This is consistent with previous findings demonstrating that IL-13 is sufficient to mediate goblet cell differentiation.[61,148] However, *Scnn1b*-Tg/*Il13*$^{-/-}$ mice still developed severe airway mucus obstruction and airway inflammation including neutrophilia and eosinophilia (Figure 12 and Figure 16). Consistent with a recent report by Gehrig *et al.*, these data demonstrate that mucus plugging occurs independent of mucin hypersecretion in *Scnn1b*-Tg mice.[94] The number of eosinophils was only slightly reduced in *Scnn1b*-Tg/*Il13*$^{-/-}$ mice compared to *Scnn1b*-Tg/*Il13*$^{+/-}$ mice suggesting that IL-4, IL-5 and eotaxin[149], known to be up-regulated in juvenile *Scnn1b*-Tg mice[15,95], may compensate for recruitment of eosinophils during spontaneous type 2 airway inflammation in juvenile *Scnn1b*-Tg mice.

Consistent with previous reports[76,77], strong GCM and a highly increased mucin expression were observed in *Il13*-Tg mice and this was less pronounced in *Scnn1b*-Tg mice. Nonetheless, juvenile *Scnn1b*-Tg mice were characterized by severe airway mucus plugging, whereas under conditions of IL-13-mediated mucin hypersecretion (*Il13*-Tg mice) airway mucus obstruction was less severe (Figure 12). This observation was not only manifested in the quantity of mucus content but also in the number of mice showing mucus plugging. Less *Il13*-Tg mice were affected by mucus obstruction than *Scnn1b*-Tg mice. According to Button *et al.* mucus dehydration and mucin hypersecretion can cause mucus hyperconcentration leading to impaired clearance.[27] Mucus clearance efficiency was impaired in juvenile *Scnn1b*-Tg mice and resulted in severe mucus plugging. In contrast, in *Il13*-Tg mice mucociliary transport was not affected enabling a better clearance of the released mucus (Figure 15). A critical factor that mediates effective MCC is airway hydration. *In vitro* studies revealed that IL-13 down-regulates Na^+ transport and increases the activity of Cl^- channels.[89,90] This IL-13-mediated hypersecretory effect was further supported *in vivo* in IL-13 treated mice.[88] Proper MCC in *Il13*-Tg mice might be ascribed to a hypersecretory phenotype that prevents severe airway mucus plugging in the presence of mucus overproduction by hydrating the airway surface. In patients with asthma, MCC was found to be impaired, but to a lesser extent compared to other chronic airway diseases.[43] Future studies are needed to evaluate the impact of the IL-13-mediated hypersecretory effect on MCC in patients with asthma. Although *Il13*-Tg mice displayed no impairment of MCC, excessive mucin production still leads to mucus accumulation in *Il13*-Tg mice suggesting that effective MCC does not necessarily prevent airway mucus obstruction. Recent studies demonstrated an involvement of IL-13 in tethering the mucus layer to airway

epithelial cells.[53] Thus, mucus adhesion to the airway surface might be another factor contributing to mucus plugging in *Il13*-Tg mice.

In contrast to juvenile mice, mucus plugging in main axial airways was similar in *Scnn1b*-Tg/*Il13*$^{-/-}$ and *Il13*-Tg/*Il13*$^{-/-}$ mice at neonatal age (Figure 12 and Figure 18). This could be explained by age-dependent differences in the localization of mucus plugs. Longitudinal studies by Mall *et al.* demonstrated that mucus plugging in *Scnn1b*-Tg mice originates in the trachea in the first week of life and then extends into proximal and distal airways in juvenile mice.[15] However, µ-CT-based analysis of all airways revealed a significantly increased mucus score for neonatal *Scnn1b*-Tg/*Il13*$^{-/-}$ mice compared to *Il13*-Tg/*Il13*$^{-/-}$ mice (Figure 19) demonstrating that mucus plugging is more severe in neonatal *Scnn1b*-Tg/*Il13*$^{-/-}$ compared to *Il13*-Tg/*Il13*$^{-/-}$ mice. These data might indicate that mucus plugging in the trachea and/or distal airways contribute to an overall severe muco-obstructive phenotype in neonatal *Scnn1b*-Tg/*Il13*$^{-/-}$ mice.

Inflammatory cells not only affect mucus accumulation through the induction of mucin production (e.g. via cytokines), they also alter mucus viscosity. Neutrophil-generated oxidation crosslinks mucin polymers to stiffen mucus in CF airways.[35] A recent study by Dunican *et al.* proposes that eosinophil-driven oxidation contributes to increased mucus viscosity in asthma.[19] Juvenile *Scnn1b*-Tg and *Il13*-Tg mice were characterized by eosinophilic and neutrophilc infiltration (Figure 16), as reported recently.[15,77,95,99] Besides the prominent effect of IL-13 on eosinophil recruitment, IL-13 has also been implicated with neutrophil accumulation.[150] These data indicate that eosinophilic and neutrophilc infiltration contributes to airway inflammation in both mouse models and thus might affect mucus rheology.

Based on the data obtained so far, it was hypothesized that both defects might reinforce each other when mediating mucus obstruction. This assumption is supported by observations gained from *Scnn1b*-Tg/*Il13*-Tg/*Il13*$^{-/-}$ mice exhibiting both airway surface dehydration and IL-13-mediated mucin hypersecretion. *Scnn1b*-Tg/*Il13*-Tg/*Il13*$^{-/-}$ mice died within the first week of life (Figure 17). Histological evaluation of the main stem bronchi revealed excessive airway mucus obstruction partially plugging the whole airway lumen (Figure 18). µ-CT measurements of the whole lung confirmed this observation on a global scale and displayed severe mucus plugging (Figure 19). Moreover, *Scnn1b*-Tg/*Il13*-Tg/*Il13*$^{-/-}$ mice were characterized by severe atelectasis, a common feature of CF[151,152] and asthma[1],

resulting from the occlusion of airways with mucus. Neonatal *Scnn1b*-Tg/*Il13*$^{-/-}$ and *Il13*-Tg/*Il13*$^{-/-}$ mice also displayed mucus plugging and atelectaic regions, but to a lesser extent and with a milder effect on mortality (Figure 17 and Figure 19). It was concluded that severe airway mucus plugging causes neonatal death in *Scnn1b*-Tg/*Il13*-Tg/*Il13*$^{-/-}$ mice. Thus, these data support the hypothesis that airway surface dehydration and IL-13-induced mucin hypersecretion contribute synergistically to the pathogenesis of airway mucus obstruction.

Another factor that substantiates the hypothesis comes from the treatment study. Hypertonic saline is used therapeutically to improve airway surface hydration and MCC in chronic airway diseases.[153] In *Scnn1b*-Tg mice, preventive treatment with 7 % HS had beneficial effects on mucus obstruction.[124] However, treatment with 7 % HS in newborn *Scnn1b*-Tg/*Il13*-Tg/*Il13*$^{-/-}$ mice did not rescue mice suggesting that airway hydration alone is not sufficient to ameliorate severe airway mucus plugging in dehydrated airways with IL-13-induced mucin overproduction (Figure 21). Further studies are needed to find an effective treatment strategy. Besides the improvement of airway hydration, it might be beneficial to consider biophysical mucus properties. This could be achieved by using mucolytic agents, which disrupt the mucus gel structure causing a reduced mucus viscosity and thereby improving mucus clearance. N-acetylcysteine, which is used in patients with COPD, might be a potential mucolytic drug.[154] To affect both pathogenic defects, a treatment combining airway hydration and mucolytic agents might prevent severe mucus plugging in *Scnn1b*-Tg/*Il13*-Tg/*Il13*$^{-/-}$ mice.

4.4 Muc5ac and Muc5b contribute to airway mucus plugging

The identification of distinct features of the major respiratory mucins Muc5ac and Muc5b indicates that the mucus composition is critical for mucus plugging. Muc5b was found to be essential for effective MCC and airway defense[57], whereas Muc5ac impedes mucus detachment from airway surfaces[53], and contributes to AHR and mucus plugging during allergic inflammation[54]. Most studies only investigated the effects of IL-13 on Muc5ac production demonstrating that IL-13 regulates Muc5ac via the induction of the transcription factors Spdef[155] and Foxa3[86]. This is also reflected by the data gained from *Il13*-Tg mice (Figure 13 and Figure 14). In contrast, the regulation of *Muc5b* by IL-13 is poorly understood.[42] By looking into *Muc5b* expression, the obtained data suggest that IL-13 (in)directly affects *Muc5b* expression. *Muc5b* transcripts were up-regulated in *Il13*-Tg mice,

and tended to be reduced in *Scnn1b*-Tg mice lacking IL-13 (Figure 13). Chen *et al.* identified *MUC5B* as an FOXA3-regulated gene[86], and Guo *et al.* recently showed a binding site of SPDEF in upstream regions of *MUC5AC* and *MUC5B* in A549 cells.[156] In *Il13*-Tg mice, *Muc5b* transcription might be mediated by Spdef and/or Foxa3. In *Scnn1b*-Tg mice, increased *Muc5ac* and *Muc5b* levels were not associated with an up-regulation of *Spdef* and *Foxa3*. One may speculate that mucin expression occurs independent of Spdef/Foxa3 in *Scnn1b*-Tg mice. This assumption is supported by a recent observation indicating Muc5ac and Muc5b production in neonatal *Spdef*-deficient *Scnn1b*-Tg mice.[157] Mucin expression in *Scnn1b*-Tg mice might be regulated by an IL-13-mediated MAPK[65] or PI3K-NFAT[158] pathway, or other mucin stimulating factors, such as IL-1β and TNF-α[159], known to be up-regulated in juvenile *Scnn1b*-Tg mice.[15,16] Further studies are needed to clarify the transcriptional mucin regulation in response to IL-13 and in *Scnn1b*-Tg mice.

Emerging evidence suggests that Muc5ac plays a crucial role for mucus adhesion. First, in fatal asthma specimen Shimura *et al.* observed that released mucus is tethered to goblet cells[160], and goblet cells in human airways are supposed to produce primarily MUC5AC.[28,30] Second, mucus analysis in piglets indicated that MUC5AC connects goblet cells with MUC5B-containing mucus.[161] Third, Bonser *et al.* recently demonstrated that MUC5AC-rich mucus is tethered to airway epithelial cells, thereby making the mucus more adhesive.[53] In neonatal and juvenile *Scnn1b*-Tg/*Il13*$^{-/-}$ mice exhibiting severe mucus plugging, mucin expression was dominated by Muc5b as shown by baseline *Muc5ac* expression, elevated *Muc5b* levels, and a low *Muc5ac/Muc5b* ratio (Figure 13 and Figure 20). These data suggest that Muc5ac might be less required for mucus plugging on dehydrated airway surfaces. In *Scnn1b*-Tg mice, mucus adhesion might be rather caused by periciliary compression due to dehydration-mediated hyperconcentrated mucus.[92] Mucin expression in neonatal *Il13*$^{-/-}$ mice was low, but was characterized by a high *Muc5ac/Muc5b* ratio. This observation might reflect recent finding of an increased expression of type 2 signature genes including *Muc5ac* at the neonatal/juvenile age.[95,162] Mucus plugs in juvenile *Il13*-Tg mice are more heterogeneous, because *Muc5ac* and *Muc5b* levels were highly upregulated (Figure 13). When compared to *Scnn1b*-Tg mice, the mucus in *Il13*-Tg mice can be described as Muc5ac-rich. Increased Muc5ac content may promote mucus adherence[53] in *Il13*-Tg mice that might cause mucus plug formation despite effective mucociliary transport. However, these data let assume that both Muc5ac and Muc5b contribute to mucus plugging.

In neonatal *Il13*-Tg/*Il13*$^{-/-}$ and *Scnn1b*-Tg/*Il13*-Tg/*Il13*$^{-/-}$ mice, total mucin expression levels were elevated to similar levels (Figure 20) suggesting that it is not the mucin quantity *per se* that determines the severity of mucus obstruction. In neonatal *Scnn1b*-Tg/*Il13*-Tg/*Il13*$^{-/-}$ mice, airway dehydration might exaggerate mucus plugging. Further, neonatal *Il13*-Tg/*Il13*$^{-/-}$ and *Scnn1b*-Tg/*Il13*-Tg/*Il13*$^{-/-}$ mice revealed similar high *Muc5ac* and *Muc5b* expression levels and a similar high *Muc5ac/Muc5b* ratio, again reflecting an IL-13-dependent high Muc5ac content compared to *Scnn1b*-Tg/*Il13*$^{-/-}$ mice. Since *Il13*-Tg/*Il13*$^{-/-}$ mice did not die due to lethal airway mucus plugging, Muc5ac-rich mucus might not be the determining factor, which further supports the hypothesis that both mucins have an adverse effect on mucus obstruction. In line with this, Ehre *et al.* reported that overexpression of Muc5ac in mice does not impair MCC and is insufficient to trigger mucus plugging.[163] The authors also demonstrated that Muc5ac-containing mucus forms a thicker mucus layer than Muc5b-rich mucus.[163] A Muc5ac-mediated thick mucus layer might further favor mucus obstruction in neonatal *Scnn1b*-Tg/*Il13*-Tg/*Il13*$^{-/-}$ mice with age-related small airway diameters. One may speculate that this might play a role in patients, since small airways are affected by mucus plugging in CF, COPD, and asthma.[9,16,22,164,165]

4.5 Conclusions and future perspectives

This study demonstrates that under conditions of muco-obstructive lung disease associated with type 2 airway inflammation, the airway epithelium provides sources of IL-13. For the first time, this study shows that epithelial IL-13 production is directly induced by IL-33 and this is mediated by the St2/Myd88/p38 signaling pathway. Considering that IL-33 serves as an alarmin in epithelial cells, these data indicate that the airway epithelium itself triggers epithelial IL-13 production in an autocrine/paracrine manner. This supports the concept that the airway epithelium is not only an important effector tissue but also an important mediator of pulmonary inflammation that contributes to the orchestration of type 2 inflammation. Further, it was demonstrated that airway epithelium-specific (over)expression of IL-13 is sufficient to cause muco-obstructive lung disease characterized by mucus plugging associated with overproduction of mucins, severe GCM, and airway inflammation. If the human airway epithelium is able to produce IL-13, this will be interesting to study in tissue samples from patients with chronic airway diseases, such as COPD and asthma. The use of primary airway epithelial cell cultures from patients and healthy controls might confirm a relevance of the IL-33/ST2-driven pathway for the epithelial IL-13 production in the human system.

This study provides novel insights into the relative roles and combined effects of airway surface dehydration and IL-13-induced mucin hypersecretion on the *in vivo* pathogenesis of airway mucus obstruction. GCM and increased mucin expression were abrogated in the absence of IL-13, but severe mucus plugging persisted in muco-static airways of *Scnn1b*-Tg/*Il13*$^{-/-}$ mice suggesting that the constitutive mucin secretion is sufficient to cause airway mucus obstruction on dehydrated airway surfaces. Further, IL-13-induced mucin hypersecretion (*Il13*-Tg) caused less severe mucus plugging than airway surface dehydration (*Snnn1b*-Tg), and the presence of both defects leads to fatal mucus plugging (*Scnn1b*-Tg/*Il13*-Tg/*Il13*$^{-/-}$). Differences in the severity of mucus plugging might be ascribed to the mucus clearance efficiency that was reduced in *Scnn1b*-Tg mice but was not impaired in *Il13*-Tg mice. To better understand the mechanism of mucus plugging under conditions of IL-13-induced mucin hypersecretion, it would be of great interest to study how the gel-on-brush model considering mucus hyperconcentration and periciliary compression is applicable in the *Il13*-Tg mouse model and of course in patients with asthma. This might be achieved by confocal microscopy and by determining the mucus osmotic pressure. This study further suggests that airway surface dehydration and IL-13-induced mucin hypersecretion act synergistically and have a detrimental effect on the pathogenesis of airway mucus obstruction. This is supported by the observation that preventive airway hydration treatment alone did not reduce lethal airway mucus plugging in *Scnn1b*-Tg/*Il13*-Tg/*Il13*$^{-/-}$ mice. A combination of agents improving airway hydration and mucolytic drugs, which decrease mucus viscosity by disrupting its structure, might be more beneficial. This study further suggests that both Muc5ac and Muc5b contribute to mucus plugging, but also point toward an impact of Muc5ac-rich mucus. IL-13 overexpressing mice revealed considerable higher levels of Muc5ac that could facilitate mucus adhesion. Knowledge about the distribution of Muc5ac and Muc5b within mucus plugs in the studied mouse models (e.g. by immunohistochemistry) might also give new insights into the complex pathophysiology of airway mucus plugging.

5 References

1. Fahy JV, Dickey BF. Airway mucus function and dysfunction. *N Engl J Med*. 2010;363(23):2233-2247.

2. Rommens JM, Iannuzzi MC, Kerem B, et al. Identification of the cystic fibrosis gene: chromosome walking and jumping. *Science*. 1989;245(4922):1059-1065.

3. Kerem B, Rommens JM, Buchanan JA, et al. Identification of the cystic fibrosis gene: genetic analysis. *Science*. 1989;245(4922):1073-1080.

4. Riordan JR, Rommens JM, Kerem B, et al. Identification of the cystic fibrosis gene: cloning and characterization of complementary DNA. *Science*. 1989;245(4922):1066-1073.

5. Mall MA, Hartl D. CFTR: cystic fibrosis and beyond. *Eur Respir J*. 2014.

6. Hector A, Kirn T, Ralhan A, et al. Microbial colonization and lung function in adolescents with cystic fibrosis. *J Cyst Fibros*. 2016;15(3):340-349.

7. Elborn JS. Cystic fibrosis. *Lancet*. 2016;388(10059):2519-2531.

8. Courtney JM, Ennis M, Elborn JS. Cytokines and inflammatory mediators in cystic fibrosis. *J Cyst Fibros*. 2004;3(4):223-231.

9. Hogg JC, Chu F, Utokaparch S, et al. The nature of small-airway obstruction in chronic obstructive pulmonary disease. *N Engl J Med*. 2004;350(26):2645-2653.

10. Sethi S, Murphy TF. Infection in the pathogenesis and course of chronic obstructive pulmonary disease. *N Engl J Med*. 2008;359(22):2355-2365.

11. Barnes PJ. Inflammatory mechanisms in patients with chronic obstructive pulmonary disease. *J Allergy Clin Immunol*. 2016;138(1):16-27.

12. Montgomery ST, Mall MA, Kicic A, Stick SM, Arest CF. Hypoxia and sterile inflammation in cystic fibrosis airways: mechanisms and potential therapies. *Eur Respir J*. 2017;49(1).

13. Sly PD, Brennan S, Gangell C, et al. Lung disease at diagnosis in infants with cystic fibrosis detected by newborn screening. *Am J Respir Crit Care Med*. 2009;180(2):146-152.

14. Sly PD, Gangell CL, Chen L, et al. Risk factors for bronchiectasis in children with cystic fibrosis. *N Engl J Med*. 2013;368(21):1963-1970.

15. Mall MA, Harkema JR, Trojanek JB, et al. Development of chronic bronchitis and emphysema in beta-epithelial Na+ channel-overexpressing mice. *Am J Respir Crit Care Med*. 2008;177(7):730-742.

16. Fritzsching B, Zhou-Suckow Z, Trojanek JB, et al. Hypoxic epithelial necrosis triggers neutrophilic inflammation via IL-1 receptor signaling in cystic fibrosis lung disease. *Am J Respir Crit Care Med*. 2015;191(8):902-913.

17. Lukens JR, Gross JM, Kanneganti TD. IL-1 family cytokines trigger sterile inflammatory disease. *Front Immunol*. 2012;3:315.

18. Brusselle GG, Joos GF, Bracke KR. New insights into the immunology of chronic obstructive pulmonary disease. *Lancet*. 2011;378(9795):1015-1026.

19. Dunican EM, Elicker BM, Gierada DS, et al. Mucus plugs in patients with asthma linked to eosinophilia and airflow obstruction. *J Clin Invest*. 2018;128(3):997-1009.

20. Brannan JD, Lougheed MD. Airway hyperresponsiveness in asthma: mechanisms, clinical significance, and treatment. *Front Physiol*. 2012;3:460.

21. Aikawa T, Shimura S, Sasaki H, Ebina M, Takishima T. Marked goblet cell hyperplasia with mucus accumulation in the airways of patients who died of severe acute asthma attack. *Chest*. 1992;101(4):916-921.

22. Kuyper LM, Pare PD, Hogg JC, et al. Characterization of airway plugging in fatal asthma. *Am J Med*. 2003;115(1):6-11.

23. Hammad H, Lambrecht BN. Barrier Epithelial Cells and the Control of Type 2 Immunity. *Immunity*. 2015;43(1):29-40.

24. Lambrecht BN, Hammad H. The immunology of asthma. *Nat Immunol*. 2015;16(1):45-56.

25. Barlow JL, Peel S, Fox J, et al. IL-33 is more potent than IL-25 in provoking IL-13-producing nuocytes (type 2 innate lymphoid cells) and airway contraction. *J Allergy Clin Immunol*. 2013;132(4):933-941.

26. Chu DK, Llop-Guevara A, Walker TD, et al. IL-33, but not thymic stromal lymphopoietin or IL-25, is central to mite and peanut allergic sensitization. *J Allergy Clin Immunol*. 2013;131(1):187-200 e181-188.

27. Button B, Cai LH, Ehre C, et al. A periciliary brush promotes the lung health by separating the mucus layer from airway epithelia. *Science*. 2012;337(6097):937-941.

28. Thornton DJ, Rousseau K, McGuckin MA. Structure and function of the polymeric mucins in airways mucus. *Annu Rev Physiol*. 2008;70:459-486.

29. Chen EY, Yang N, Quinton PM, Chin WC. A new role for bicarbonate in mucus formation. *Am J Physiol Lung Cell Mol Physiol*. 2010;299(4):L542-549.

30. Groneberg DA, Eynott PR, Oates T, et al. Expression of MUC5AC and MUC5B mucins in normal and cystic fibrosis lung. *Respir Med*. 2002;96(2):81-86.

31. Ghosh A, Boucher RC, Tarran R. Airway hydration and COPD. *Cell Mol Life Sci*. 2015;72(19):3637-3652.

32. Anderson WH, Coakley RD, Button B, et al. The Relationship of Mucus Concentration (Hydration) to Mucus Osmotic Pressure and Transport in Chronic Bronchitis. *Am J Respir Crit Care Med*. 2015;192(2):182-190.

33. Henderson AG, Ehre C, Button B, et al. Cystic fibrosis airway secretions exhibit mucin hyperconcentration and increased osmotic pressure. *J Clin Invest*. 2014;124(7):3047-3060.

34. Abdullah LH, Coakley R, Webster MJ, et al. Mucin Production and Hydration Responses to Mucopurulent Materials in Normal vs. CF Airway Epithelia. *Am J Respir Crit Care Med*. 2017.

35. Yuan S, Hollinger M, Lachowicz-Scroggins ME, et al. Oxidation increases mucin polymer cross-links to stiffen airway mucus gels. *Sci Transl Med*. 2015;7(276):276ra227.

36. Abdullah LH, Evans JR, Wang TT, et al. Defective postsecretory maturation of MUC5B mucin in cystic fibrosis airways. *JCI Insight*. 2017;2(6):e89752.

37. Shao MX, Nakanaga T, Nadel JA. Cigarette smoke induces MUC5AC mucin overproduction via tumor necrosis factor-alpha-converting enzyme in human airway epithelial (NCI-H292) cells. *Am J Physiol Lung Cell Mol Physiol*. 2004;287(2):L420-427.

38. Gensch E, Gallup M, Sucher A, et al. Tobacco smoke control of mucin production in lung cells requires oxygen radicals AP-1 and JNK. *J Biol Chem*. 2004;279(37):39085-39093.

39. Zhou JS, Zhao Y, Zhou HB, et al. Autophagy plays an essential role in cigarette smoke-induced expression of MUC5AC in airway epithelium. *Am J Physiol Lung Cell Mol Physiol*. 2016;310(11):L1042-1052.

40. Innes AL, Woodruff PG, Ferrando RE, et al. Epithelial mucin stores are increased in the large airways of smokers with airflow obstruction. *Chest*. 2006;130(4):1102-1108.

41. Kim EY, Battaile JT, Patel AC, et al. Persistent activation of an innate immune response translates respiratory viral infection into chronic lung disease. *Nat Med*. 2008;14(6):633-640.

42. Thai P, Loukoianov A, Wachi S, Wu R. Regulation of airway mucin gene expression. *Annu Rev Physiol*. 2008;70:405-429.

43. Del Donno M, Bittesnich D, Chetta A, Olivieri D, Lopez-Vidriero MT. The effect of inflammation on mucociliary clearance in asthma: an overview. *Chest*. 2000;118(4):1142-1149.

44. Messina MS, O'Riordan TG, Smaldone GC. Changes in mucociliary clearance during acute exacerbations of asthma. *Am Rev Respir Dis*. 1991;143(5 Pt 1):993-997.

45. Lachowicz-Scroggins ME, Yuan S, Kerr SC, et al. Abnormalities in MUC5AC and MUC5B Protein in Airway Mucus in Asthma. *Am J Respir Crit Care Med*. 2016;194(10):1296-1299.

46. Evans CM, Kim K, Tuvim MJ, Dickey BF. Mucus hypersecretion in asthma: causes and effects. *Curr Opin Pulm Med*. 2009;15(1):4-11.

47. Curran DR, Cohn L. Advances in mucous cell metaplasia: a plug for mucus as a therapeutic focus in chronic airway disease. *Am J Respir Cell Mol Biol*. 2010;42(3):268-275.

48. Kesimer M, Ford AA, Ceppe A, et al. Airway Mucin Concentration as a Marker of Chronic Bronchitis. *N Engl J Med*. 2017;377(10):911-922.

49. Ordonez CL, Khashayar R, Wong HH, et al. Mild and moderate asthma is associated with airway goblet cell hyperplasia and abnormalities in mucin gene expression. *Am J Respir Crit Care Med*. 2001;163(2):517-523.

50. Fahy JV. Goblet cell and mucin gene abnormalities in asthma. *Chest*. 2002;122(6 Suppl):320S-326S.

51. Welsh KG, Rousseau K, Fisher G, et al. MUC5AC and a Glycosylated Variant of MUC5B Alter Mucin Composition in Children With Acute Asthma. *Chest*. 2017.

52. Kirkham S, Sheehan JK, Knight D, Richardson PS, Thornton DJ. Heterogeneity of airways mucus: variations in the amounts and glycoforms of the major oligomeric mucins MUC5AC and MUC5B. *Biochem J*. 2002;361(Pt 3):537-546.

53. Bonser LR, Zlock L, Finkbeiner W, Erle DJ. Epithelial tethering of MUC5AC-rich mucus impairs mucociliary transport in asthma. *J Clin Invest*. 2016;126(6):2367-2371.

54. Evans CM, Raclawska DS, Ttofali F, et al. The polymeric mucin Muc5ac is required for allergic airway hyperreactivity. *Nat Commun*. 2015;6:6281.

55. Janssen WJ, Stefanski AL, Bochner BS, Evans CM. Control of lung defence by mucins and macrophages: ancient defence mechanisms with modern functions. *Eur Respir J*. 2016;48(4):1201-1214.

56. Woodruff PG, Modrek B, Choy DF, et al. T-helper type 2-driven inflammation defines major subphenotypes of asthma. *Am J Respir Crit Care Med*. 2009;180(5):388-395.

57. Roy MG, Livraghi-Butrico A, Fletcher AA, et al. Muc5b is required for airway defence. *Nature*. 2014;505(7483):412-416.

58. Humbert M, Durham SR, Kimmitt P, et al. Elevated expression of messenger ribonucleic acid encoding IL-13 in the bronchial mucosa of atopic and nonatopic subjects with asthma. *J Allergy Clin Immunol*. 1997;99(5):657-665.

59. Naseer T, Minshall EM, Leung DY, et al. Expression of IL-12 and IL-13 mRNA in asthma and their modulation in response to steroid therapy. *Am J Respir Crit Care Med*. 1997;155(3):845-851.

60. Wills-Karp M, Luyimbazi J, Xu X, et al. Interleukin-13: central mediator of allergic asthma. *Science*. 1998;282(5397):2258-2261.

61. Grunig G, Warnock M, Wakil AE, et al. Requirement for IL-13 independently of IL-4 in experimental asthma. *Science*. 1998;282(5397):2261-2263.

62. Tiringer K, Treis A, Fucik P, et al. A Th17- and Th2-skewed cytokine profile in cystic fibrosis lungs represents a potential risk factor for Pseudomonas aeruginosa infection. *Am J Respir Crit Care Med*. 2013;187(6):621-629.

63. Hartl D, Griese M, Kappler M, et al. Pulmonary T(H)2 response in Pseudomonas aeruginosa-infected patients with cystic fibrosis. *J Allergy Clin Immunol*. 2006;117(1):204-211.

64. Byers DE, Alexander-Brett J, Patel AC, et al. Long-term IL-33-producing epithelial progenitor cells in chronic obstructive lung disease. *J Clin Invest*. 2013;123(9):3967-3982.

65. Alevy YG, Patel AC, Romero AG, et al. IL-13-induced airway mucus production is attenuated by MAPK13 inhibition. *J Clin Invest*. 2012;122(12):4555-4568.

66. Grubek-Jaworska H, Paplinska M, Hermanowicz-Salamon J, et al. IL-6 and IL-13 in induced sputum of COPD and asthma patients: correlation with respiratory tests. *Respiration*. 2012;84(2):101-107.

67. Cowley AC, Thornton DJ, Denning DW, Horsley A. Aspergillosis and the role of mucins in cystic fibrosis. *Pediatr Pulmonol*. 2017;52(4):548-555.

68. Agarwal R, Srinivas R, Jindal SK. Allergic bronchopulmonary aspergillosis complicating chronic obstructive pulmonary disease. *Mycoses*. 2008;51(1):83-85.

69. Everaerts S, Lagrou K, Dubbeldam A, et al. Sensitization to Aspergillus fumigatus as a risk factor for bronchiectasis in COPD. *Int J Chron Obstruct Pulmon Dis*. 2017;12:2629-2638.

70. Knutsen AP, Slavin RG. Allergic bronchopulmonary aspergillosis in asthma and cystic fibrosis. *Clin Dev Immunol*. 2011;2011:843763.

71. Agarwal R, Nath A, Aggarwal AN, Gupta D, Chakrabarti A. Aspergillus hypersensitivity and allergic bronchopulmonary aspergillosis in patients with acute severe asthma in a respiratory intensive care unit in North India. *Mycoses*. 2010;53(2):138-143.

72. Christenson SA, Steiling K, van den Berge M, et al. Asthma-COPD overlap. Clinical relevance of genomic signatures of type 2 inflammation in chronic obstructive pulmonary disease. *Am J Respir Crit Care Med*. 2015;191(7):758-766.

73. Postma DS, Rabe KF. The Asthma-COPD Overlap Syndrome. *N Engl J Med*. 2015;373(13):1241-1249.

74. Gao J, Iwamoto H, Koskela J, et al. Characterization of sputum biomarkers for asthma-COPD overlap syndrome. *Int J Chron Obstruct Pulmon Dis*. 2016;11:2457-2465.

75. Piehler D, Eschke M, Schulze B, et al. The IL-33 receptor (ST2) regulates early IL-13 production in fungus-induced allergic airway inflammation. *Mucosal Immunol*. 2016;9(4):937-949.

76. Zhu Z, Homer RJ, Wang Z, et al. Pulmonary expression of interleukin-13 causes inflammation, mucus hypersecretion, subepithelial fibrosis, physiologic abnormalities, and eotaxin production. *J Clin Invest*. 1999;103(6):779-788.

77. Kuperman DA, Huang X, Koth LL, et al. Direct effects of interleukin-13 on epithelial cells cause airway hyperreactivity and mucus overproduction in asthma. *Nat Med*. 2002;8(8):885-889.

78. Gour N, Wills-Karp M. IL-4 and IL-13 signaling in allergic airway disease. *Cytokine*. 2015;75(1):68-78.

79. Oh CK, Geba GP, Molfino N. Investigational therapeutics targeting the IL-4/IL-13/STAT-6 pathway for the treatment of asthma. *Eur Respir Rev*. 2010;19(115):46-54.

80. Park KS, Korfhagen TR, Bruno MD, et al. SPDEF regulates goblet cell hyperplasia in the airway epithelium. *J Clin Invest*. 2007;117(4):978-988.

81. Wan H, Kaestner KH, Ang SL, et al. Foxa2 regulates alveolarization and goblet cell hyperplasia. *Development*. 2004;131(4):953-964.

82. Qin Y, Jiang Y, Sheikh AS, Shen S, Liu J, Jiang D. Interleukin-13 stimulates MUC5AC expression via a STAT6-TMEM16A-ERK1/2 pathway in human airway epithelial cells. *Int Immunopharmacol*. 2016;40:106-114.

83. Lin J, Jiang Y, Li L, Liu Y, Tang H, Jiang D. TMEM16A mediates the hypersecretion of mucus induced by Interleukin-13. *Exp Cell Res*. 2015;334(2):260-269.

84. Huang F, Zhang H, Wu M, et al. Calcium-activated chloride channel TMEM16A modulates mucin secretion and airway smooth muscle contraction. *Proc Natl Acad Sci U S A*. 2012;109(40):16354-16359.

85. Erle DJ, Sheppard D. The cell biology of asthma. *J Cell Biol*. 2014;205(5):621-631.

86. Chen G, Korfhagen TR, Karp CL, et al. Foxa3 induces goblet cell metaplasia and inhibits innate antiviral immunity. *Am J Respir Crit Care Med*. 2014;189(3):301-313.

87. Laoukili J, Perret E, Willems T, et al. IL-13 alters mucociliary differentiation and ciliary beating of human respiratory epithelial cells. *J Clin Invest*. 2001;108(12):1817-1824.

88. Anagnostopoulou P, Dai L, Schatterny J, Hirtz S, Duerr J, Mall MA. Allergic airway inflammation induces a pro-secretory epithelial ion transport phenotype in mice. *Eur Respir J*. 2010;36(6):1436-1447.

89. Galietta LJ, Pagesy P, Folli C, et al. IL-4 is a potent modulator of ion transport in the human bronchial epithelium in vitro. *J Immunol*. 2002;168(2):839-845.

90. Danahay H, Atherton H, Jones G, Bridges RJ, Poll CT. Interleukin-13 induces a hypersecretory ion transport phenotype in human bronchial epithelial cells. *Am J Physiol Lung Cell Mol Physiol*. 2002;282(2):L226-236.

91. Anagnostopoulou P, Riederer B, Duerr J, et al. SLC26A9-mediated chloride secretion prevents mucus obstruction in airway inflammation. *J Clin Invest*. 2012;122(10):3629-3634.

92. Mall M, Grubb BR, Harkema JR, O'Neal WK, Boucher RC. Increased airway epithelial Na+ absorption produces cystic fibrosis-like lung disease in mice. *Nat Med*. 2004;10(5):487-493.

93. Trojanek JB, Cobos-Correa A, Diemer S, et al. Airway Mucus Obstruction Triggers Macrophage Activation and MMP12-dependent Emphysema. *Am J Respir Cell Mol Biol*. 2014.

94. Gehrig S, Duerr J, Weitnauer M, et al. Lack of neutrophil elastase reduces inflammation, mucus hypersecretion, and emphysema, but not mucus obstruction, in mice with cystic fibrosis-like lung disease. *Am J Respir Crit Care Med*. 2014;189(9):1082-1092.

95. Fritzsching B, Hagner M, Dai L, et al. Impaired mucus clearance exacerbates allergen-induced type 2 airway inflammation in juvenile mice. *J Allergy Clin Immunol*. 2017;140(1):190-203 e195.

96. Boucher RC. An overview of the pathogenesis of cystic fibrosis lung disease. *Adv Drug Deliv Rev*. 2002;54(11):1359-1371.

97. Hogg JC. Pathophysiology of airflow limitation in chronic obstructive pulmonary disease. *Lancet*. 2004;364(9435):709-721.

98. Hogg JC. The pathology of asthma. *APMIS*. 1997;105(10):735-745.

99. Lee CG, Homer RJ, Zhu Z, et al. Interleukin-13 induces tissue fibrosis by selectively stimulating and activating transforming growth factor beta(1). *J Exp Med*. 2001;194(6):809-821.

100. Zheng T, Zhu Z, Wang Z, et al. Inducible targeting of IL-13 to the adult lung causes matrix metalloproteinase- and cathepsin-dependent emphysema. *J Clin Invest*. 2000;106(9):1081-1093.

101. Dahdah A, Gautier G, Attout T, et al. Mast cells aggravate sepsis by inhibiting peritoneal macrophage phagocytosis. *J Clin Invest*. 2014;124(10):4577-4589.

102. Zhu Z, Ma B, Homer RJ, Zheng T, Elias JA. Use of the tetracycline-controlled transcriptional silencer (tTS) to eliminate transgene leak in inducible overexpression transgenic mice. *J Biol Chem*. 2001;276(27):25222-25229.

103. Neill DR, Wong SH, Bellosi A, et al. Nuocytes represent a new innate effector leukocyte that mediates type-2 immunity. *Nature*. 2010;464(7293):1367-1370.

104. Perl AK, Wert SE, Loudy DE, Shan Z, Blair PA, Whitsett JA. Conditional recombination reveals distinct subsets of epithelial cells in trachea, bronchi, and alveoli. *Am J Respir Cell Mol Biol*. 2005;33(5):455-462.

105. Harkema JR, Plopper CG, Hyde DM, St George JA. Regional differences in quantities of histochemically detectable mucosubstances in nasal, paranasal, and nasopharyngeal epithelium of the bonnet monkey. *J Histochem Cytochem*. 1987;35(3):279-286.

106. Weibel ER. Principles and methods for the morphometric study of the lung and other organs. *Lab Invest*. 1963;12:131-155.

107. Vasilescu DM, Knudsen L, Ochs M, Weibel ER, Hoffman EA. Optimized murine lung preparation for detailed structural evaluation via micro-computed tomography. *J Appl Physiol (1985)*. 2012;112(1):159-166.

108. Tapia JC, Kasthuri N, Hayworth KJ, et al. High-contrast en bloc staining of neuronal tissue for field emission scanning electron microscopy. *Nat Protoc*. 2012;7(2):193-206.

109. Thiesse J, Namati E, Sieren JC, et al. Lung structure phenotype variation in inbred mouse strains revealed through in vivo micro-CT imaging. *J Appl Physiol (1985)*. 2010;109(6):1960-1968.

110. Mayer AK, Bartz H, Fey F, Schmidt LM, Dalpke AH. Airway epithelial cells modify immune responses by inducing an anti-inflammatory microenvironment. *Eur J Immunol*. 2008;38(6):1689-1699.

111. Pfaffl MW. A new mathematical model for relative quantification in real-time RT-PCR. *Nucleic Acids Res*. 2001;29(9):e45.

112. Allahverdian S, Harada N, Singhera GK, Knight DA, Dorscheid DR. Secretion of IL-13 by airway epithelial cells enhances epithelial repair via HB-EGF. *Am J Respir Cell Mol Biol*. 2008;38(2):153-160.

113. Temann UA, Laouar Y, Eynon EE, Homer R, Flavell RA. IL9 leads to airway inflammation by inducing IL13 expression in airway epithelial cells. *Int Immunol*. 2007;19(1):1-10.

114. Semlali A, Jacques E, Koussih L, Gounni AS, Chakir J. Thymic stromal lymphopoietin-induced human asthmatic airway epithelial cell proliferation through an IL-13-dependent pathway. *J Allergy Clin Immunol*. 2010;125(4):844-850.

115. Park SW, Ahn MH, Jang HK, et al. Interleukin-13 and its receptors in idiopathic interstitial pneumonia: clinical implications for lung function. *J Korean Med Sci*. 2009;24(4):614-620.

116. Hocke AC, Ermert M, Althoff A, et al. Regulation of interleukin IL-4, IL-13, IL-10, and their downstream components in lipopolysaccharide-exposed rat lungs. Comparison of the constitutive expression between rats and humans. *Cytokine*. 2006;33(4):199-211.

117. Kuperman DA, Huang X, Nguyenvu L, Holscher C, Brombacher F, Erle DJ. IL-4 receptor signaling in Clara cells is required for allergen-induced mucus production. *J Immunol*. 2005;175(6):3746-3752.

118. Chatila T, Silverman L, Miller R, Geha R. Mechanisms of T cell activation by the calcium ionophore ionomycin. *J Immunol*. 1989;143(4):1283-1289.

119. Schmitz J, Owyang A, Oldham E, et al. IL-33, an interleukin-1-like cytokine that signals via the IL-1 receptor-related protein ST2 and induces T helper type 2-associated cytokines. *Immunity*. 2005;23(5):479-490.

120. Martin NT, Martin MU. Interleukin 33 is a guardian of barriers and a local alarmin. *Nat Immunol*. 2016;17(2):122-131.

121. Ho IC, Tai TS, Pai SY. GATA3 and the T-cell lineage: essential functions before and after T-helper-2-cell differentiation. *Nat Rev Immunol*. 2009;9(2):125-135.

122. Spilianakis CG, Flavell RA. Long-range intrachromosomal interactions in the T helper type 2 cytokine locus. *Nat Immunol*. 2004;5(10):1017-1027.

123. Lee PJ, Zhang X, Shan P, et al. ERK1/2 mitogen-activated protein kinase selectively mediates IL-13-induced lung inflammation and remodeling in vivo. *J Clin Invest*. 2006;116(1):163-173.

124. Graeber SY, Zhou-Suckow Z, Schatterny J, Hirtz S, Boucher RC, Mall MA. Hypertonic saline is effective in the prevention and treatment of mucus obstruction, but not airway inflammation, in mice with chronic obstructive lung disease. *Am J Respir Cell Mol Biol*. 2013;49(3):410-417.

125. Holtzman MJ, Byers DE, Alexander-Brett J, Wang X. The role of airway epithelial cells and innate immune cells in chronic respiratory disease. *Nat Rev Immunol*. 2014;14(10):686-698.

126. Croft CA, Culibrk L, Moore MM, Tebbutt SJ. Interactions of Aspergillus fumigatus Conidia with Airway Epithelial Cells: A Critical Review. *Front Microbiol*. 2016;7:472.

127. Namvar S, Warn P, Farnell E, et al. Aspergillus fumigatus proteases, Asp f 5 and Asp f 13, are essential for airway inflammation and remodelling in a murine inhalation model. *Clin Exp Allergy*. 2015;45(5):982-993.

128. Kauffman HF, Tomee JF, van de Riet MA, Timmerman AJ, Borger P. Protease-dependent activation of epithelial cells by fungal allergens leads to morphologic

changes and cytokine production. *J Allergy Clin Immunol*. 2000;105(6 Pt 1):1185-1193.

129. Liew FY, Girard JP, Turnquist HR. Interleukin-33 in health and disease. *Nat Rev Immunol*. 2016;16(11):676-689.

130. Yang Z, Sun R, Grinchuk V, et al. IL-33-induced alterations in murine intestinal function and cytokine responses are MyD88, STAT6, and IL-13 dependent. *Am J Physiol Gastrointest Liver Physiol*. 2013;304(4):G381-389.

131. Endo Y, Hirahara K, Iinuma T, et al. The interleukin-33-p38 kinase axis confers memory T helper 2 cell pathogenicity in the airway. *Immunity*. 2015;42(2):294-308.

132. Yagami A, Orihara K, Morita H, et al. IL-33 mediates inflammatory responses in human lung tissue cells. *J Immunol*. 2010;185(10):5743-5750.

133. Traister RS, Uvalle CE, Hawkins GA, Meyers DA, Bleecker ER, Wenzel SE. Phenotypic and genotypic association of epithelial IL1RL1 to human TH2-like asthma. *J Allergy Clin Immunol*. 2015;135(1):92-99.

134. Wu H, Yang S, Wu X, et al. Interleukin-33/ST2 signaling promotes production of interleukin-6 and interleukin-8 in systemic inflammation in cigarette smoke-induced chronic obstructive pulmonary disease mice. *Biochem Biophys Res Commun*. 2014;450(1):110-116.

135. Tiringer K, Treis A, Kanolzer S, et al. Differential expression of IL-33 and HMGB1 in the lungs of stable cystic fibrosis patients. *Eur Respir J*. 2014;44(3):802-805.

136. Roussel L, Farias R, Rousseau S. IL-33 is expressed in epithelia from patients with cystic fibrosis and potentiates neutrophil recruitment. *J Allergy Clin Immunol*. 2013;131(3):913-916.

137. Holtzman MJ, Byers DE, Brett JA, et al. Linking acute infection to chronic lung disease. The role of IL-33-expressing epithelial progenitor cells. *Ann Am Thorac Soc*. 2014;11 Suppl 5:S287-291.

138. Prefontaine D, Lajoie-Kadoch S, Foley S, et al. Increased expression of IL-33 in severe asthma: evidence of expression by airway smooth muscle cells. *J Immunol*. 2009;183(8):5094-5103.

139. Prefontaine D, Nadigel J, Chouiali F, et al. Increased IL-33 expression by epithelial cells in bronchial asthma. *J Allergy Clin Immunol*. 2010;125(3):752-754.

140. Kouzaki H, Iijima K, Kobayashi T, O'Grady SM, Kita H. The danger signal, extracellular ATP, is a sensor for an airborne allergen and triggers IL-33 release and innate Th2-type responses. *J Immunol*. 2011;186(7):4375-4387.

141. Boucher RC. Evidence for airway surface dehydration as the initiating event in CF airway disease. *J Intern Med*. 2007;261(1):5-16.

142. Barnes PJ. Immunology of asthma and chronic obstructive pulmonary disease. *Nat Rev Immunol*. 2008;8(3):183-192.

143. Button B, Anderson WH, Boucher RC. Mucus Hyperconcentration as a Unifying Aspect of the Chronic Bronchitic Phenotype. *Ann Am Thorac Soc*. 2016;13 Suppl 2:S156-162.

144. Clunes LA, Davies CM, Coakley RD, et al. Cigarette smoke exposure induces CFTR internalization and insolubility, leading to airway surface liquid dehydration. *FASEB J*. 2012;26(2):533-545.

145. Sloane PA, Shastry S, Wilhelm A, et al. A pharmacologic approach to acquired cystic fibrosis transmembrane conductance regulator dysfunction in smoking related lung disease. *PLoS One*. 2012;7(6):e39809.

146. Livraghi A, Grubb BR, Hudson EJ, et al. Airway and lung pathology due to mucosal surface dehydration in {beta}-epithelial Na+ channel-overexpressing mice: role of TNF-{alpha} and IL-4R{alpha} signaling, influence of neonatal development, and limited efficacy of glucocorticoid treatment. *J Immunol*. 2009;182(7):4357-4367.

147. Kuperman DA, Schleimer RP. Interleukin-4, interleukin-13, signal transducer and activator of transcription factor 6, and allergic asthma. *Curr Mol Med*. 2008;8(5):384-392.

148. Kondo M, Tamaoki J, Takeyama K, Nakata J, Nagai A. Interleukin-13 induces goblet cell differentiation in primary cell culture from Guinea pig tracheal epithelium. *Am J Respir Cell Mol Biol*. 2002;27(5):536-541.

149. Rosenberg HF, Phipps S, Foster PS. Eosinophil trafficking in allergy and asthma. *J Allergy Clin Immunol*. 2007;119(6):1303-1310; quiz 1311-1302.

150. Shim JJ, Dabbagh K, Ueki IF, et al. IL-13 induces mucin production by stimulating epidermal growth factor receptors and by activating neutrophils. *Am J Physiol Lung Cell Mol Physiol*. 2001;280(1):L134-140.

151. Salamone I, Mondello B, Lucanto MC, Cristadoro S, Lombardo M, Barone M. Bronchial tree-shaped mucous plug in cystic fibrosis: imaging-guided management. *Respirol Case Rep*. 2017;5(2):e00214.

152. Amaxopoulou C, Gnannt R, Higashigaito K, Jung A, Kellenberger CJ. Structural and perfusion magnetic resonance imaging of the lung in cystic fibrosis. *Pediatr Radiol*. 2017.

153. Daviskas E, Anderson SD, Gonda I, et al. Inhalation of hypertonic saline aerosol enhances mucociliary clearance in asthmatic and healthy subjects. *Eur Respir J*. 1996;9(4):725-732.

154. Decramer M, Janssens W. Mucoactive therapy in COPD. *Eur Respir Rev*. 2010;19(116):134-140.

155. Chen G, Korfhagen TR, Xu Y, et al. SPDEF is required for mouse pulmonary goblet cell differentiation and regulates a network of genes associated with mucus production. *J Clin Invest*. 2009;119(10):2914-2924.

156. Guo M, Tomoshige K, Meister M, et al. Gene signature driving invasive mucinous adenocarcinoma of the lung. *EMBO Mol Med*. 2017;9(4):462-481.

157. Chen G, Volmer AS, Wilkinson KJ, et al. Spdef-Independent Mucin Production During Non-Th2-Dominated Pulmonary Inflammation Revealed In The Scnn1b-Tg Muco-Obstructive Mouse Model. *Am J Respir Crit Care Med*. 2016;193:A5558.

158. Yan F, Li W, Zhou H, et al. Interleukin-13-induced MUC5AC expression is regulated by a PI3K-NFAT3 pathway in mouse tracheal epithelial cells. *Biochem Biophys Res Commun*. 2014;446(1):49-53.

159. Song KS, Lee WJ, Chung KC, et al. Interleukin-1 beta and tumor necrosis factor-alpha induce MUC5AC overexpression through a mechanism involving ERK/p38 mitogen-activated protein kinases-MSK1-CREB activation in human airway epithelial cells. *J Biol Chem*. 2003;278(26):23243-23250.

160. Shimura S, Andoh Y, Haraguchi M, Shirato K. Continuity of airway goblet cells and intraluminal mucus in the airways of patients with bronchial asthma. *Eur Respir J*. 1996;9(7):1395-1401.

161. Ermund A, Meiss LN, Rodriguez-Pineiro AM, et al. The normal trachea is cleaned by MUC5B mucin bundles from the submucosal glands coated with the MUC5AC mucin. *Biochem Biophys Res Commun*. 2017;492(3):331-337.

162. Lewis CC, Aronow B, Hutton J, et al. Unique and overlapping gene expression patterns driven by IL-4 and IL-13 in the mouse lung. *J Allergy Clin Immunol*. 2009;123(4):795-804 e798.

163. Ehre C, Worthington EN, Liesman RM, et al. Overexpressing mouse model demonstrates the protective role of Muc5ac in the lungs. *Proc Natl Acad Sci U S A*. 2012;109(41):16528-16533.

164. Williams OW, Sharafkhaneh A, Kim V, Dickey BF, Evans CM. Airway mucus: From production to secretion. *Am J Respir Cell Mol Biol*. 2006;34(5):527-536.

165. Burgel PR, Montani D, Danel C, Dusser DJ, Nadel JA. A morphometric study of mucins and small airway plugging in cystic fibrosis. *Thorax*. 2007;62(2):153-161.

Publications

Original articles

Fritzsching B*, Hagner M*, Dai L*, Christochowitz S, Agrawal R, van Bodegom C, et al. Impaired mucus clearance exacerbates allergen-induced type 2 airway inflammation in juvenile mice. J Allergy Clin Immunol **2017**; 140:190-203 e5. (*These authors contributed equally to this work.)

Abstracts

Christochowitz S, Millar-Büchner P, Schmidt S, Wagner WL, Löser T, Hagner M, Schatterney J, Kauczor HU, Mall MA. Relative roles of mucus dehydration and mucin hypersecretion in the in vivo pathogenesis of airway mucus obstruction. Deutsches Zentrum für Lungenforschung Annual Meeting, Bad Nauheim, **2018**

Christochowitz S, Schmidt S, Schatterny J, Hagner M, Mall MA. Relative roles of reduced mucus clearance and mucus hypersecretion in the pathogenesis of airway mucus plugging in mice. Gordon Research Conference (GRC) on Cilia, Mucus & Mucociliary Interactions, Texas, USA, **2017**

Christochowitz S, Schmidt S, Schatterny J, Hagner M, Mall MA. Relative roles of reduced mucus clearance and mucus hypersecretion in the pathogenesis of airway mucus plugging in mice. 14th European Cystic Fibrosis Society Basic Science Conference, Albufeira, Portugal, **2017**

M, Fritzsching B, Dai L, van Bodegom C, Christochowitz S, Schmidt S, Schatterny J, Hirtz S, Dürr J, Zhou-Suckow Z, Mall MA. Impaired mucus clearance promotes Aspergillus fumigatus-induced type 2 airway inflammation in cystic fibrosis-like lung disease in mice. Cyst Fibros **2016**; 15: S6.

Hagner M, Fritzsching B, Dai L, van Bodegom C, Christochowitz S, Schmidt S, Schatterny J, Hirtz S, Dürr J, Zhou-Suckow Z, Mall MA. Impaired mucus clearance promotes Aspergillus fumigatus-induced type 2 airway inflammation in cystic fibrosis-like lung disease in mice. Pediatr Pulmonol **2016**; 51: S229.

Christochowitz S, van Bodegom C, Schmidt S, Maier E, Hagner M, Fellenberg J, Mall MA, Fritzsching B. Pulmonary IL-13 expression is increased by airway surface dehydration in vivo. Pneumologie **2015**; 69 - A29

Hagner M, Schmidt S, Maier E, Christochowitz S, Lampe M, Mall MA, Fritzsching B. Pulmonary allergen clearance is impaired by airway surface dehydration. Pneumologie **2015**; 69 - A28

Fritzsching B, Dai L, van Bodegom C, Schatterny J, Hirtz S, Zhou-Suckow Z, Hagner M, Christochowitz S, Mall MA. Airway surface dehydration is a novel risk factor for allergic airway inflammation. Pneumologie **2015**; 69 - A30

Christochowitz S, van Bodegom C, Schmidt S, Maier E, Hagner M, Fellenberg J, Mall MA, Fritzsching B. Airway dehydration increases pulmonary IL-13 expression in vivo. Allergo J Int **2014**; 24: 41.

B Fritzsching, L Dai, C van Bodegom, J Schatterny, S Hirtz, Z Zhou-Suckow, M Hagner, S Christochowitz, MA Mall. Airway surface dehydration is a novel risk factor for allergic airway inflammation. Allergo J Int **2014**; 24: 31.

Oral Presentation

Relative roles of reduced mucus clearance and mucus hypersecretion in the pathogenesis of airway mucus plugging in mice. 14th European Cystic Fibrosis Society Basic Science Conference, Albufeira, Portugal, 29 March – 01 April **2017**

Acknowledgements

I want to thank my supervisor Prof. Dr. Marcus Mall for excellent scientific input, for his encouragement and constructive advice. My work benefited greatly from his extensive experience.

I want to thank Prof. Dr. Benedikt Fritzsching for initial guidance, which enabled the successful first period of my project. I also want to thank my thesis advisory committee Prof. Dr. Volker Daniel and Prof. Dr. Karsten Mahnke for their interest in my project and helpful recommendations for the progress of my work.

Many thanks to Dr. Johanna Salomon for her continued advice and proofreading, for going to sports courses with me, and for nice times also outside the lab. Many thanks to Dr. Matthias Hagner for his constructive proofreading, for the good team spirit, and for having entertaining times during exhausting PhD phases.

I am thankful to Simone Schmidt for her continuous experimental support that continued also during my parental leave. I thank Jolanthe Schatterny, Heike Scheuermann, Stephanie Hirtz, Angela Frank, and Martin Finke for their technical help. I also want to thank Inge Frommer for performing the osmium impregnation technique, as well as Willi Wagner and Timo Löser for helping with the analysis of µ-CT scans. I want to thank Dr. Michelle Paulsen for proofreading of my thesis.

I am grateful to all the colleagues of the Department of Translational Pulmonology for their help and for creating such a friendly working atmosphere extending into barbecues and humorous lunch and coffee breaks.

Many thanks to my parents Silvana and Berndt Christochowitz for their endless support.

Finally, I want to thank Sebastian Olschewski for all his support, for being understanding and for always being there for me. I am so proud to have my daughter Selma, who always cheered me up with her smile.